University of Szeged

Faculty of Pharmacy

Institute of Pharmaceutical Technology and Regulatory Affairs

Head: Prof. Dr. Ildikó Csóka Ph.D.

Ph.D. Thesis

FORMULATION AND CHARACTERIZATION OF INNOVATIVE DERMAL FOAM SYSTEMS

By

Dr. Fanni Falusi

Pharmacist

Supervisors:

Dr. habil. Anita Kovács, Ph.D.

Dr. habil. Szilvia Berkó, Ph.D.

Szeged

2024

PUBLICATIONS RELATED TO THE SUBJECT OF THE THESIS

I. **Fanni Falusi**; Mária Budai-Szűcs; Erzsébet Csányi; Szilvia Berkó; Tamás Spaits; Ildikó Csóka; Anita Kovács: Investigation of the effect of polymers on dermal foam properties using the QbD approach.
European Journal of Pharmaceutical Sciences, 173, 106160 (2022) **(Q1, IF:4.6 by JCR)**

II. **Fanni Falusi**; Szilvia Berkó; Anita Kovács; Mária Budai-Szűcs: Application of Xanthan Gum and Hyaluronic Acid as Dermal Foam Stabilizers.
Gels, 8(7), 413. (2022) **(Q1, IF: 4.6 by JCR)**

III. **Fanni Falusi**, Szilvia Berkó, Mária Budai-Szűcs, Zoltán Veréb, Anita Kovács: Foams Set a New Pace for the Release of Diclofenac Sodium.
Pharmaceutics 16, 287 (2024) **(Q1, IF:5.4 by JCR)**

PUBLICATIONS NOT RELATED TO THE SUBJECT OF THE THESIS

I. Anita Kovács, Stella Zsikó, **Fanni Falusi**, Erzsébet Csányi, Mária Budai-Szűcs, Ildikó Csóka, Szilvia Berkó: Comparison of Synthetic Membranes to Heat-Separated Human Epidermis in Skin Permeation Studies *In Vitro*.
Pharmaceutics 13, 2106 (2021) **(Q1, IF:6.525 by JCR)**

II. Anita Kovács, **Fanni Falusi,** Attila Gácsi, Mária Budai-Szűcs, Erzsébet Csányi, Zoltán Veréb, Tamás Monostori, Ildikó Csóka, Szilvia Berkó: Formulation and investigation of hydrogels containing an increased level of diclofenac sodium using risk assessment tools.
European Journal of Pharmaceutical Sciences 193, 106666, (2024) **(Q1, IF:4.6 by JCR)**

PRESENTATIONS RELATED TO THE SUBJECT OF THE THESIS

Verbal presentations

I. **Fanni Falusi**; Anita Kovács; Erzsébet Csányi
Investigation of foams for topical use
III. Symposium of Young Researchers on Pharmaceutical Technology, Biotechnology and Regulatory Science, Szeged, 2021

II. **Falusi Fanni**
Dermális habok formulálása és vizsgálata
IV. Fiatal Technológusok Fóruma, online, 2021

III. **Falusi Fanni**; Berkó Szilvia; Csóka Ildikó; Kovács Anita
Dermális habok jellemzése és vizsgálata
MKE Kozmetikai Szimpózium, Budapest, 2021

IV. **Falusi Fanni**
Különböző polimer tartalmú habok formulációja és vizsgálata
XIV. Clauder Ottó Emlékverseny, Budapest, 2021

V. **Fanni Falusi**; Anita Kovács; Szilvia Berkó
Formulation and investigation of the effect of polymers on dermal foam properties using the QbD approach
IV. Symposium of Young Researchers on Pharmaceutical Technology, Biotechnology and Regulatory Science, Szeged, 2022

VI. **Falusi Fanni**; Kovács Anita; Budai-Szűcs Mária; Berkó Szilvia
Dermális habok, mint innovatív gyógyszerformák formulálása és vizsgálata
Gyógyszerkémiai és Gyógyszertechnológiai Szimpózium '22, Herceghalom, 2022

VII. **Falusi Fanni**; Kovács Anita; Budai-Szűcs Mária; Csóka Ildikó; Berkó Szilvia
Dermálisan alkalmazott készítmények hatóanyag-felszabadulásának és penetrációjának *in vitro* modellezése
MKE Kozmetikai Szimpózium, Budapest, 2022

VIII. **Fanni Falusi**; Szilvia Berkó; Anita Kovács
Influence of polymers and active substances on foam stability
V. Symposium of Young Researchers on Pharmaceutical Technology, Biotechnology and Regulatory Science, Szeged, 2023

IX. **Falusi Fanni**
A gyógyszeres habok nyújtotta ígéretes lehetőségek a hagyományos gyógyszerhordozó rendszerekkel szemben
VI. Fiatal Technológusok Fóruma, Budapest, 2023

X. **Falusi Fanni**; Berkó Szilvia; Kovács Anita
Dermálisan alkalmazott gyógyszerhordozó rendszerek komparatív vizsgálata
Gyógyszerkémiai és Gyógyszertechnológiai Szimpózium '23, Herceghalom, 2023

XI. **Falusi Fanni**
A dermális habok nyújtotta ígéretes lehetőségek
MKE Kozmetikai Szimpózium, Budapest, 2023

Poster Presentations

I. **Fanni Falusi**; Szilvia Berkó; Mária Budai-Szűcs; Anita Kovács
Formulation and investigation of the effect of polymers on dermal foam properties using the Quality by Design (QbD) approach
9th BBBB International Conference on Pharmaceutical Sciences - Pharma Sciences of Tomorrow, Ljubljana, 2022

II. **Falusi Fanni**; Berkó Szilvia; Budai-Szűcs Mária; Kovács Anita
Hialuronsav és xantángumi, mint habstabilitás növelő komponensek vizsgálata
Gyógyszertechnológiai és Ipari Gyógyszerészeti Konferencia, Siófok, 2022

III. **Fanni Falusi**; Szilvia Berkó; Mária Budai-Szűcs; Anita Kovács
Development and evaluation of stable hydrogel formulations with enhanced diclofenac sodium concentration for effective topical drug delivery
14th Central European Symposium on Pharmaceutical Technology, Ohrid, 2023

PRESENTATIONS NOT RELATED TO THE SUBJECT OF THE THESIS

I. **Fanni Falusi**; Szilvia Berkó; Anita Kovács
Advancements in formulation and investigation of innovative foam-based *in situ* film-forming systems
VI. Symposium of Young Researchers on Pharmaceutical Technology, Biotechnology and Regulatory Science, Szeged, 2024

TABLE OF CONTENTS

ABBREVIATIONS

AD-MSC	Human adipose-derived mesenchymal stem cell
ANOVA	Analysis of variance
CAM	Chorioallantoic membrane assay
CMA	Critical Material Attributes
CPP	Critical Process Parameters
CQA	Critical Quality Attributes
DEXP	Dexpanthenol
DMEM-HG	Dulbecco's Modified Eagle's Medium with high D-Glucose concentration
DS	Diclofenac sodium
FE	Foam expansion
FVS	Foam volume stability
HA	Hyaluronic acid
HA_{CL}	Cross-linked Hyaluronic acid
HA_{HMW}	High molecular weight Hyaluronic acid
HA_{LMW}	Low molecular weight Hyaluronic acid
HEC	Hydroxyethylcellulose
HET-CAM	Hen's Egg Chorioallantoic Membrane Test
HPMC	Hydroxypropyl methylcellulose
ICCVAM	Interagency Coordinating Committee on the Validation of Alternative Methods
IPA	Isopropanol
IS	Irritation score
IVPT	*In vitro* permeation test
IVRT	*In vitro* release test
logP	Logarithmic octanol-water partition coefficient
LVE	Viscoelastic range
NIAC	Niacinamide
PEG 200	Polyethylene glycol 200
QbD	Quality by Design
QTPP	Quality Target Product Profile

REM	Risk Estimation Matrix
RI	Relative intensity
RFD	Relative foam density
SDS	Sodium dodecyl sulfate
SLES	Sodium laureth sulfate
TPP	Target Product Profile
UHPLC	Ultra-high performance liquid chromatography
XANT	Xanthan gum

1. INTRODUCTION

A wide range of dermal formulations is available during the development of preparations (Figure 1). According to the classification of the 8th edition of the European Pharmacopoeia, within traditional forms, solid, semisolid, and liquid preparations are distinguished. Solid forms applied dermally include powders, while semisolid forms are represented by ointments, creams, gels, patches, and pastes. Liquid forms encompass solutions, emulsions, and suspensions [1]. In addition to traditional forms, the pharmaceutical industry has seen an increasing number of new, innovative forms, such as nanoemulsions [2], niosomes [3], film-forming systems [4], foams, etc. [5]. In the dermal field, foams have gained focus in recent years, especially in the treatment of burns and wound healing [6,7]. They are being applied in several new areas, and environmentally friendly designs have become increasingly important. Consequently, propellant-containing systems are gradually being replaced by propellant-free systems.

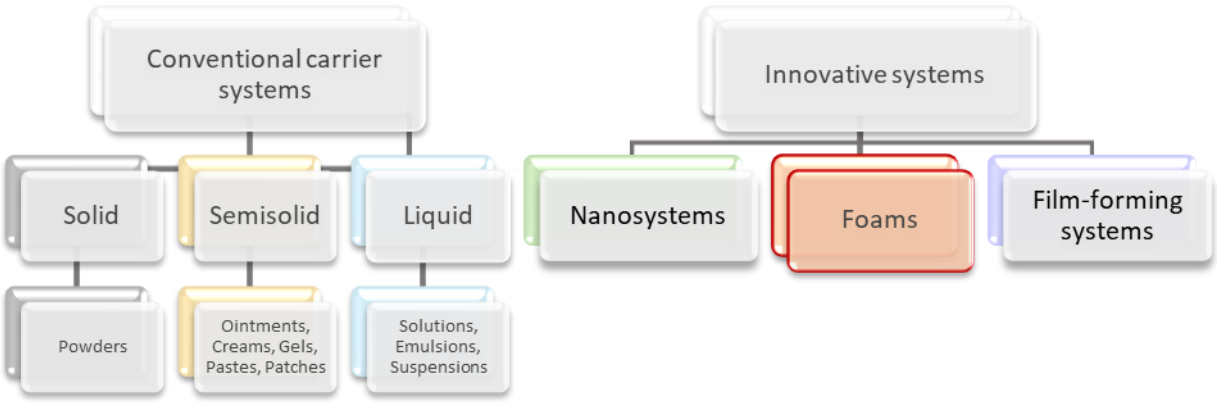

Figure 1. Classification of preparations for dermal use.

Foam-forming systems offer significant potential, providing advantages to both the pharmaceutical and cosmetic industries. They provide easy and convenient application with precise dosage, allowing complete removal from the skin surface. Despite their numerous advantages, formulating these systems poses considerable challenges. The key consideration in composition design is ensuring the product to remain on the skin for a sufficient duration. Meeting user needs, the product should spread quickly and provide a pleasant skin feel.

There are limited studies on medicated foams, therefore understanding, developing, and investigating these systems can result in a formulation with significantly improved properties.

2. THEORETICAL BACKGROUND

2.1. The structure of the skin

The largest organ of our body is the skin (Figure 2), comprising 10-15% of the body weight of an average adult [8,9].

Fundamentally, the skin is a complex structure consisting of three distinct layers: the epidermis, dermis, and hypodermis. These layers are not only clearly differentiated in terms of their structural composition but also exhibit distinct functionalities [10].

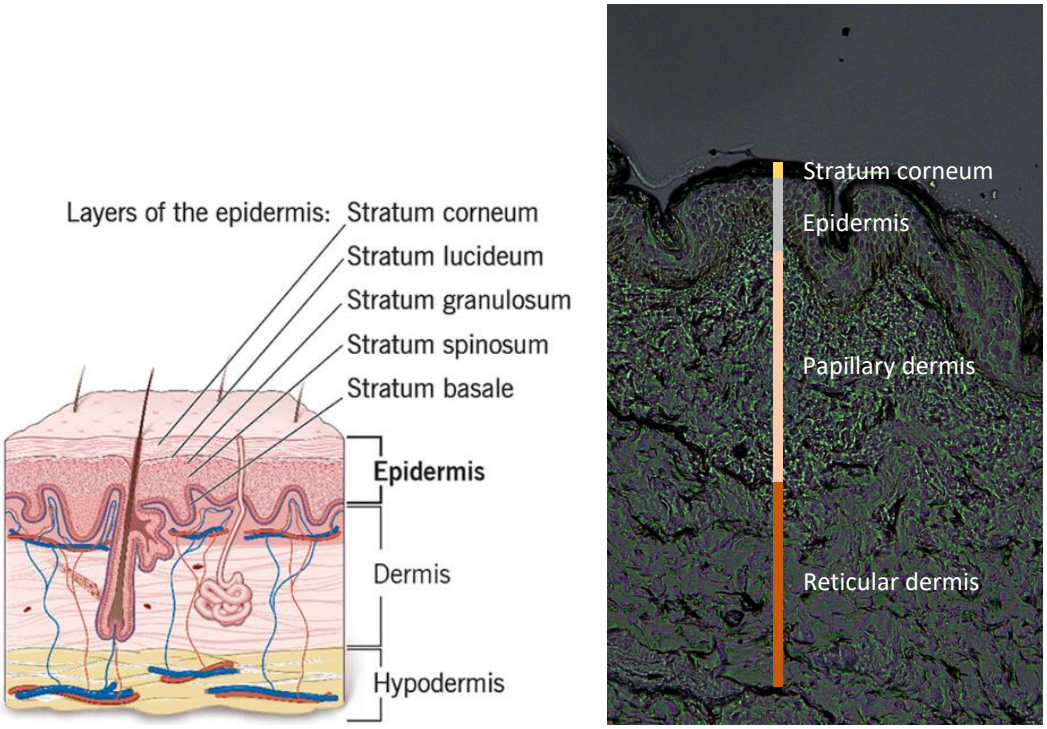

Figure 2. The structure of the skin [11].

Epidermis

The epidermis, the outermost skin layer, is primarily composed of keratinocytes, making up 95% of its cells, with the remaining 5% consisting of melanocytes, Langerhans cells, and Merkel cells. It comprises five distinct layers: the basal cell layer (*stratum basale*), spinous or prickle cell layer (*stratum spinosum*), granular cell layer (*stratum granulosum*), clear cell layer (*stratum lucidum*), and the outermost horny layer (*stratum corneum*) [9].

In the basal cell layer, cells divide continuously on the basal membrane, ensuring ongoing layer renewal. Desmosomes in the spinous cell layer create prickles, enhancing the mechanical resistance of the epidermis. Keratinization commences in the granular layer, producing keratohyalin protein granules. Finally, in the clear layer, cells lose their nuclei as they press tightly together [12].

The tight-sealing cells of the clear layer, the horny layer, and the lipid mantle (produced by the granular cell layer) play a crucial role in the skin's barrier function. In pharmaceutical technology, the primary challenge during dermal drug delivery is overcoming the skin barrier [13]. The skin barrier function is maintained by corneocytes and epidermal lipids, forming a "bricks and mortar" structure. Corneocytes lack nuclei and are filled with keratin filaments [14]. Surrounding them are extracellular lipids, primarily ceramides, cholesterol, and fatty acids [15,16]. The hydro-lipid film layer on the epidermis serves as the primary defense against microbes, while the acid mantle, sustained by substances from sweat glands (e.g., lactic acid, amino acids) and sebaceous gland (e.g., free fatty acids) and cornification process (e.g., amino acids, pyrrolidone carboxylic acid), creates an acidic environment that protects against infections [17].

Besides, the Natural Moisturizing Factor, containing polar molecules such as salts, amino acids, and urea, is present in corneocytes, aiding in the mobility of compounds of the *stratum corneum* [18,19]. The multilamellar lipid structure of the *stratum corneum* protects the body from excessive transepidermal water loss and prevents the penetration of compounds into the body via the epidermis [20].

Dermis

The dermis, situated beneath the epidermis, is the thick and elastic layer of the skin, comprised of two sublayers. The deeper *stratum reticulare*, a loose fibrous connective tissue, separates the dermis from the subcutaneous tissue, while the closer-to-surface *stratum papillare*, consisting of dense fibrous connective tissue, forms a wavy boundary with the epidermis. Differentiating between these sublayers is difficult due to the lack of a distinct boundary. Collagen fibers provide tensile strength, while elastic fibers contribute to elasticity. The dermis contains a dense vascular network that nourishes the epidermis and regulates heat. In addition, as blood vessels are located in the dermis, it is paramount to deliver the active ingredient there to achieve systemic effects [21,22].

Hypodermis

The hypodermis consists of a dense network of blood vessels and nerves, along with fat cells, located below the dermis. It plays a role in nourishing the skin, providing mechanical protection to organs, serving as an insulator for heat regulation, and acting as an energy reservoir [23].

2.2. Drug delivery through the skin

In the case of liquid and semisolid dermal preparations, the release of the active ingredient is essential. The diffusion of the active ingredient is influenced by several factors including the composition of the formula, interactions among the components, the viscosity or rheological properties of the formulation, and whether the active ingredient is in a dissolved or dispersed form within the dosage form [24]. The therapy must ensure that the released active ingredient can penetrate and permeate the deeper layers of the skin. Pathways for drug absorption through the skin involve different routes. Drugs pass through the *stratum corneum*, in a process known as transepidermal transport, which can be divided into intracellular and intercellular pathways. In the intracellular route, compounds are transported through the cells of the *stratum corneum*, while in the intercellular route, molecules traverse the lipid matrix between corneocytes [25]. Additionally, drugs can be transported via the transappendageal route, which involves passage through sweat ducts and hair follicles. The route of drug permeation is influenced by their physicochemical properties, although it should be noted that most drugs go through the combination of these routes. This understanding of drug transport mechanisms is crucial for delivering drugs topically or transdermally, as they need to overcome the *stratum corneum*, the primary skin barrier, reaching the viable epidermis or entering the systemic circulation in the dermis. The distribution between the *stratum corneum* and the formulation is crucial and depends on the properties of the active ingredient [26].

The cells of the *stratum corneum* mainly contain keratin, which is a nonpolar substance. Therefore, the distribution becomes favorable for the active ingredient only if it dissolves well in an apolar environment. When delivering active ingredients, it is essential to consider that only those with both lipid solubility and a certain water solubility can reach the highly water-containing cells of the epidermis and the deeper layers of the skin [27].

Substances exhibiting a well-balanced partition coefficient, specifically those having a logarithmic octanol-water partition coefficient (logP) ranging from 1 to 3, are linked with optimal skin permeability [28].

Furthermore, achieving the right therapeutic concentration poses a challenge, especially for high molecular weight molecules, which struggle to penetrate or traverse the skin [29]. The "500 Dalton Rule" [30] suggests that drugs with a molecular weight below 500 Daltons can passively penetrate the *stratum corneum* and be delivered through the skin.

Only a small number of active ingredients can effectively penetrate the skin on their own due to requirements of appropriate solubility and permeability. To attain a systemic impact, it is essential to develop a formulation that can penetrate this protective barrier by temporarily disrupting it and then rapidly restoring its original structure [31].

2.3. Characterization of dermal foams

Difficulties in the application of traditional dosage forms (e.g., greasy skin sensation, rubbing) can adversely impact patients' quality of life, leading to dissatisfaction with the treatment, especially in patients diagnosed with chronic skin diseases [32,33].

Foams are created by dispersing a gaseous substance in a solid or liquid dispersion medium. Dermal foams present a promising pharmaceutical dosage form for dermal drug delivery and the cosmetic industry. Foams may contain one or more active ingredients that exert their effects on or through the skin. Foam formulations can be applied more easily and uniformly on the treated skin surface, providing better coverage for affected areas [34]. Moreover, foams can reach hard-to-reach areas, including skin folds, and hirsute regions, making them particularly advantageous for treating inflamed, swollen, abraded, infected, and sensitive skin. They minimize the need for skin contact and rubbing due to their excellent spreading capability [35]. They are easy and convenient to apply, allow precise dosage, are non-dripping, and do not leave traces on clothes. In terms of shelf life, they are stored in sealed containers, minimizing the risk of contamination. Dermal foams are utilized to target the skin or particular mucosal surfaces, either exerting localized effects or facilitating absorption through the skin. The transdermal delivery route enables achieving a local effect with a smaller drug quantity, circumventing gastrointestinal tract issues and enterohepatic circulation, thereby reducing the likelihood of systemic side effects. Despite these advantages (Figure 3), the number of available foam preparations in the market is relatively low compared to traditional formulations like creams and gels.

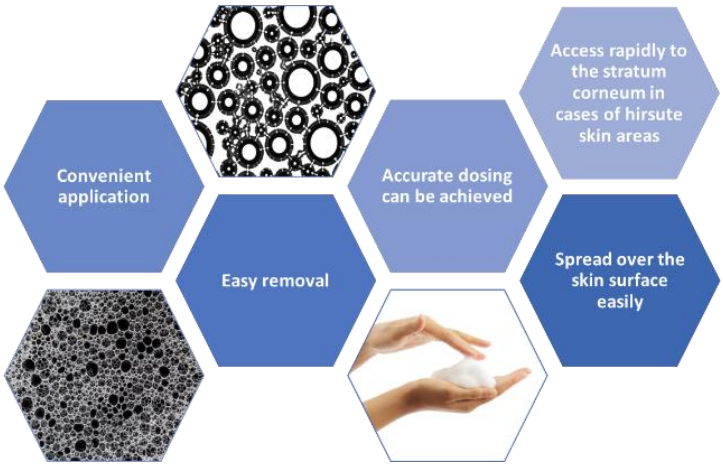

Figure 3. Advantages of dermal foams.

The thermodynamic instability of foams presents a significant limitation, making them prone to decay. The kinetic stability and quality of foams can be influenced by the composition, encompassing both excipients and active ingredients [36].

The choice of appropriate excipients, crucial for foam stability, needs consideration before formulation. Typically, they consist of surface-active agents, solvents, foam stabilizers, preservatives, and may incorporate penetration enhancers. Incorporating surfactants and foam-stabilizing excipients, as indicated by studies [37,38], can enhance the lifetime and stability of the foam. When selecting a surfactant, several factors must be considered. While ionic surfactants are effective, their known skin-irritating effects suggest the use of non-ionic surfactants, especially when treating inflamed areas [39,40].

In addition to surfactants, foam stabilizers such as polymers are also used in foam formation, which stabilize the foam after its generation, by increasing the viscosity of the liquid phase [41]. Examples of polymers used in foams include naturally occurring ones like agar-agar, xanthan gum, hyaluronic acid, and tragacanth gum; acidic polymers like palmitic acid, stearic acid; and semi-synthetic polymers such as cellulose ethers [42].

During the formulation process, it is important to ensure the complete dissolution of the active ingredient in the system. Once applied, the volatile components of the foam quickly evaporate from the foam on the skin. Consequently, a supersaturated liquid layer [43,44] of the active ingredient forms on the epidermis, from which rapid permeation begins due to the significant driving force within the system (Figure 4). If this process occurs rapidly, there is no chance for the active ingredient to crystallize, as swift permeation causes a reduction in its concentration in the foam layer.

Additionally, the interconnected network of foam facilitates effective medication transport across the layers of the epidermis, enhancing absorption and bioavailability [45].

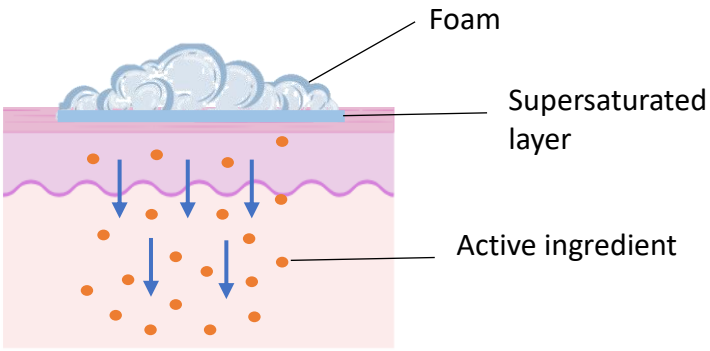

Figure 4. The phenomenon of supersaturation in the case of foams.

Foams have unique physical properties and structure, distinguishing them from traditional drug delivery systems. Investigating their physical properties and structure is vital to understanding why they are advantageous for transdermal drug delivery. Foams are characterized by a porous structure formed during foam formation [46]. These pores are voids within the foam structure contributing to its dense, sponge-like appearance. These pores are essential for drug delivery as they allow the incorporation of drug active ingredients into the foam structure, enabling sustained release following application to the skin [47–49]. Additionally, this porous nature increases the surface area available for drug absorption, allowing for faster (immediate) drug diffusion [47].

Depending on the physiological condition of the skin, a wide range of active ingredients can be used in formulating dermal foams, such as antibacterial, antifungal, and wound-healing agents. Foams containing corticosteroids or anti-inflammatory agents can reduce inflammation, itching, and irritation associated with these conditions. Additionally, foams may promote wound healing by creating a moist environment and delivering therapeutic agents. The specific indication for dermal foams depends on the underlying condition being treated and the formulation of the foam.

2.4. QbD concept as a quality improvement tool

Achieving stability and ensuring the correct quality stand out as the primary and foremost requirements during the development of pharmaceuticals [50,51]. In contemporary pharmaceutical industry practices, the Quality by Design (QbD) approach during the design stage has proven to be beneficial [52].

Initially, it documents critical quality attributes and critical process parameters influencing the quality of the product. In essence, QbD represents a science-based, risk-based approach to drug development, commencing with predetermined goals. Integrating the QbD approach into the research phase, particularly in designing the active substance and pharmaceutical form, allows for more effective assimilation of research findings into the development process. The initial step of the QbD approach involves defining the Quality Target Product Profile (QTTP) as the development goal. Subsequently, critical quality attributes (CQA), critical material attributes (CMAs), and critical process parameters (CPPs) are identified, and potential factors affecting product quality are selected through risk assessment. The QbD concept relies on risk assessment, which helps identify critical parameters influencing critical quality attributes [53–55].

3. EXPERIMENTAL AIMS

This Ph.D. work aimed to design stable foam formulations and to determine the proper methods to investigate their physicochemical, biopharmaceutical and biocompatibility properties. Another goal was to examine the permeation of foams through the skin and gain a deeper understanding of the mechanism of their action.

The research was carried out in accordance with the following steps:

I. In the initial part of my Ph.D. work, stable foam compositions were formulated based on the QbD approach, and appropriate methods were developed to analyze their physicochemical, structural characteristics, and stability. In addition, the effect of different polymers on foam stability as well as on foam structure were investigated.

II. During the second part of my work, emphasis was placed on the formulation of a foam drug delivery system with diclofenac sodium and investigation of its biopharmaceutical properties. Furthermore, a comparative assessment of the research results was carried out with the foam bulk liquid and a conventional hydrogel, which falls within the category of traditional carrier systems.

III. In the subsequent part of my research, the biocompatibility of foam formulations was examined with *in vitro* cytotoxicity tests and an *in ovo* model.

The cytotoxicity of the components was assessed using human adipose-derived mesenchymal stem cells (AD-MSCs) and keratinocytes. Additionally, the formulations were evaluated for their effects on wound healing using two types of wound healing models involving AD-MSCs.

The *in ovo* model was employed to assess the irritation potential of the formulations.

4. MATERIALS AND METHODS

4.1. Materials

Polyoxyl castor oil was purchased from BASF SE Chemtrade GmbH (Ludwigshafen, Germany). Caprylocaproyl Polyoxyl-8 glycerides, obtained from Gattefossé (Saint-Priest Cedex, France), were provided by Azelis Hungary Ltd. (Budapest, Hungary). Xanthan gum (XANT) from CP Kelco A Huber Company (Atlanta, GA, USA) and the blend of Phenoxyethanol and Caprylyl Glycol were both provided as gifts by Biesterfeld Speciális Kemikáliák Magyarország Ltd. (Budapest, Hungary). Hydroxyethylcellulose (HEC) was acquired from Molar Chemicals Ltd. (Budapest, Hungary), and purified, deionized water from the Milli-Q system by Millipore (Milford, MA, USA). Additionally, HyaCare50 (HA_{LMW}), HyaCare Filler CL (HA_{CL}), and HyaCare Tremella (HA_{HMW}) were product samples from Finecon s.r.o. (Bratislava, Slovakia). Diclofenac sodium (DS) and fluorescein sodium were obtained from Sigma-Aldrich (Budapest, Hungary), Isopropanol (IPA) from Avantor (Radnor, PA, USA), Hydroxypropyl methylcellulose (HPMC) from Colorcon (Budapest, Hungary), Polyethylene glycol 200 (PEG 200) from Merck KGaA (Darmstadt, Germany), and the cellulose acetate filter from Macherey-Nagel GmbH & Co. KG (Düren, Germany). Additionally, 70% Sodium laureth sulfate (SLES) and Niacinamide (NIAC) was provided by Biesterfeld Speciális Kemikáliák Magyarország Ltd. (Budapest, Hungary), and Dexpanthenol (DEXP) by DSM Nutritional Products Ltd. (Basel, Switzerland). For the chorioallantoic membrane assay, Sodium dodecyl sulfate (SDS) was purchased from Sigma-Aldrich (Steinheim, Germany).

4.2. Methods of experiment part 1 – Formulation and characterization of the physicochemical properties of foams

4.2.1. The Quality by Design approach

The initial stage in QbD-based development (Figure 5) involves outlining the Target Product Profile (TPP), and then QTPP summarizes its quality characteristics, encompassing factors such as efficiency, delivery route, dosage form, packaging, appearance, and therapeutic indication. Throughout the development process, the QTPP parameters forms the basis [56–58].

To ensure the desired quality of the pharmaceutical product during both development and production, the second stage is to define the CQAs. The third crucial step involves identifying material (CMA) and process parameters (CPP) that could impact the CQAs of the foams. The determination of these parameters helps to find the relationship between material properties and process parameters that are related to critical product quality parameters [53,59].

Assessment identifies critical parameters affecting quality attributes, using various quality tools [60]. The Ishikawa diagram helps identify potential root causes affecting product quality, while Pareto analysis categorizes risks based on impact: Category A for high-risk, Category B for medium-risk, and Category C for low-risk parameters. Risk estimation matrix (REM) establishes the level of risk parameters and the relationship between quality attributes, CPPs, and CMAs.

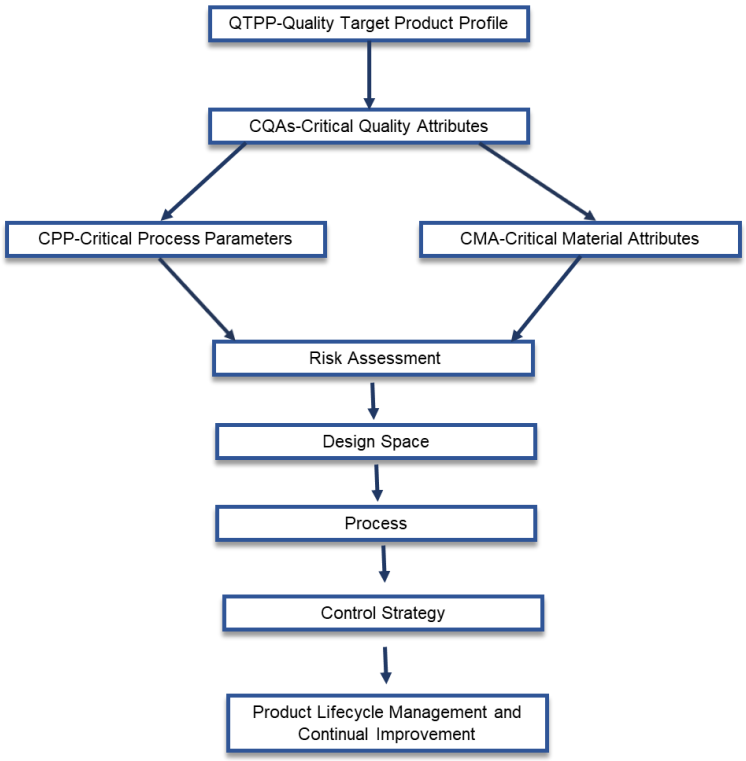

Figure 5. Process of the QbD approach in the development of pharmaceutical formulations.

4.2.2. Preparation of foams

Firstly, different foam compositions were prepared, as outlined in Table 1. The lifetime of the foam can be extended by increasing the viscosity of the liquid phase among the air bubbles. One possible solution is the use of polymers in the composition. Therefore, the formulated foams contained different types of polymers in different concentrations (Phase B) [61]. The foaming agents were mainly surfactants (Phase A). All formulations contained the same amount of surfactants. Phase C contains the microbiological preservative.

The initial step in foam preparation involved preparing Phase B, where polymer swelling lasted for 2 hours in purified water. Subsequently, Phase C was added to Phase A. The final step was the addition of Phase B to the mixture of Phases A and C. Following sample preparation, the liquids were stored in well-sealed jars until the start of the examination. Before each analysis, 30 grams of bulk liquid underwent stirring with an IKA stirrer for 5 minutes at 2000 rpm, as determined by preformulation studies.

Table 1. Composition of different formulations ('+' indicates that the formulation contains the excipient, '–' indicates that the formulation does not contain the excipient).

	F-0polymer	**F-XANT_0.1**	**F-XANT_0.2**	**F-HEC_0.2**	**F-HEC_0.4**	**F-HA_{LMW}–0.1**	**F-HA_{LMW}–0.2**	**F-HA_{HMW}–0.1**	**F-HA_{HMW}–0.2**	**F-HA_{CL}–0.1**	**F-HA_{CL}–0.2**
Phase A											
Caprylocaproyl Polyoxyl-8 glycerides /surfactant/	+	+	+	+	+	+	+	+	+	+	+
Polyoxyl castor oil /surfactant/	+	+	+	+	+	+	+	+	+	+	+
Phase B											
Xanthan gum /polymer/	–	0.1%	0.2%	–	–	–	–	–	–	–	–
HEC /polymer/	–	–	–	0.2%	0.4%	–	–	–	–	–	–
HA_{LMW} /polymer/	–	–	–	–	–	0.1%	0.2%	–	–	–	–
HA_{HMW} /polymer/	–	–	–	–	–	–	–	0.1%	0.2%	–	–
HA_{CL} /polymer/	–	–	–	–	–	–	–	–	–	0.1%	0.2%
Purified water /solvent/	+	+	+	+	+	+	+	+	+	+	+
Phase C											
Blend of Phenoxyethanol and Caprylyl Glycol /preservative/	+	+	+	+	+	+	+	+	+	+	+

4.2.3. Characterization of the critical parameters of the foams

4.2.3.1. Macroscopic characterization of foams

The macroscopic properties of the foams were determined by using the cylinder method [42]. After stirring the bulk liquid for 5 minutes, the foam was filled into a glass measuring cylinder and the initial and the aged volumes of the foam after 30 minutes were recorded. The following parameters can be determined by macroscopic tests:

- relative foam density (RFD);
- foam expansion (FE, %);
- foam volume stability (FVS, %).

These parameters were calculated using the formula below [62,63].

$$RFD = \frac{m(foam)}{m(water)} \quad (1)$$

The European Pharmacopoeia describes RFD in the Monograph "Medicated foams". It equals the weight of the test sample of foam compared to the weight of the same volume of water.

$$FE(\%) = \frac{V(foam) - V(formulation)}{V(formulation)} \cdot 100\% \quad (2)$$

where V(formulation) is the volume of the formulation [mL] required to produce V(foam) [mL] [42].

$$FVS(\%) = \frac{V(foam,30\ min)}{V(foam)} \cdot 100\% \quad (3)$$

where V(foam,30min) is the foam volume after 30 min [mL] [64,65].

4.2.3.2. Microscopic characterization of foam kinetics and bubble morphology

The microscopic measurements were performed with Leica DM6 B Fully Automated Upright Microscope System (Leica Biosystems GmbH, Wetzlar, Germany) Through microscopic examination, the structure and bubble size of the foams can be determined, providing information about the foam kinetics.

The structure of the foam from the microscopic images was analyzed after a predetermined time (0, 10, 20, 30 minutes). The results of the bubble size analysis can be found in Annex I. Foam uniformity can also be determined with this method as the homogeneity of air bubbles.

The size, roundness, and the aspect ratio of incorporated air bubbles as well as bubble amount in a predetermined area are the parameters of interest in foam characterization [66].

4.2.3.3. Rheological investigations

The rheological properties of the foams were investigated using an Anton Paar Physica MCR302 Rheometer (Anton Paar, Graz, Austria) employing a parallel plate type measuring device (diameter: 50 mm, gap height: 2 mm). Flow curves of the bulk liquids were recorded with a cone-plate type measuring device (diameter: 25 mm, gap height: 0.1 mm), over the shear rate range from 0.1 to 100 1/s and from 100 to 0.1 1/s at 25°C. The analysis of the foams involved amplitude sweeps, wherein the strain value increased from 0.1% to 100%, with an angular frequency of 10 rad/s [67].

4.2.3.4. Assessment of spreadability

The spreadability of foams was assessed using a TA.XT plus Texture Analyzer (Stable Micro Systems Ltd., UK) equipped with a TTC Spreadability Rig, involving a male 90° cone probe and a precisely matched female perspex cone-shaped product holder [68]. The male cone immersed into the sample in the female cone until a 1 mm gap was reached.

The force required for the product to flow outward at 45° between the male and female cone surfaces determined the spreadability, with the maximum force (firmness) recorded in the force-distance curve. This method models the application of semisolid dermal dosage forms.

4.3. Methods of experiment part 2 - Biopharmaceutical analysis of a diclofenac sodium-containing foam drug delivery system compared to foam bulk liquid and hydrogel

4.3.1. Preparation of the formulations

In this part, properties of the foam formula were compared to the foam bulk liquid (which is a polymer solution) and to a conventional hydrogel. Regarding the formulations, both the foam and hydrogel shared identical concentrations of non-ionic emulsifiers and preservatives. The variations were observed in solvent types, polymer types, and concentrations. In our preliminary research, xanthan gum-based foam (F-XANT_0.2) demonstrated superior stability and physicochemical properties [69], while HPMC-containing hydrogels exhibited optimal results [70].

In the hydrogel preparation, HPMC underwent a 2-hour hydration in purified water, and a mixture of polyethylene glycol 200 and isopropanol was simultaneously prepared.

After polymer swelling, a predetermined amount of diclofenac sodium was dissolved in the solvent mixture and gradually added to the hydrated polymer. Mechanical stirring homogenized the formulation, which was then stored in a sealed container.

For foam preparation, a polymer solution was prepared with a 2-hour swelling process in purified water. The preservative solution was mixed with emulsifiers, and the swelled polymer was incorporated into this mixture. After homogenization with a mechanical stirrer, the liquid was stored until examination, mirroring the bulk liquid preparation process. The foams used in the experiments were generated using a propellant-free foam pump.

Detailed compositions are provided in Table 2.

Table 2. The composition of foam, hydrogel, and bulk liquid ('–' indicates that the formulation does not contain the excipient).

	Hydrogel	**Foam/Foam bulk liquid**
DS (%) /active ingredient/	1	1
PEG 200 (%) /solvent/	3.5	–
IPA (%) /solvent/	15	–
HPMC (%) /polymer/	3	–
Xanthan gum (%) /polymer/	–	0.2
Caprylocaproyl Polyoxyl-8 glycerides (%) /surfactant/	2	2
Polyoxyl castor oil (%) /surfactant/	2	2
Blend of Phenoxyethanol and Caprylyl Glycol (%) /preservative/	0.5	0.5
Purified water (%) /solvent/	up to 100	up to 100

4.3.2. Preformulation test of foam formula: Investigation of *ex vivo* permeation through the skin using fluorescent microscope

To model whether the formulation can permeate the *stratum corneum*, fluorescent microscopy was employed. The investigation included assessing the permeation capacity of the blank foam (without active ingredient).

Experiments on *ex vivo* skin permeation were conducted using excised human skin obtained from a Caucasian female patient who had undergone routine plastic surgery at the Department of Dermatology and Allergology, University of Szeged (Ethical Permission: BMEÜ/2339-3/2022/EKU). After plastic surgery, the skin underwent a gentle cleansing process and was stored at −20 °C for a maximum of 6 months before use.

Fluorescein sodium water-soluble dye was used to visualize the permeation of the foam system. At room temperature, full-thickness subcutaneous fat-free human abdominal skin was used in the experiment. The skin samples were defrosted and kept on filter papers soaked in phosphate-buffered solution to preserve their hydration. To ensure the permeation of formulations, 0.2 g of each formulation was applied to the skin surface, and observation times of 10 and 30 minutes were employed. Following the treatment, any excess preparation remaining on the skin was carefully wiped off. Subsequently, a section of the treated skin was frozen and sliced using a Leica CM1950 Cryostat (Leica Biosystems GmbH, Wetzlar, Germany). Cross-sections with a thickness of 10 μm were placed on slides and examined using a light microscope (LEICA DM6 B, Leica Microsystems GmbH, Wetzlar, Germany) at room temperature. A red fluorescence filter (580–660 nm) was utilized to prevent interference from skin autofluorescence during analysis. The examination was conducted at a magnification of 200× [71].

Images of the untreated skin were captured as a negative control, while skin pretreated with a solution containing sodium laureth sulfate (SLES) was used as a positive control. Images of the treatments were taken and visually compared to the control groups. The ImageJ software was employed to assess the color intensity of the images, representing the distribution of color intensity within each image. The increase in intensity is indicated as relative intensity (RI), signifying how many times the intensity increases compared to the negative control (untreated skin) [72].

4.3.3. Rheological properties of the foam formula compared to bulk liquid and hydrogel

The viscosity of the bulk liquid, foam, and hydrogel was assessed using an Anton Paar Physica MCR302 Rheometer (Anton Paar, Graz, Austria) at 25°C. A cone-plate type measuring device with a 50 mm diameter and a 0.045 mm gap height in the middle of the cone was employed. Utilizing the RheoCompass software, the instrument calculated the viscosity of the preparations at a shear rate of 50 1/s through interpolation. Three measurements were simultaneously conducted, and flow curves for the examined formulations were plotted over a shear rate range from 0.1 to 100 1/s.

4.3.4. Biopharmaceutical investigation of the foam formula compared to bulk liquid and hydrogel

4.3.4.1. *In vitro* drug release and permeation tests (IVRT and IVPT) using Franz Diffusion Cell System

The drug release through the synthetic membrane from the bulk liquid, foam, and hydrogel, as well as its permeation through human heat-separated epidermis, were modeled using the vertical Franz Diffusion Cell (Hanson Microette TM Topical & Trans-dermal Diffusion Cell System, Hanson Research Corporation, Chatsworth, CA USA). The excised human skin, just like in the case of the fluorescent microscope method, was obtained through plastic surgery.

For *in vitro* release tests, as a donor phase, 0.3 g of the sample (in the case of the hydrogel and bulk liquid) was applied onto a synthetic membrane filter. In the case of foam (due to its large volume), 0.085 g was placed onto the membrane (Porafil cellulose acetate membrane with a pore diameter of 0.45 μm, Macherey-Nagel GmbH & Co. KG, Düren, Germany). In contrast, for the *in vitro* permeation test, a heat-separated human epidermis [73,74] was employed as the membrane. Both the drug release and permeation tests lasted 6 hours and the sampling dates were 10, 20, 30 mins; 1; 2; 4; and 6 hours. The amount of the active pharmaceutical ingredient released from the formulation and transported through the skin was determined by using ultra-high performance liquid chromatography (UHPLC) (Shimadzu Nexera X2 ultra high-performance liquid chromatography system).

The UHPLC was equipped with a Phenomenex Kinetex XB-C18 (50×2.1 mm, 2.6 μm) column, which was used as a stationary phase. Separation was achieved through isocratic elution employing a 36:64 mixture of 0.136 g/L KH_2PO_4 solution and methanol as the eluent.

The separation procedure occurred at 40°C with a flow rate of 0.5 mL/min, spanning a 3-minute analysis time. The retention time for DS was noted at 1.5 minutes. A sample volume of 3 µL was injected for analysis. Detection was carried out using a di-ode array UV-VIS detector at a wavelength of 247 nm [75].

The calculation of *in vitro* permeation was based on the cumulative amount of diclofenac sodium that permeated through the epidermis, considering the diffusion area. These findings were graphed over time, and the steady-state flux (J) was calculated from the slope of the permeation curve, quantified in terms of µg/cm^2/h. For this analysis, the incubation period ranged from 1 to 6 hours, during which the flux data for diclofenac sodium was determined.

4.3.4.2. Investigation of *ex vivo* drug permeation using Raman Spectroscopy

The confocal Raman spectroscopy can be employed to investigate topical formulations, for both determining permeation and permeation depth. In my research, Raman microscopy was utilized to capture images depicting the spatial distribution of diclofenac sodium within *ex vivo* human skin.

The skin preparation and sectioning followed the same procedure as for fluorescence microscopy but with a 3-hour incubation time. Subsequently, approximately 15-micrometer thick cross-sectional skin samples were placed on aluminium-coated slides. Raman spectroscopic assessments were performed using a Thermo Fisher DXR Dispersive Raman Spectrometer (Thermo Fisher Scientific Inc., Waltham, MA, USA) equipped with a CCD camera and a diode laser emitting at 780 nm with a peak power of 24 mW. This wavelength is optimal for studying biological specimens, minimizing fluorescence interference. A microscopic lens with 50× magnification and a pinhole aperture with a 25 µm diameter were used for the measurements [76]. Mapping was conducted over a 100 × 500 µm area with vertical and horizontal step sizes of 50 µm. The untreated skin map served as a control throughout the measurement.

The spectra of diclofenac sodium in the bulk liquid and hydrogel were employed as a basis for comparing treated and untreated skin samples. To capture the spectra of diclofenac sodium, a 780 nm laser source was utilized. A total of 24 scans were recorded for each spectrum with an exposure time of 6 seconds. The Raman microscope featured 50× optical magnification with a 25 µm slit aperture.

Data collection and analysis were carried out using the Dispersive Raman software package OMNICTM 8.2 (ThermoFisher Scientific Inc., Waltham, MA, USA) [77].

4.3.5. Statistical analysis

The results of the *in vitro* drug release tests underwent statistical analysis utilizing the two-way ANOVA (analysis of variance) test with Bonferroni's multiple comparison method, using Prism 5.0 software for Windows 10 (GraphPad Software Inc., La Jolla, CA, USA). The presented data comprise the mean values obtained from six experiments, accompanied by standard deviations. Significant distinctions from the foam formulation were noted at the significance levels of $*p \leq 0.05$ and $***p \leq 0.001$.

4.4. Methods of experiment part 3 - Assessment of biocompatibility and wound healing potential of foam components and formulations

4.4.1. Composition of the investigated formulations

For cytotoxicity tests, the components were individually dissolved in Dulbecco's Modified Eagle's Medium with high D-Glucose concentration (DMEM-HG) medium in a 100-fold dilution compared to the applied concentrations in the formulations.

The aim of the wound scratch and impedance-based assay was to investigate the effects of the polymers and active ingredients.

On the other hand, the *in ovo* assay targeted the examination of irritation of the promising materials. In these studies, formulations including F-0polymer, F-XANT_0.2, and F-HA_{HMW}_0.2, among the previously blank compositions, as well as formulations containing active ingredients, were also tested (Table 3).

Table 3. The composition of active ingredient-containing foam formulations ('–' indicates that the formulation does not contain the excipient).

	F-XANT_0.2-DS_1	**F-XANT_0.2-HA_{HMW}_0.2-DEXP_1-NIAC_1**	**F-HA_{HMW}_0.2-NIAC_5**	**F-HA_{HMW}_0.2-DEXP_5**	**F-HA_{HMW}_0.2-DS_1**
DS (%) /active ingredient/	1	–	–	–	1
DEXP (%) /active ingredient/	–	1	–	5	–
NIAC (%) /active ingredient/	–	1	5	–	–
HA_{HMW} (%) /polymer/	–	0.2	0.2	0.2	0.2
Xanthan gum (%) /polymer/	0.2	0.2	–	–	–
Caprylocaproyl Polyoxyl-8 glycerides (%) /surfactant/	2	2	2	2	2
Polyoxyl castor oil (%) /surfactant/	2	2	2	2	2
Blend of Phenoxyethanol and Caprylyl Glycol (%) /preservative/	0.5	0.5	0.5	0.5	0.5
Purified water (%) /solvent/	up to 100	up to 100	up to 100	up to 100	up to 100

During the experiments, the foam bulk liquids were examined, with pure DMEM-HG medium serving as the control.

4.4.2. Cell culturing

Abdominal human keratinocytes and AD-MSCs were extracted using enzymatic digestion and then cultured in Dulbecco's Modified Eagle's Medium with 4.5 g/L D-Glucose (DMEM-HG) (REF: LM-D1111/500, Biosera, Nuaille, France), supplemented with 10% fetal bovine serum (REF: FB-1090/500, Biosera, Nuaille, France), 1% L-Glutamine (REF: XC-T1715/100, Biosera, Nuaille, France), and 1% Antibiotic-antimycotic (AB/AM) (REF: XC-A4110/100, Biosera, Nuaille, France). The cells were then incubated at 37°C with 5% CO_2. At passage 5, the expression of stem cell markers and differentiation ability were confirmed using flow cytometry and standard tri-lineage differentiation assays with StemPro™ Differentiation Kits (Gibco) for adipogenesis, osteogenesis, and chondrogenesis [78,79].

4.4.3. Citotoxicity assay

The impact of the utilized components on cell toxicity was assessed through MTT (3-(4,5-dimethylthiazol-2-yl)-2,5-diphenyl-2H-tetrazolium bromide) assays following the manufacturer's guidelines. AD-MSCs and keratinocytes were distributed into 96-well plates, with each well initially containing 5×10^3 cells. These cells were then exposed to a solution containing the components, in the same concentrations as used in the foam formulations, for 24 hours in triplicate. Absorbance was measured using the Synergy HTX multi-plate reader (Agilent/BioTek, Santa Clara, CA, USA) at 550 nm, with a reference wavelength set at 650 nm [80].

4.4.4. Investigation of the effect of foam preparations on an *in vitro* wound healing model

4.4.4.1. Wound scratch assay with AD-MSCs

The effects of dermal agents on the wound-healing potential of AD-MSCs were examined under *in vitro* conditions. For this, 5×10^4 cells/well were seeded into 24-well plates. Uniform wounds were made on the cell layer using the AutoScratch wound-making device (Agilent/BioTek, Santa Clara, CA, USA). After scratching, dermal agents – diluted in media – were added to the wells. Wound healing was examined with an Olympus IX83 microscope in the microscope's Okolab incubation system (37°C, 5% CO_2), at 10× magnification for 48 hours, with 1-hour intervals. To evaluate the wound-healing test, the area of the wounds between first and last time points was manually measured and compared to the untreated control, which were graphically represented and analyzed [81].

4.4.4.2. Impedance-based measurement of wound healing

The effects of dermal agents on the wound-healing potential of AD-MSCs were examined under *in vitro* conditions. For this, 1.5×10^4 cells per well were seeded into E-Plate WOUND 96 plates (REF: 300600970, Agilent/BioTek, Santa Clara, CA, USA). Uniform wounds were prepared using the AccuWound 96 wound-making device (Agilent/BioTek, Santa Clara, CA, USA). Wound healing was assessed using the xCELLigence Real-Time Cell Analyzer (Agilent/BioTek, Santa Clara, CA, USA), which measured impedance via golden electrodes. Cellular impedance was monitored for 48 hours to evaluate wound healing, and the resulting data were visually represented and analyzed. Impedance-based cell monitoring operates on the fundamental principle that adherent cells are cultivated on flat gold-film electrodes positioned at the base of a cell culture dish.

The presence of dielectric cell bodies augments electrochemical impedance, as current must navigate around or through the cells. Impedance measurements are responsive to alterations in cell coverage on the electrode and modifications in the morphology of the adherent cells [82–84].

4.4.5. Irritation evaluation by the HET-CAM assay

To evaluate biocompatibility, an *in vivo* assessment was conducted using the *in ovo* chorioallantoic membrane assay (CAM). In brief, fertilized chicken (*Gallus gallus domesticus*) eggs were kept in a controlled, humidified atmosphere at a temperature of 37°C. Subsequently, 4-5 mL of egg white was extracted, and openings were made in the upper shells. The embryos were then maintained until the experimental procedure, with all tests conducted in triplicate [85–87].

The potential toxicity on mucosal or skin tissues was investigated using the *in vivo* Hen's Egg Chorioallantoic Membrane Test (HET-CAM) carried out according the Interagency Coordinating Committee on the Validation of Alternative Methods (ICCVAM) recommendations and adapted to the condition of the laboratory. The protocol evaluates the potential irritant effect on the vascular plexus of the chorioallantoic membrane, assessing the *in vivo* biocompatibility with multiple applications in ophthalmology, cosmetology and dermatology [88–90].

The sample volume of 300 µL were applied on the CAM surface on the 10^{th} day of incubation, followed by a 5-minute continuous observation of the modifications produced at the CAM level by means of stereomicroscopy (ZEISS SteREO Discovery.V8, Göttingen, Germany).

Distilled water served as the negative control, whereas SDS at a concentration of 0.5% acted as the positive control. Significant images were registered before the application (t_0) and after 5 minutes (300 seconds, t_5) of contact with the samples. All images were processed using Axiocam 105 color, AxioVision SE64. Rel. 4.9.1 Software, (ZEISS Göttingen, Germany), ImageJ (ImageJ Version 1.50e, [91]) and GIMP software (GIMP v 2.8, [92]).

The evaluation of potential irritative effects on vascularized CAM tissues involved noting the occurrence time, in seconds, of parameters such as hemorrhage (H), vascular lysis (L), and coagulation (C). An irritation score (IS) was then calculated using a specific equation:

$$IS = 5x\left[\frac{301 - \text{Sec H}}{300}\right] + 7x\left[\frac{301 - \text{Sec L}}{300}\right] + 9x\left[\frac{301 - \text{Sec C}}{300}\right] \quad (4)$$

where: hemorrhage (Sec H) = start of observation (in seconds) of bleeding reactions on the membrane, lysis time (Sec L) = start of observation (in seconds) of lysis of the vessel on the membrane, coagulation time (Sec L) = start of observation (in seconds) of the formation of coagulation on the membrane.

Means values are obtained. The IS values range on a scale between 0 and 21, according to the irritation scale recommended by Luepke [93], the irritation scores can be classified as following: 0–0.9 – non-irritant, 1–4.9 weak irritant, 5–8.9 moderate irritant, 9–21 strong irritant.

4.4.6. Statistical analysis

The results of the cytotoxicity assay and impedance-based measurement of wound healing underwent statistical evaluation using the one-way ANOVA analysis of variance test (Dunnett's Multiple Comparison Test) with Prism 5.0 for Windows 10 software (GraphPad Software Inc., La Jolla, CA, USA). The data represent the mean values derived from four (in the case of cytotoxicity test) and three (in the case of impedance-based wound healing measurement) experiments, along with the standard error of the means, and significant differences from the control were observed at the levels of ***$p \leq 0.001$ vs. Control, **$p \leq 0.01$ vs. Control, *$p \leq 0.05$ vs. Control.

5. RESULTS AND DISCUSSION

5.1. Experiment part 1 - Formulation and characterization of the physicochemical properties of foams

5.1.1. Definition of QTPP, CQAs, CMAs, and CPPs for foam systems

The experimental aim outlined the QTPP, which included the skin as the route of administration, foam as the dosage form, topical application as the site of action, stability of the formula, and a transparent or white, homogeneous appearance for the liquid systems, and a white appearance for the foam systems.

The characteristics of excipients influence the properties of both the liquid system and the resulting foam, with polymer content playing a role in foam stability.

The liquid systems were assessed for physical properties like viscosity, pH, and surface tension, while the foam systems are evaluated for attributes such as bubble size, stability, expansion, density, rheological properties, and spreadability. The criteria for the specified QTPPs and CQAs were determined based on existing literature. Following this, the CMAs and CPPs for the foam formulae, containing different polymers, were identified through risk assessment.

Risk assessment involves evaluating the potential risks associated with foams. An Ishikawa diagram illustrates the impact of key attributes and parameters on foam quality, revealing the causes and sub-causes influencing foam system characteristics (Figure 6).

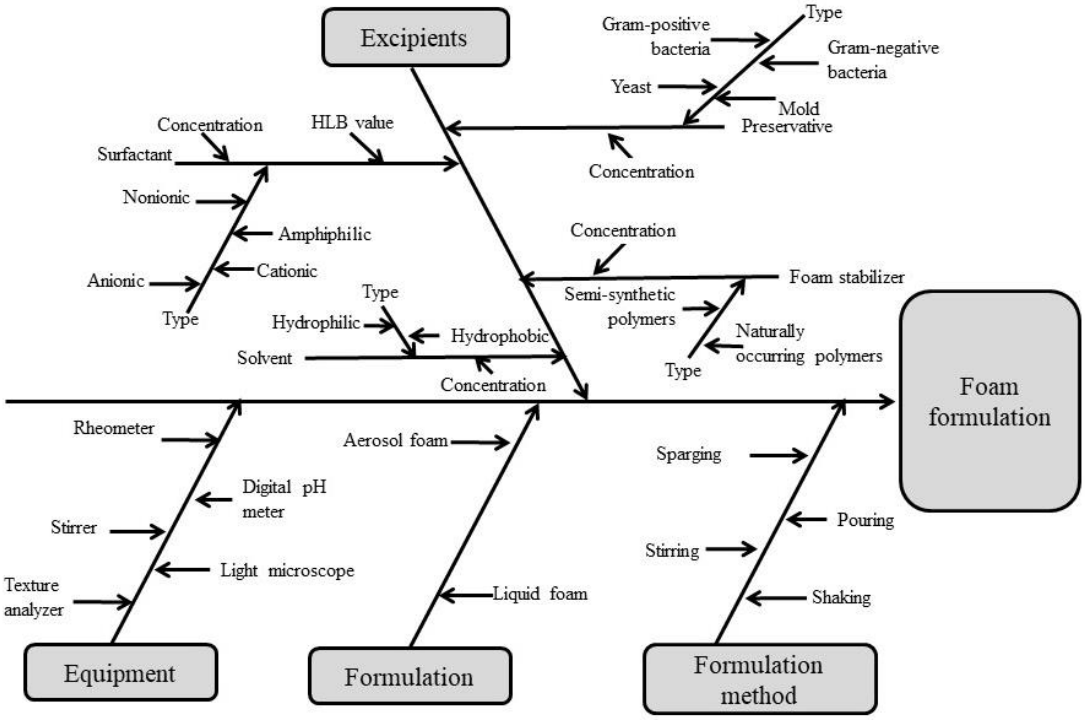

Figure 6. Ishikawa diagram of material attributes and process parameters of foams.

Subsequently, REM was employed to evaluate the relationship between CQAs and QTPPs. A three-step scale was utilized to classify the connection between the parameters of CQAs and QTPPs for the foam formulations: Low (indicating low-risk parameters), Medium (signifying medium-risk parameters), and High (representing high-risk parameters). Using the REM outcomes, Pareto charts (Figure 7) was generated to illustrate the severity scores of the CQAs.

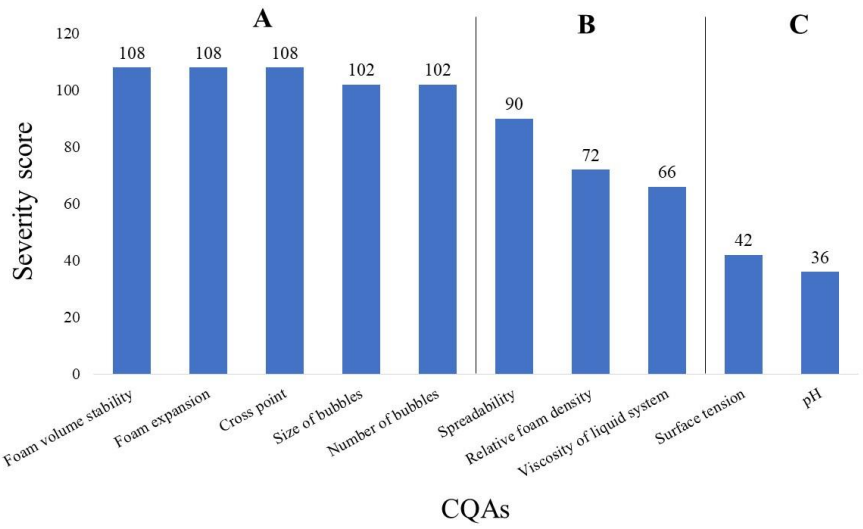

Figure 7. Pareto chart of CQA parameters.

The findings identified five critical foam properties, including macroscopic foam stability, foam expansion, cross point, size of the bubbles, and number of the bubbles, as the most critical parameters categorized under Category A, with severity scores exceeding 100, indicating their criticality during development. Category B parameters, such as spreadability, relative foam density, and viscosity of the liquid system, had severity scores ranging from 60 to 90, while Category C parameters (surface tension, pH) had minimal impact on product quality. Among the defined CPPs and CMAs, polymer concentration and type, as well as stirring speed and time, had the highest influence on the target product, which were the parameters investigated (Figure 8).

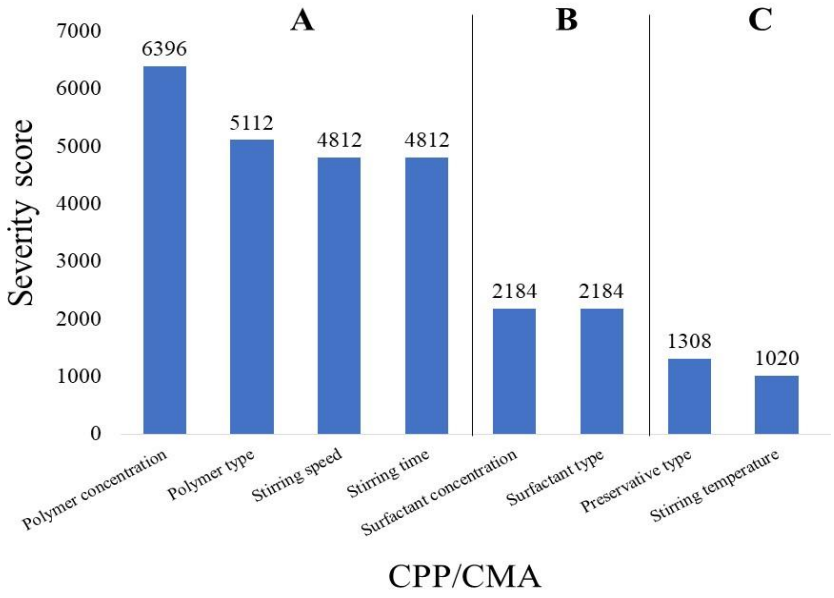

Figure 8. Pareto chart of CPP/CMA parameters.

5.1.2. Preformulation study of foams

Preformulation tests were conducted to optimize mixing time and speed crucial for achieving the desired foam consistency. Various stirring speeds (1000 rpm, 1500 rpm, 2000 rpm) and durations (5, 10, 15 min) were evaluated to attain a foam volume twice that of the liquid for testing. Results indicated that a suitable foam consistency for testing purposes was achieved at 2000 rpm for 5 minutes.

5.1.3. Characterization of the critical formulation parameters

5.1.3.1. Macroscopic characterization of foams

During the macroscopic examination, the effect of polymer concentration and type on the quality characteristics of the foam were investigated using the cylinder method. This allows gathering insights into the stability of foam formulations, including foam expansion, foam volume stability, and relative foam density. The results can be found in Table 3.

Table 3. The results of macroscopic cylinder test.

	FE [%]	**FVS [%]**	**RFD**
F-0polymer	172 ± 15.7	14 ± 1.81	0.2028
F-XANT_0.1	158 ± 3.84	95 ± 0.78	0.3879
F-XANT_0.2	134 ± 1.92	100 ± 0	0.4265
F-HEC_0.2	177 ± 0	15 ± 1.39	0.3614
F-HEC_0.4	164 ± 1.92	29 ± 1.28	0.3781
F-HA$_{LMW}$_0.1	179 ± 1.92	14 ± 0.09	0.3585
F-HA$_{LMW}$_0.2	177 ± 0	14 ± 0.35	0.3614
F-HA$_{HMW}$_0.1	130 ± 3.33	77 ± 14.22	0.4348
F-HA$_{HMW}$_0.2	126 ± 3.85	94 ± 0.09	0.4434
F-HA$_{CL}$_0.1	130 ± 3.33	15 ± 0.87	0.4348
F-HA$_{CL}$_0.2	130 ± 3.33	14 ± 0.21	0.4348

Macroscopic analysis revealed that the polymer-free composition exhibited high foam expansion but poor foam stability, resulting in rapid breakdown of the foam structure.

Similarly, formulations F-HEC_0.2, F-HA_{LMW}_0.1, and F-HA_{LMW}_0.2 demonstrated high foam expansion but low foam stability. F-HA_{CL} displayed low foam stability at both concentrations tested, with moderate foam expansion. In contrast, formulations F-XANT and F-HA_{HMW} exhibited high foam stability across both concentrations. Remarkably, increasing polymer concentration led to higher foam density for all polymers, although this did not consistently correlate with foam stability and expansion. Formulations with foam expansion exceeding 150% demonstrated optimal foaming characteristics. The most stable formulations were those with foam volume stability above 70%, notably F-XANT_0.2 and F-HA_{HMW}_0.2.

5.1.3.2. Microscopic characterization of foam kinetics and bubble morphology

Microscopic examinations were employed to follow the kinetics of foam destabilization and investigated the structure of each foam containing different polymers.

Bubble sizes were assessed in microscopic images captured at specific time intervals (0, 10, 20, 30 min), revealing that increasing bubble size led to foam destabilization over time. Foams which contain larger bubbles from the beginning were more friable. The size of the bubbles depends on the concentration of the polymer. In the case of F-XANT, F-HA_{HMW}, and F-HA_{CL} with increasing polymer concentration, the initial size of the bubbles was also larger.

Kinetic analysis enabled the determination of foam stability, with Figure 9 illustrating the relationship between the number of bubbles and time. Foams with an initial bubble count in a predetermined area exceeding 100 demonstrated microscopic stability, aligning well with results obtained from macroscopic foam volume stability test using the cylinder method.

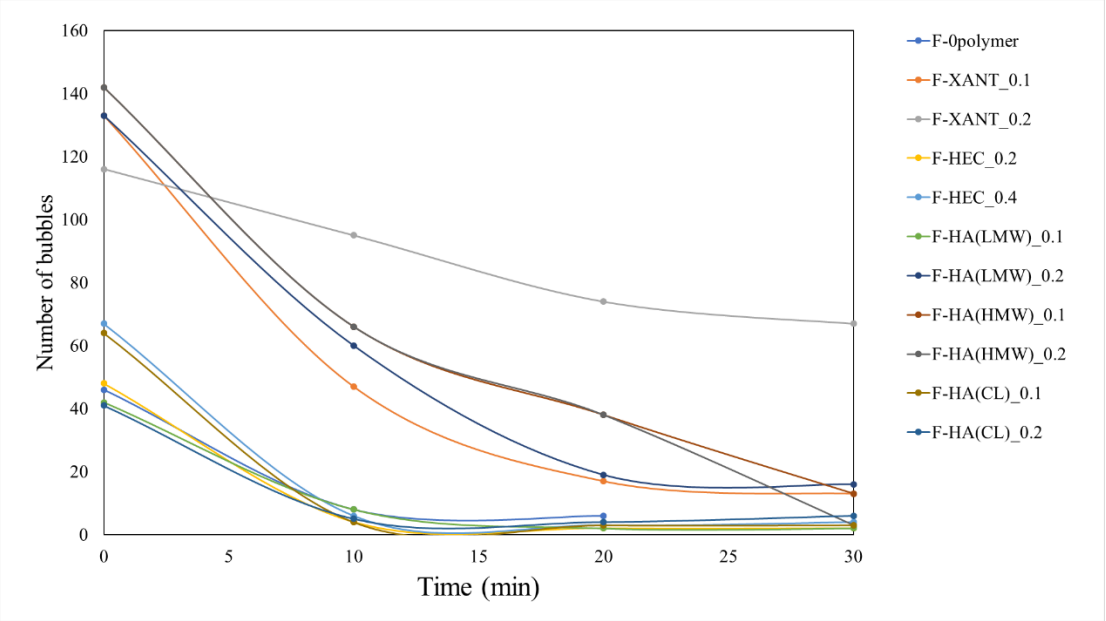

Figure 9. Kinetics of foam destabilization.

5.1.3.3. Rheological investigation of the foams (Oscillometric measurements)

Foam structure is characterized by a network of bubbles held together by a cohesive dispersion medium, which can be analyzed using oscillatory rheology [94,95]. The viscoelastic properties of a material, characterized by G' (storage modulus) and G" (loss modulus), and their relationship to each other, offer insights into its behavior. The point of intersection in an amplitude sweep signifies a flow point (γ_f), the linear viscoelastic (LVE) range and its limit (yield point, γ_y) represent the end of the linear range of the moduli. The two points indicate structural stability of the coherent systems. A broader LVE range suggests greater stability, with constant G' and G". Observations revealed two distinct amplitude sweep curves: one with a wider LVE range and higher elastic modulus, indicating stability, and another where G" dominates, signifying a lack of coherent foam structure (Figure 10). Some foam formulations behaved like liquids with higher G" than G' values in the LVE region, lacking flow points. Instability in other cases prevented measurements. Polymer-free foam immediately flowed and displayed its highest LVE range limit after 10 minutes due to liquid drainage. F-XANT_0.1 and F-XANT_0.2 were more stable than polymer-free foam, but higher concentrations decreased stability after 30 minutes. F-HEC_0.2 and F-HEC_0.4 showed decreasing coherence over time, correlating with polymer concentration. F-HA_{LMW} formulations remained stable for 20 minutes, improving stability with higher polymer content.

F-HA_{HMW}_0.1 exhibited better coherence after 30 minutes, while cross-linked hyaluronic acid accelerated foam breakdown with higher polymer concentrations. Xanthan gum-containing and high molecular weight hyaluronic acid foams demonstrated promising long-term stability, aligning with FVS% values.

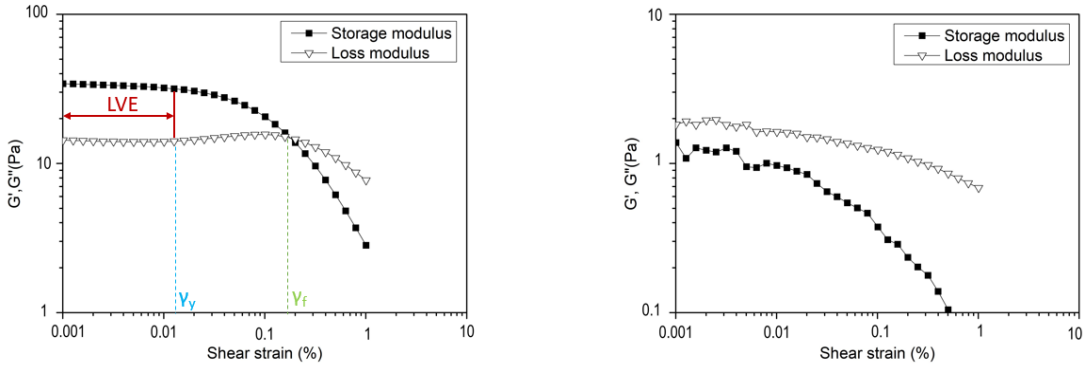

Figure 10. Typical rheological behavior of the formulated foams; stable (left) and unstable (right) foams.

The amplitude sweep curves of the polymers and rheological parameters derived from the curves can be found in Annex I and II.

5.1.3.4. Rheological investigation: Flow and viscosity characteristics of foam bulk liquids

Initially, viscosity assessment of bulk liquids, conducted after risk assessment, involves the use of rheological parameters as sensitive indicators for liquid, semisolid, and foam formulations. These parameters aid in characterizing spreadability, consistency, and stability. Viscosity can influence foam formation; excessive viscosity may hinder it, while insufficient viscosity can lead to quick destabilization. Polymer solutions typically exhibited shear-thinning behavior due to macromolecular alignment under shear, notably observed with xanthan gum and HEC-containing solutions where viscosity increased with concentration. Low molecular weight hyaluronic acid and cross-linked hyaluronic acid solutions showed similar rheological behavior to polymer-free solutions, while high molecular weight hyaluronic acid exhibited shear-thinning behavior akin to xanthan gum, alongside slight thixotropy. The flow curves can be found in Annex I.

5.1.3.5. Assessment of spreadability

Spreadability, indicating how easily a foam spreads on the skin, inversely correlates with application ease [96]. Using a male cone probe, force is applied to penetrate the foam to a specified depth, with maximum force indicating firmness. Viscosity, the connection between bubbles, distribution, and geometry of bubbles influence foam firmness. Lower force means easier spreading, while higher force suggests greater foam stability. Polymer-free foam exhibited poor spreadability and quick flow, while polymer content generally enhances firmness, preventing from flowing off the skin. Figure 11 illustrates that higher polymer concentrations require more force for spreading. High molecular weight hyaluronic acid foams demanded the most force, while xanthan gum and high molecular weight hyaluronic acid foams have met spreadability requirements, and correlated with macroscopic findings.

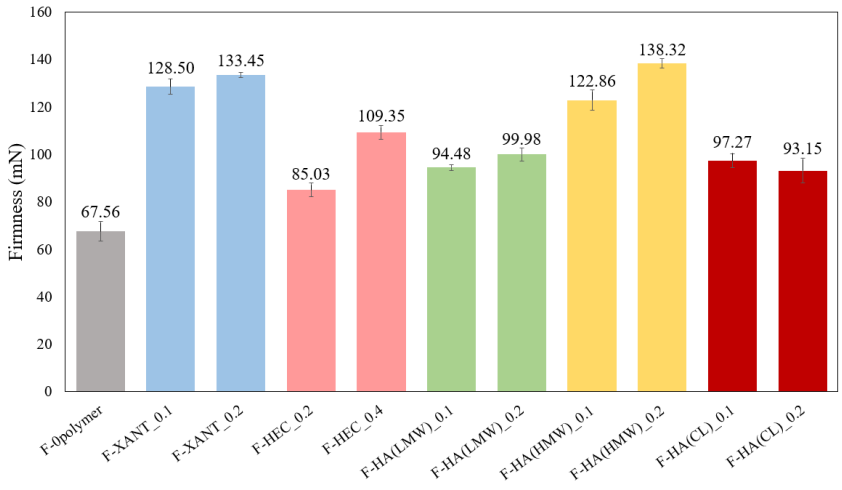

Figure 11. Firmness values of the investigated formulations.

5.1.4. Summary of Experiment 1

Based on the initial risk assessment, eleven compositions were formed and analyzed. CQAs identified included foam volume stability, expansion, cross point, bubble size, and number, alongside medium-critical attributes like spreadability, foam density, and liquid viscosity. Polymer concentration and type emerged as highly critical material parameters affecting CQAs, while surfactant had a moderate impact. Polymer content significantly influenced foam properties in different ways.

Among my findings, formulations like F-XANT_0.1, F-XANT_0.2, F-HA_{HMW}_0.1, and F-HA_{HMW}_0.2 showed promising foam properties. Results from various methods exhibited strong correlation.

The optimal formula can be determined by combining the macroscopic method of assessing foam stability, examining the microscopic kinetics using a light microscope, and employing oscillometric measurements to find cross-points. In contrast to prior researches, this study has developed a protocol that combines these methods to choose the optimal foam formulation.

5.2. Experiment part 2 - Biopharmaceutical analysis of a diclofenac sodium-containing foam drug delivery system compared to foam bulk liquid and hydrogel

5.2.1. Preformulation study of foam formula: *Ex vivo* permeation through fluorescent microscope

The foam underwent comparison with both negative and positive controls during the study. The negative control involved evaluating the appearance of untreated skin under a fluorescent microscope. Microscopic images revealed a high fluorescence intensity in the *stratum corneum* (Figure 12A), consistent with previous literature documenting the physiological appearance of this skin layer [97]. To assess the permeation of the fluorescent dye-marked formulation, examination of the lower epidermal and dermal layers was necessary, as these layers exhibit low intensity under the fluorescent filter and are unaffected by skin autofluorescence (Figure 12B).

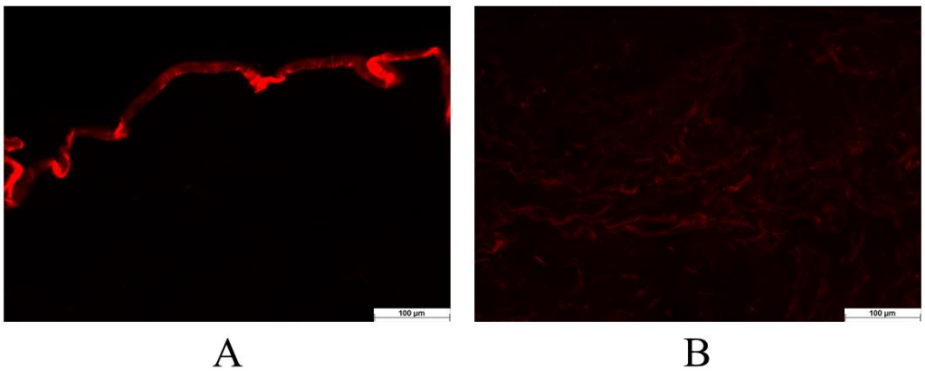

Figure 12. Microscopic images of the negative control (untreated skin): Image of *stratum corneum* with upper skin layers (A) and lower skin layers (B).

For the positive control, the skin underwent pretreatment with a solution containing SLES to enhance permeation.

Alkyl sulfates can disrupt the skin barrier, enabling the passage of fluorescein dye solution through the *stratum corneum*. Relative intensity was then evaluated to determine the increase compared to untreated skin (negative control).

Results (depicted in Figure 13) revealed a significant rise in light intensity following the SLES pretreatment. This indicates that SLES reduced the protective function of *stratum corneum*, enabling the dye solution to penetrate deeper skin layers. After 10 minutes of treatment, intensity increased by 7.81 times, while after 30 minutes, it only increased by 6.41 times compared to the untreated skin.

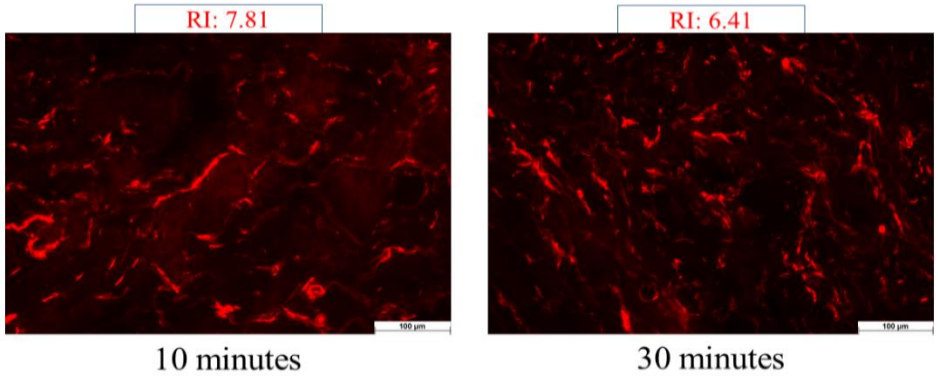

Figure 13. Microscopic images of the positive control, indicating the values of relative intensity at 10 and 30 minutes.

For the foam, as the observation time progressed, there was a noticeable rise in fluorescence intensity. Following 10 minutes, permeation increased by 3.76-fold, whereas after 30 minutes, this value increased by 6.68-fold (Figure 14). Initially, intensity was low with the foam preparation at 10 minutes, but after 30 minutes, it reached the relative intensity of the positive control. Based on the results, the foam formulation could achieve deep permeation similarly to the positive control.

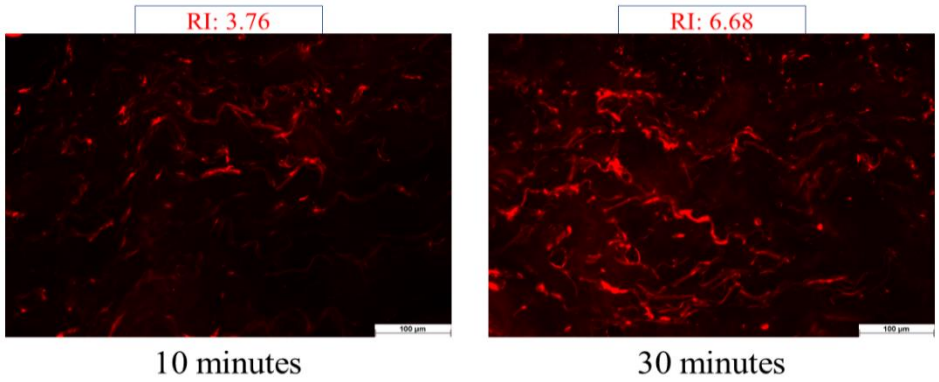

Figure 14. Microscopic images of the foam formulation, indicating the values of relative intensity at 10 and 30 minutes.

5.2.2. Rheological properties of the foam formula compared to bulk liquid and hydrogel

Rheological measurements were employed to examine the consistency of the systems. The viscosities of both the initial bulk liquid and the residual liquid film after foam breakdown were analyzed and compared with those of a standard hydrogel formulation (Table 4).

Table 4. The viscosity of the prepared formulations under a shear rate of 50 1/s.

	Viscosity (mPas)
Bulk liquid	46.99 ± 0.80
Liquid film (after the foam decay)	58.68 ± 1.07
Hydrogel	378.78 ± 4.39

The foam initially formed from the bulk liquid, combining with air through a propellant-free foam pump. Over time, the foam decayed into a liquid film due to binding forces and chain interactions, leading to a more organized network compared to the initial bulk liquid. This structured network increased the viscosity of the liquid film, resulting in decreased volume filling and higher density. The hydrogel exhibited significantly higher viscosity, typical of semisolid formulations. Rheological analysis showed that all three systems displayed shear-thinning behavior common in polymer solutions, where viscosity decreases with shear. The high viscosity of the hydrogel was attributed to its higher polymer content. Since the viscosity of the hydrogel increased by 6.5 times compared to the bulk liquid and liquid film, it may lead to a delay in skin permeation due to increased resistance to deformation.

5.2.3. Biopharmaceutical investigation of the foam formula compared to bulk liquid and hydrogel

5.2.3.1. *In vitro* drug release and permeation tests (IVRT and IVPT) using Franz Diffusion Cell System

The results indicated rapid release of diclofenac sodium from the foam, with about 80% released in 30 minutes, compared to approximately 5 hours for the hydrogel (Figure 15). This rapid release from the foam may be attributed to its porous structure, facilitating easier dispersion of active ingredients and quicker delivery to the target site.

The surfactants and polymers used contribute to the formation and stabilization of this porous structure. These excipients prevents thinning and destabilization of the liquid film between air bubbles, stabilizing the foam [94].

Surfactant molecules orient with polar parts in contact with water and hydrophobic chains facing the air, both at the interface and within the water film, facilitating rapid active ingredient release [38]. While the release kinetics were slower in case of the bulk liquid and hydrogel, diclofenac sodium exhibited slightly faster diffusion from the bulk liquid. This could be due to the lower viscosity of polymer solutions, allowing for easier diffusion of active ingredients. Conversely, hydrogels, with their higher viscosity and more organized structure, may contribute slower release, potentially influenced by the more organized and interconnected structure typical of hydrogels.

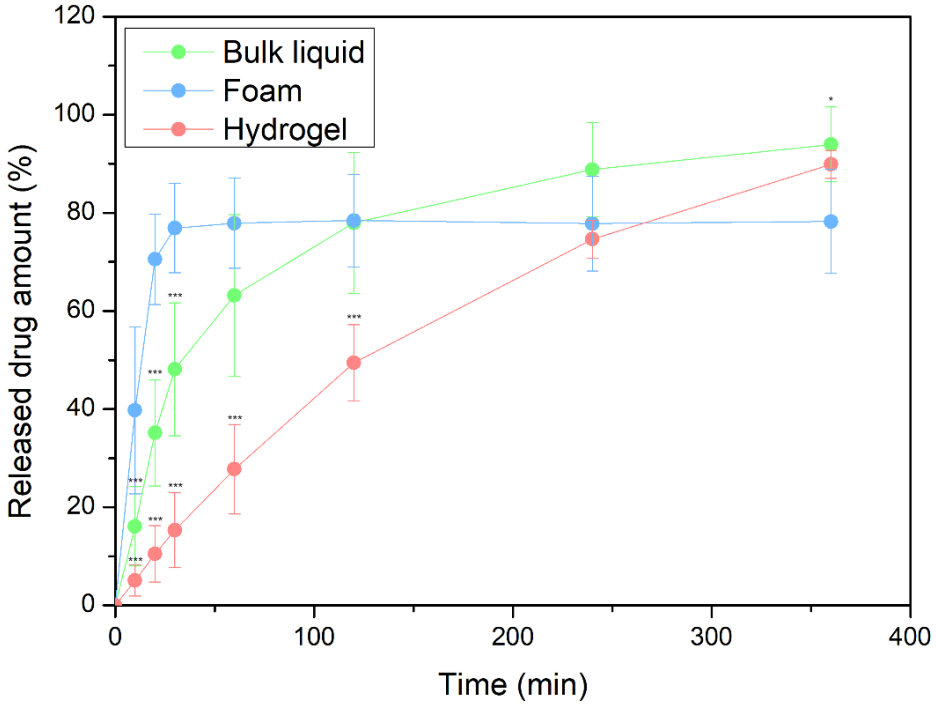

Figure 15. Release profile of diclofenac sodium in various dosage forms (***$p \leq 0.001$ vs. Foam, *$p \leq 0.05$ vs. Foam).

The data of the permeation rate (Table 5) indicated that rapid drug release from the foam led to swift drug permeation. Due to its ability to cover a large skin surface area, the foam allows for quick absorption of the active ingredient, enhancing its rapid delivery to the skin and accelerating its efficacy. Additionally, the liquid film formed after foam decaying may have become supersaturated, leading to faster permeation compared to hydrogel and bulk liquid formulations.

Table 5. The flux of diclofenac sodium through the human epidermis.

	J (μg/cm^2/h)	R^2
Bulk liquid	0.866	0.9811
Foam	5.838	0.9921
Hydrogel	1.65	0.9173

5.2.3.2. Investigation of *ex vivo* drug permeation using Raman spectroscopy

The *ex vivo* permeation was studied with Raman spectroscopy. Figures 16–18 demonstrate the qualitative distribution of diclofenac sodium in human skin samples following the application of foam, bulk liquid, and hydrogel, aiming to determine the permeation of diclofenac sodium into the epidermis or dermis.

Warmer colors on the maps indicated the higher presence of the active ingredient. In the case of bulk liquid, diclofenac sodium was detectable in deeper skin layers within 10 minutes, becoming more pronounced by 30 minutes (Figure 16). Conversely, in foam-treated skin sections, diclofenac sodium was concentrated in upper epidermal layers initially, with presence in deeper layers increasing over time (Figure 17). Gradual foam decay led to liquid leakage between bubbles onto the skin after 10 minutes, creating a supersaturated layer. Consequently, the increased diclofenac sodium presence in the foam became more prominent, with increased active substance concentrations observed between 20 to 30 minutes.

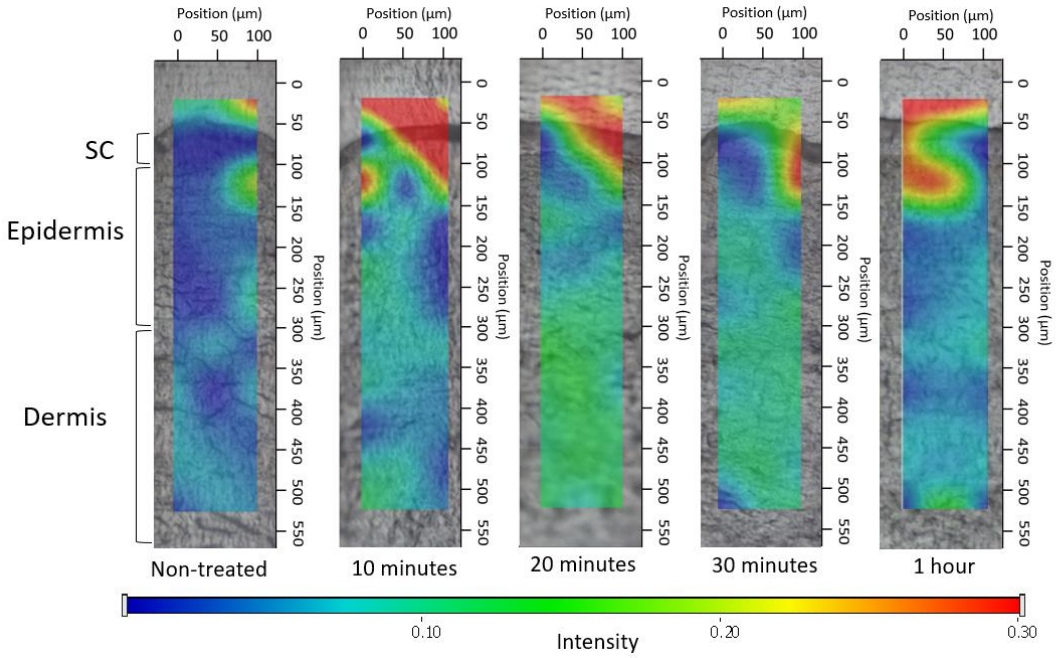

Figure 16. Raman correlation map of bulk liquid.

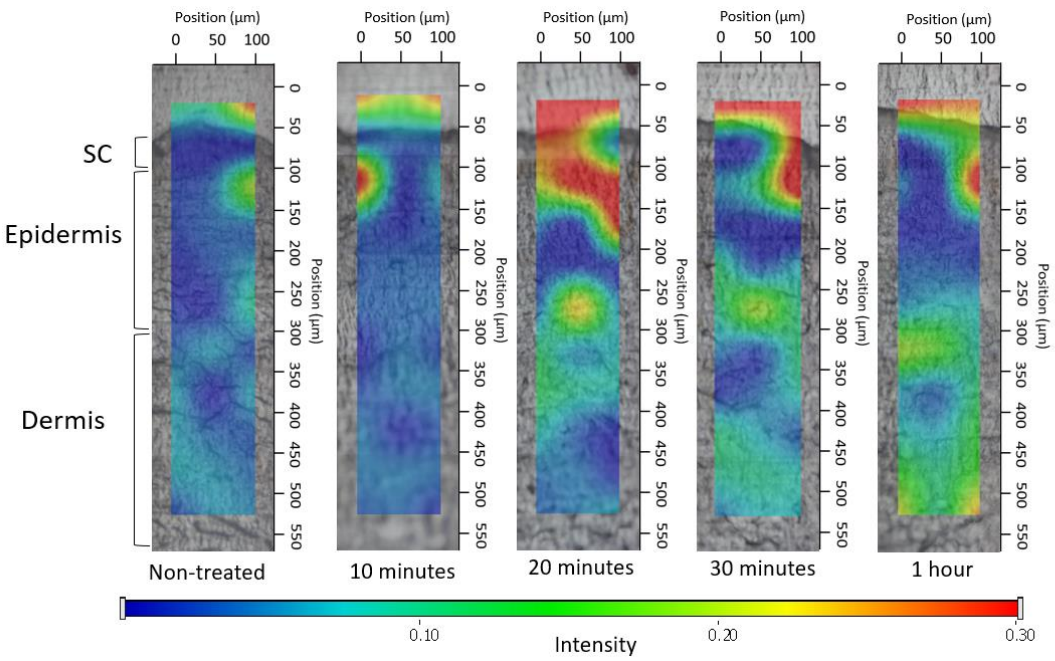

Figure 17. Raman correlation map of foam.

In terms of the hydrogel (Figure 18), the findings suggested that diclofenac sodium permeated only into the outermost epidermal layer during the entire study period. Subsequently, after 1 hour, elevated concentrations were observed only in the upper part of the skin.

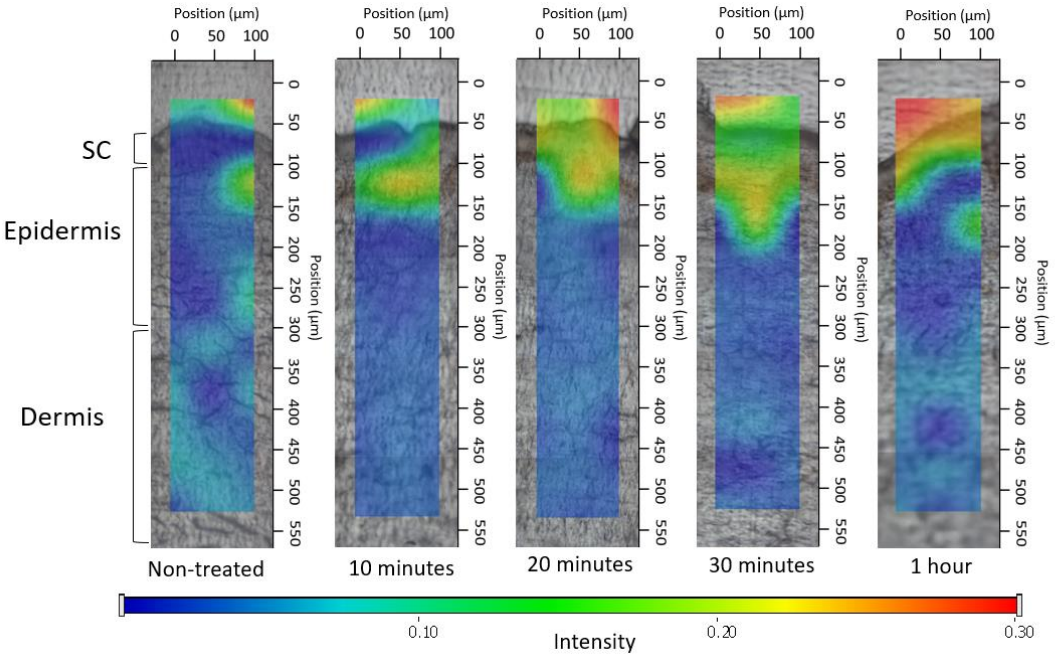

Figure 18. Raman correlation map of hydrogel.

5.2.4. Summary of Experiment 2

In this part of research, the biopharmaceutical properties of foams with those of traditional hydrogel and polymer solutions were compared. The results indicated that compared to the hydrogel, the foam as a drug delivery system achieved rapid drug release and deeper skin permeation. Within just 30 minutes, approximately 80% of the active ingredient was released using the foam, while it took about 5 hours for the hydrogel to reach the same level of release. The rapid release observed from the foam could be attributed to its porous structure, which aids in the efficient dispersion of active ingredients, leading to faster delivery to the target area. Based on the IVPT results, the permeation rate of the foam was the highest which results showed good correlation with *ex vivo* Raman measurements. Raman skin permeation studies revealed that the foam concentrated in the upper epidermal layers within 10 minutes and gradually permeated deeper layers over time. Despite having the same composition as the bulk liquid, the foam formulation exhibited higher permeation of the active ingredient after 20 minutes. In contrast, the hydrogel, with the highest viscosity, impeded diclofenac sodium permeation into deeper skin layers even after one hour.

5.3. Experiment part 3 - Assessment of biocompatibility and wound healing potential of foam components and formulations

Due to their advantageous properties, foams may have the potential to assist in maintaining a moist environment around the wound, which promotes ideal conditions for effective wound healing. It is suitable for treating hard-to-reach areas and it is flexible and conformable to wound contours, ensuring optimal contact with the wound bed.

The wound healing process involves the sequential phases of inflammation, proliferation, and remodeling, following initial injury [98,99]. Inflammation, after hemostasis, is crucial for activating the innate immune system to protect against pathogens and remove dead tissue [100]. During proliferation, the wound surface undergoes re-epithelialization, collagen synthesis, extracellular matrix formation, and vascular network restoration. In the final remodeling phase, regenerative processes diminish, giving way to connective tissue reorganization and the onset of the contractile response [98]. In the next series of experiments, the aim was to incorporate active ingredients into foams such as dexpanthenol which plays a significant role in all three main phases of wound healing [101], while diclofenac sodium acts as an anti-inflammatory agent. Additionally, niacinamide, which is more involved in the remodeling phase, has anti-inflammatory effects [102,103].

Furthermore, the foam formulations contained xanthan gum [104] and hyaluronic acid [105] as polymers, which may demonstrate activity in wound healing and could be beneficial for treating minor wounds and scars.

5.3.1. Cytotoxicity assay

The MTT assay was performed on the ingredients of the investigated foam formulations. Both the polymers, and active agents had a similar effect on cell viability. Results showed (Figure 19) that, in the case of AD-MSCs, components slightly reduced cell viability (except Polyoxyl 40 castor oil), with diclofenac sodium having the most significant reducing effect. Nonetheless, all tested components maintained viability above 70%, meeting the criteria for non-cytotoxicity to mesenchymal cells according to ISO 10993-5 standards [106]. The control group displayed 100% viability (measured in quadruplicates, N=4).

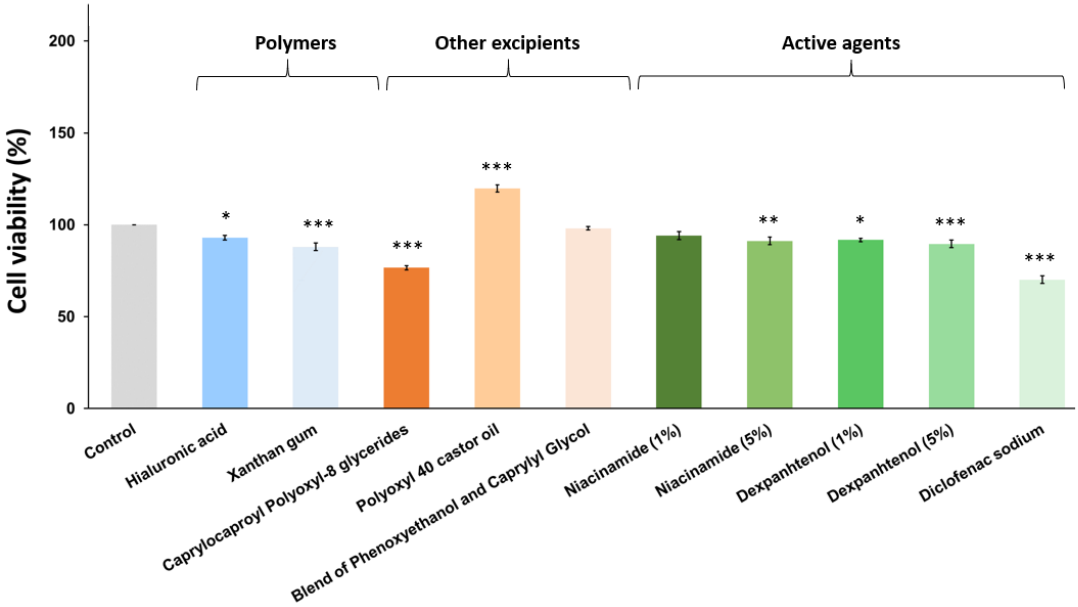

Figure 19. Effect of foam components on cell viability of AD-MSCs (***$p \leq 0.001$ vs. Control, **$p \leq 0.01$ vs. Control, *$p \leq 0.05$ vs. Control).

For keratinocytes (Figure 20), except for diclofenac sodium and one of the non-ionic surfactants, all applied components increased cell viability; Polyoxyl 40 castor oil demonstrated even significantly greater cell viability than all of the active agents and polymers. Because of the higher standard error of the mean values, no more significant differences could be observed in this study. The results also indicated that each component reached the 70% cell viability value set by the ISO 10993-5 standard.

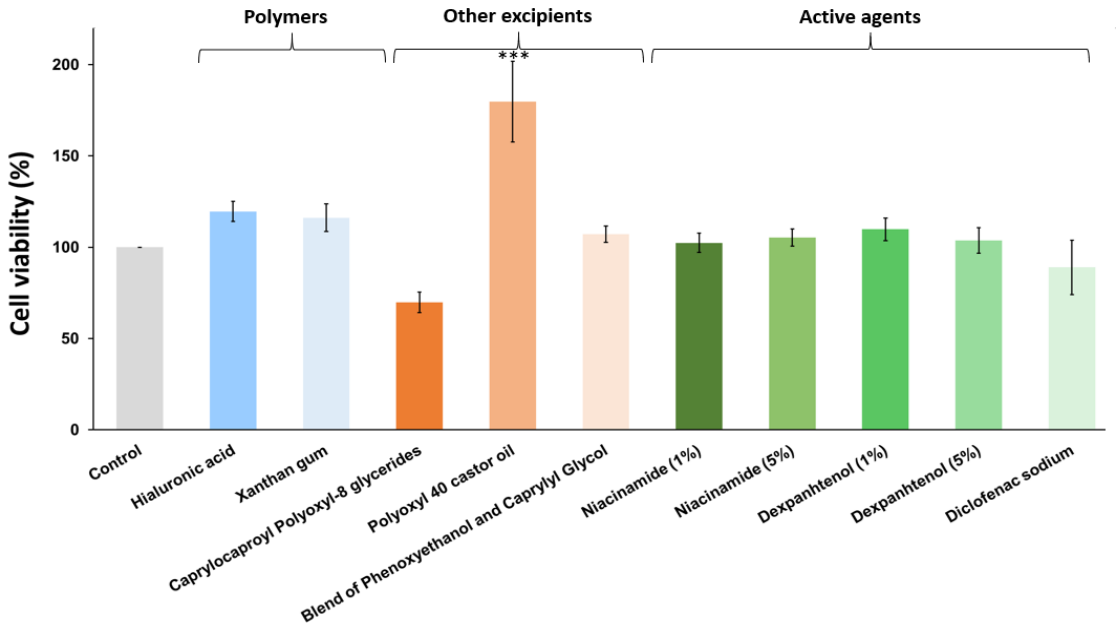

Figure 20. Effect of foam components on cell viability of keratinocytes (***$p \leq 0.001$ vs. Control).

Based on the cytotoxicity evaluation, the components within the formulations showed no cytotoxic effects on mesenchymal cells and keratinocytes at the concentrations used. Comparing the two cell types, AD-MSC cells were less sensitive to changes in the applied conditions than keratinocytes, therefore they are more suitable for detecting the significant effects of the components on the cells.

5.3.2. Comparison of the wound scratch and impedance-based wound healing assays

In this part of the research, the effects of five foam formulae were examined on two widely used wound healing models. One method, the wound scratch assay, is a simple yet useful tool for analyzing cell migration in two dimensions [107]. The other method, the impedance-based approach, which has gained prominence in recent years, has been identified as promising for three-dimensional proliferation assays [108].

Before the scratching, cells formed a contiguous monolayer (Figure 21). Scratching with Autoscratch device resulted in about 40-45 μm^2 wound on the monolayer with a sharp wound edge. During the wound healing AD-MSCs from the wound edge migrated into the inner region of wounds.

F-0polymer

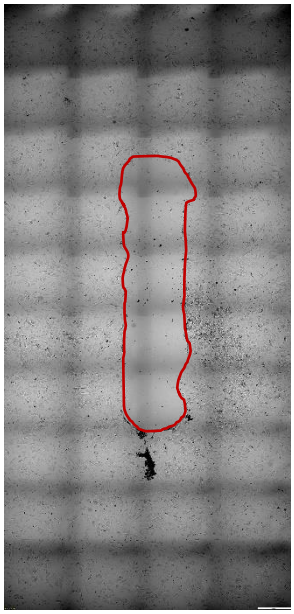

Initial state

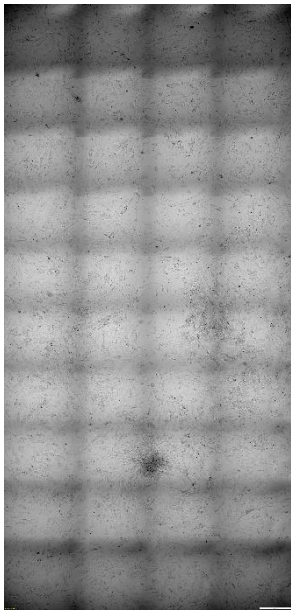

After 48 hours

F-XANT_0.2

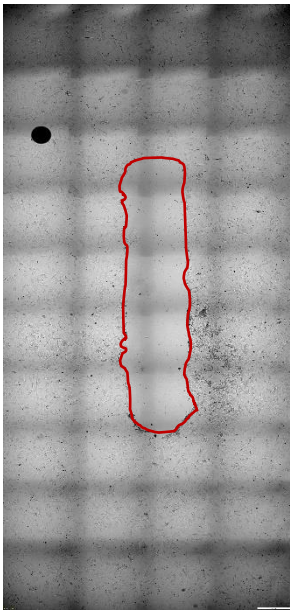

Initial state

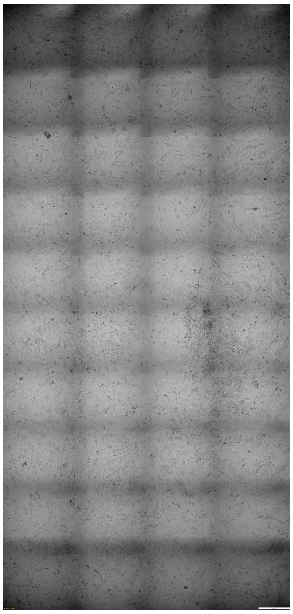

After 48 hours

F-HA_{HMW}_0.2

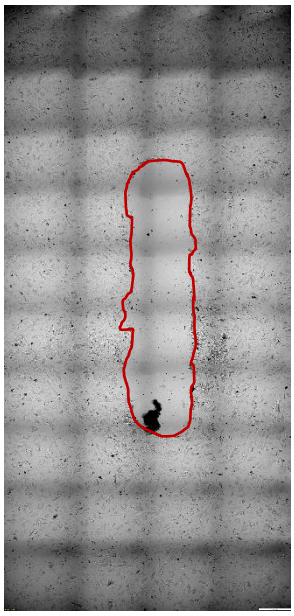

Initial state

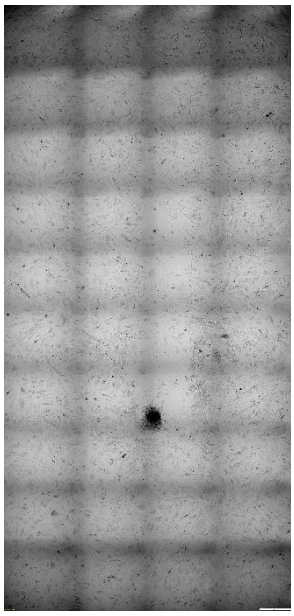

After 48 hours

F-XANT_0.2-DS_1

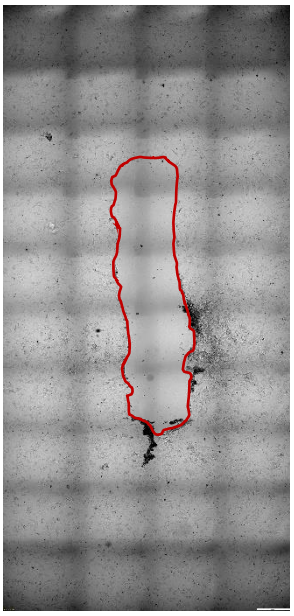

Initial state

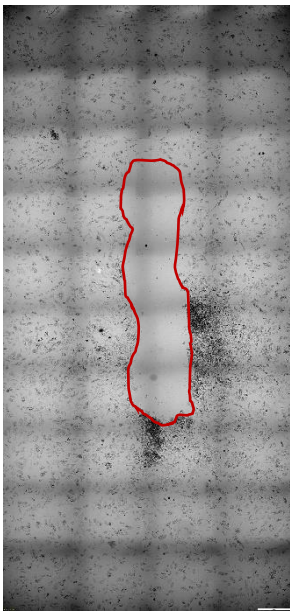

After 48 hours

F-XANT_0.2-HA_{HMW}_0.2-DEXP_1-NIAC-1

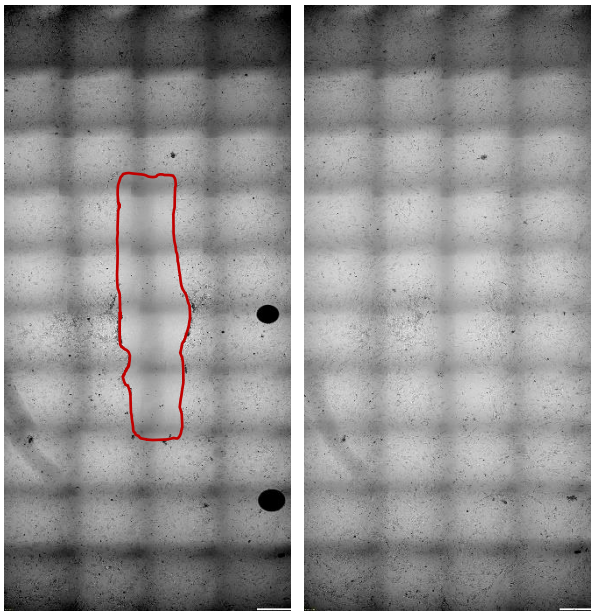

Initial state **After 48 hours**

Figure 21. The process of wound closure with different foam formulations.

It was notable that the majority of wounds had successfully closed, indicating effective wound-healing properties. However, one notable exception was observed in the case of the wound treated with foam containing diclofenac sodium, which exhibited incomplete closure compared to the other wounds. This suggests a potential inhibitory effect of diclofenac sodium on the initial wound healing process. Supported by previous studies, diclofenac inhibits the proliferation, migration, and differentiation of neural stem cells [109] and mesenchymal stem cells [110], however, in an appropriate combination, it can promote rapid wound healing [111].

According to the results of the impedance-based wound healing assay (Figure 22), the polymers had a beneficial effect on wound healing and improved cell migration from 30.9% (F-0polymer) to 43.05% with xanthan gum and to 46.13% with hyaluronic acid. In contrast, diclofenac sodium-containing foam formulations exhibited a relatively low migration percentage (15.99%). Combining the polymer-containing foam formula with dexpanthenol and niacinamide slightly decreased the migration percentage, but higher values were obtained compared to the polymer-free formulation.

Overall, the results of the wound scratch assay and the impedance-based measurement of wound healing showed a correlation, thus, due to the low migration percentage observed with diclofenac sodium-containing foam, wound closure did not occur.

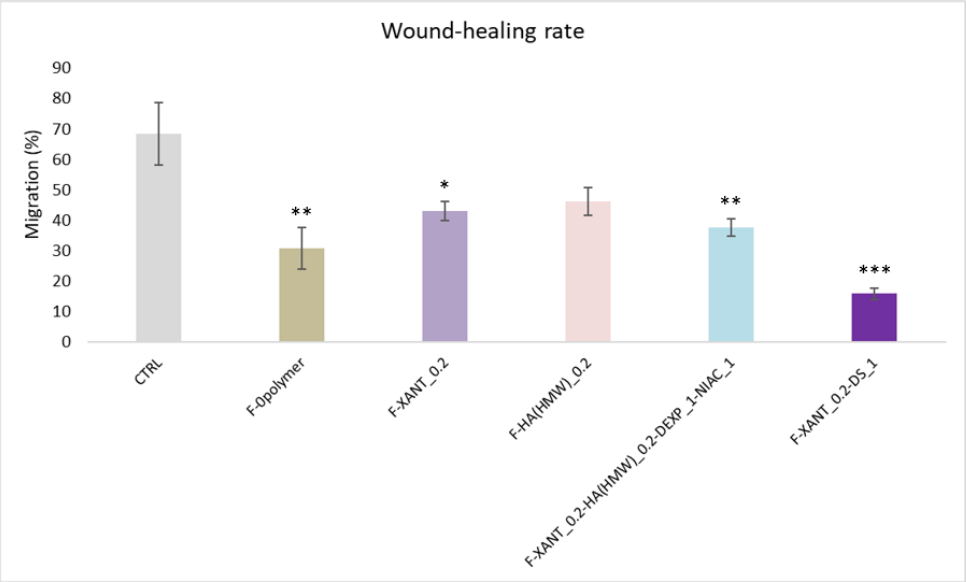

Figure 22. Wound-healing rate of AD-MSCs (***$p \leq 0.001$ vs. Control, **$p \leq 0.01$ vs. Control, *$p \leq 0.05$ vs. Control).

5.3.3. *In ovo* examination of foam formulations

Based on the results of the wound scratch assay, the effect of hyaluronic acid alone and in combination improved the extent of wound healing. Therefore, during the *in ovo* examinations, I investigated hyaluronic acid-containing foam formulations alone and in combination.

5.3.3.1. Irritation potential on HET-CAM assay

The images in Figure 23 (t_5) and the irritative scores outlined in Table 6, which are based on observations made within 5 minutes after application, suggested the absence of irritation in all samples compared to the positive control (treated with sodium dodecyl sulfate). However, a distinct observation emerges upon extending the observation period to 30 minutes after application, a distinct observation emerges. After 30 minutes, only the negative control and the F-HA_{HMW}_0.2-DEXP_5 formulation showed no irritation in the measurement.

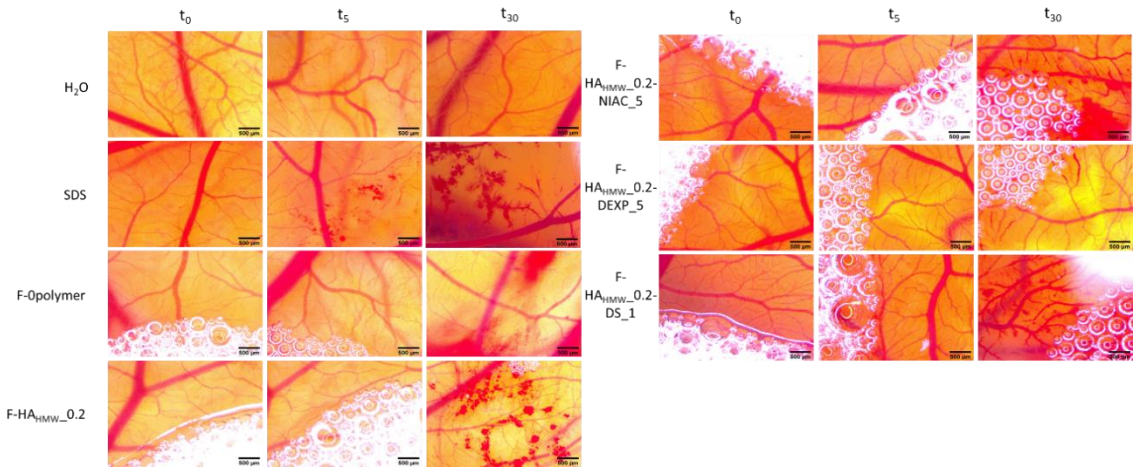

Figure 23. Irritation potential of hyaluronic-acid containing foam systems using HET-CAM assay; images represent the initial moment, before application (t_0), and 5 minutes after application of the samples (t_5) and 30 minutes post-application (t_{30}); scale bars represent 500 µm.

Table 6. The irritative scores of the analyzed samples in the HET-CAM assay.

SAMPLES	IF (5MINUTES)	EFFECT (5 MINUTES)
H_2O	0	No irritation
SDS	16.4 ± 0.54	Severe irritation
F-0polymer	0	No irritation
F-HA_{HMW}_0.2	0	No irritation
F-HA_{HMW}_0.2-NIAC_5	0	No irritation
F-HA_{HMW}_0.2-DEXP_5	0	No irritation
F-HA_{HMW}_0.2-DS_1	0	No irritation

5.3.4. Summary of Experiment 3

In conclusion, the formulated foam systems presented advantageous properties that may contribute to maintaining a moist wound environment, thus facilitating effective wound healing. Incorporating active ingredients such as dexpanthenol, niacinamide, and diclofenac sodium into foam formulations addresses specific aspects of wound healing, from inflammation control to tissue repair. Cytotoxicity assays demonstrated the safety of these formulations on both mesenchymal stem cells and keratinocytes.

Comparative analyses of wound scratch and impedance-based assays underscored the importance of polymer content in promoting cell migration and wound closure.

Notably, foam formulations containing diclofenac sodium exhibited incomplete wound closure, suggesting a potential inhibitory effect on the initial healing process. The impedance-based measurement also showed the lowest migration value (15%) with the foam containing diclofenac.

In ovo examinations have further clarified the effects of dexpanthenol-containing foam formulation, revealing no signs of irritation, indicating their potential to promote tissue repair.

6. CONCLUSION

The medicinal use of dermal foams is increasingly popular among the public. Their application is aesthetic, non-greasy, and easily removable from the skin, thus enhancing patient adherence. Foams have excellent spreadability on the skin, facilitating immediate absorption of active ingredients without the need for intense rubbing. Despite their numerous advantages, formulating dermal foams poses significant challenges. Meeting user demands for quick spreadability and pleasant skin sensation while ensuring environmental friendliness has become crucial. Additionally, while foams offer many benefits, their availability in the market remains relatively low compared to traditional products like creams and gels.

In my Ph.D. work, novel foam systems were formulated and new investigational methods were established suitable for testing the physicochemical and subsequently the biopharmaceutical properties of foams. Finally, I investigated the biocompatibility and the effects of the formulated products on wound healing.

During my work, I managed to develop testing methods capable of assessing the mechanical properties of foam, and the results indicated that foam, as a dosage form, is suitable for providing rapid drug release, deeper permeation, and may serve as alternatives to conventional carrier systems.

7. FINDINGS AND PRACTICAL RELEVANCE OF THE WORK

- The QbD approach was employed for the first time in foam development, demonstrating its efficacy in identifying and quantifying the critical parameters of these systems.
- A new light microscopy measurement method has been successfully developed for measuring foam kinetics and bubble morphology.

- The effect of stability enhancing polymers used in foams has been demonstrated and the effect of different polymers on the physicochemical properties of foams has been investigated. It has been determined that the combined application of macroscopic, microscopic, and rheological measurement methods allows for the appropriate selection of excipients used in foam formulations.
- The Texture Analyzer device was first employed to determine the physical stability of the foams.
- Through biopharmaceutical investigations, it was demonstrated that foam dosage forms enable immediate drug release and achieving deeper skin permeation. The *in vitro* quantitative IVPT and qualitative *ex vivo* Raman mapping studies were well-correlated. The combination of IVRT, IVPT, and Raman spectroscopy was first employed to determine the biopharmaceutical properties of the foams, establishing that rapid drug release and deep permeation can be achieved.
- The Raman mapping results exhibited a strong correlation with the fluorescent microscopic examination providing additional evidence for the system's rapid permeation.
- The biocompatibility of components in dermally applied foams was demonstrated using human adipose-derived mesenchymal stem cells and keratinocytes extracted from viable human skin, supporting the safety of application on the skin. The correlation between the two MTT tests indicated that, due to their sensitivity, assays conducted on human adipose-derived mesenchymal stem cells are more suitable for determining the cell viability of foam components.
- The wound healing effects of the foam bulk liquids were confirmed in two different models. The combined use of these two models showed good correlation, which may be suitable for selecting the optimal formula for wound treatment.
- The *in ovo* HET-CAM assay was suitable for determining the irritation of foam formulations.

8. REFERENCES

1. Lein, A.; Oussoren, C. Dermal. In *Practical Pharmaceutics*; Bouwman-Boer, Y., Fenton-May, V., Le Brun, P., Eds.; Springer International Publishing: Cham, 2015; pp. 229–263 ISBN 978-3-319-15813-6.
2. Zaid Alkilani, A.; Hamed, R.; Hussein, G.; Alnadi, S. Nanoemulsion-Based Patch for the Dermal Delivery of Ascorbic Acid. *J. Dispers. Sci. Technol.* **2022**, *43*, 1801–1811, doi:10.1080/01932691.2021.1880924.
3. Akbari, J.; Saeedi, M.; Enayatifard, R.; Morteza-Semnani, K.; Hassan Hashemi, S.M.; Babaei, A.; Rahimnia, S.M.; Rostamkalaei, S.S.; Nokhodchi, A. Curcumin Niosomes (Curcusomes) as an Alternative to Conventional Vehicles: A Potential for Efficient Dermal Delivery. *J. Drug Deliv. Sci. Technol.* **2020**, *60*, 102035, doi:10.1016/j.jddst.2020.102035.
4. Pünnel, L.C.; Lunter, D.J. Film-Forming Systems for Dermal Drug Delivery. *Pharmaceutics* **2021**, *13*, 932, doi:10.3390/pharmaceutics13070932.
5. Fu, X.; Ping, Q.; Gao, Y. Effects of Formulation Factors on Encapsulation Efficiency and Release Behaviour *in Vitro* of Huperzine A-PLGA Microspheres. *J. Microencapsul.* **2005**, *22*, 705–714, doi:10.1080/02652040500162196.
6. Kurowska, A.; Ghate, V.; Kodoth, A.; Shah, A.; Shah, A.; Vishalakshi, B.; Prakash, B.; Lewis, S.A. Non-Propellant Foams of Green Nano-Silver and Sulfadiazine: Development and In Vivo Evaluation for Burn Wounds. *Pharm. Res.* **2019**, *36*, 122, doi:10.1007/s11095-019-2658-8.
7. Trucillo, P.; Di Maio, E. Classification and Production of Polymeric Foams among the Systems for Wound Treatment. *Polymers* **2021**, *13*, 1608, doi:10.3390/polym13101608.
8. Hernández-Rangel, A.; Martin-Martinez, E.S. Collagen Based Electrospun Materials for Skin Wounds Treatment. *J. Biomed. Mater. Res. A* **2021**, *109*, 1751–1764, doi:10.1002/jbm.a.37154.
9. Lai-Cheong, J.E.; McGrath, J.A. Structure and Function of Skin, Hair and Nails. *Medicine (Baltimore)* **2021**, *49*, 337–342, doi:10.1016/j.mpmed.2021.03.001.
10. Hofmann, E.; Schwarz, A.; Fink, J.; Kamolz, L.-P.; Kotzbeck, P. Modelling the Complexity of Human Skin In Vitro. *Biomedicines* **2023**, *11*, 794, doi:10.3390/biomedicines11030794.
11. Epidermis (Outer Layer of Skin): Layers, Function, Structure Available online: https://my.clevelandclinic.org/health/body/21901-epidermis (accessed on 13 March 2024).
12. Simpson, C.L.; Patel, D.M.; Green, K.J. Deconstructing the Skin: Cytoarchitectural Determinants of Epidermal Morphogenesis. *Nat. Rev. Mol. Cell Biol.* **2011**, *12*, 565–580, doi:10.1038/nrm3175.
13. Gorzelanny, C.; Mess, C.; Schneider, S.W.; Huck, V.; Brandner, J.M. Skin Barriers in Dermal Drug Delivery: Which Barriers Have to Be Overcome and How Can We Measure Them? *Pharmaceutics* **2020**, *12*, 684, doi:10.3390/pharmaceutics12070684.
14. Pham, Q.D.; Björklund, S.; Engblom, J.; Topgaard, D.; Sparr, E. Chemical Penetration Enhancers in Stratum Corneum — Relation between Molecular Effects and Barrier Function. *J. Controlled Release* **2016**, *232*, 175–187, doi:10.1016/j.jconrel.2016.04.030.
15. Del Rosso, J.Q.; Levin, J. The Clinical Relevance of Maintaining the Functional Integrity of the Stratum Corneum in Both Healthy and Disease-Affected Skin. *J. Clin. Aesthetic Dermatol.* **2011**, *4*, 22–42.
16. Mojumdar, E.H.; Madsen, L.B.; Hansson, H.; Taavoniku, I.; Kristensen, K.; Persson, C.; Morén, A.K.; Mokso, R.; Schmidtchen, A.; Ruzgas, T.; et al. Probing Skin Barrier Recovery on Molecular Level Following Acute Wounds: An In Vivo/Ex Vivo Study on Pigs. *Biomedicines* **2021**, *9*, 360, doi:10.3390/biomedicines9040360.
17. Yang, G.; Seok, J.K.; Kang, H.C.; Cho, Y.-Y.; Lee, H.S.; Lee, J.Y. Skin Barrier Abnormalities and Immune Dysfunction in Atopic Dermatitis. *Int. J. Mol. Sci.* **2020**, *21*, 2867, doi:10.3390/ijms21082867.
18. Hussain, H.; Ziegler, J.; Hause, G.; Wohlrab, J.; Neubert, R.H.H. Quantitative Analysis of Free Amino Acids and Urea Derived from Isolated Corneocytes of Healthy Young, Healthy Aged, and Diseased Skin. *Skin Pharmacol. Physiol.* **2019**, *32*, 94–100, doi:10.1159/000495992.
19. Maeno, K. Direct Quantification of Natural Moisturizing Factors in Stratum Corneum Using Direct Analysis in Real Time Mass Spectrometry with Inkjet-Printing Technique. *Sci. Rep.* **2019**, *9*, 17789, doi:10.1038/s41598-019-54454-x.
20. van Smeden, J.; Janssens, M.; Gooris, G.S.; Bouwstra, J.A. The Important Role of Stratum Corneum Lipids for the Cutaneous Barrier Function. *Biochim. Biophys. Acta BBA - Mol. Cell Biol. Lipids* **2014**, *1841*, 295–313, doi:10.1016/j.bbalip.2013.11.006.
21. Richard, C.; Cassel, S.; Blanzat, M. Vesicular Systems for Dermal and Transdermal Drug Delivery. *RSC Adv.* **2021**, *11*, 442–451, doi:10.1039/D0RA09561C.
22. National Academies of Sciences, E.; Division, H. and M.; Policy, B. on H.S.; Creams, C. on the A. of the A.S.D.R. the S. and E. of I.U. in C.T.P.; Jackson, L.M.; Schwinn, D.A. Science of Compounded Topical Pain Creams. In *Compounded Topical Pain Creams: Review of Select Ingredients for Safety, Effectiveness, and Use*; National Academies Press (US), 2020.
23. Chamcheu, J.C.; Roy, T.; Uddin, M.B.; Banang-Mbeumi, S.; Chamcheu, R.-C.N.; Walker, A.L.; Liu, Y.-Y.; Huang, S. Role and Therapeutic Targeting of the PI3K/Akt/mTOR Signaling Pathway in Skin Cancer: A

Review of Current Status and Future Trends on Natural and Synthetic Agents Therapy. *Cells* **2019**, *8*, 803, doi:10.3390/cells8080803.
24. Lee, J.H.; Yeo, Y. Controlled Drug Release from Pharmaceutical Nanocarriers. *Chem. Eng. Sci.* **2015**, *125*, 75–84, doi:10.1016/j.ces.2014.08.046.
25. Tapfumaneyi, P.; Imran, M.; Alavi, S.E.; Mohammed, Y. Science of, and Insights into, Thermodynamic Principles for Dermal Formulations. *Drug Discov. Today* **2023**, *28*, 103521, doi:10.1016/j.drudis.2023.103521.
26. Petrilli, R.; Lopez, R.F.V. Physical Methods for Topical Skin Drug Delivery: Concepts and Applications. *Braz. J. Pharm. Sci.* **2018**, *54*, doi:10.1590/s2175-97902018000001008.
27. N'Da, D.D. Prodrug Strategies for Enhancing the Percutaneous Absorption of Drugs. *Molecules* **2014**, *19*, 20780–20807, doi:10.3390/molecules191220780.
28. Mitragotri, S.; Anissimov, Y.G.; Bunge, A.L.; Frasch, H.F.; Guy, R.H.; Hadgraft, J.; Kasting, G.B.; Lane, M.E.; Roberts, M.S. Mathematical Models of Skin Permeability: An Overview. *Int. J. Pharm.* **2011**, *418*, 115–129, doi:10.1016/j.ijpharm.2011.02.023.
29. Goyal, R.; Macri, L.K.; Kaplan, H.M.; Kohn, J. Nanoparticles and Nanofibers for Topical Drug Delivery. *J. Controlled Release* **2016**, *240*, 77–92, doi:10.1016/j.jconrel.2015.10.049.
30. Guo, J.-W.; Jee, S.-H. Strategies to Develop a Suitable Formulation for Inflammatory Skin Disease Treatment. *Int. J. Mol. Sci.* **2021**, *22*, 6078, doi:10.3390/ijms22116078.
31. Wang, M.; Marepally, S.K.; Vemula, P.K.; Xu, C. Chapter 5 - Inorganic Nanoparticles for Transdermal Drug Delivery and Topical Application. In *Nanoscience in Dermatology*; Hamblin, M.R., Avci, P., Prow, T.W., Eds.; Academic Press: Boston, 2016; pp. 57–72 ISBN 978-0-12-802926-8.
32. van Cranenburgh, O.D.; de Korte, J.; Sprangers, M.A.G.; de Rie, M.A.; Smets, E.M.A. Satisfaction with Treatment among Patients with Psoriasis: A Web-Based Survey Study. *Br. J. Dermatol.* **2013**, *169*, 398–405, doi:10.1111/bjd.12372.
33. Sampogna, F.; Tabolli, S.; Abeni, D. Living with Psoriasis: Prevalence of Shame, Anger, Worry, and Problems in Daily Activities and Social Life. *Acta Derm. Venereol.* **2012**, *92*, 299–303, doi:10.2340/00015555-1273.
34. Farkas, D.; Kállai-Szabó, N.; Antal, I. Foams as Carrier Systems for Pharmaceuticals and Cosmetics. *Acta Pharm. Hung.* **2019**, *89*, 5–15, doi:10.33892/aph.2019.89.5-15.
35. Purdon, C.H.; Haigh, J.M.; Surber, C.; Smith, E.W. Foam Drug Delivery in Dermatology: Beyond the Scalp. *Am. J. Drug Deliv.* **2003**, *1*, 71–75, doi:10.2165/00137696-200301010-00006.
36. Cantat, I.; Cohen-Addad, S.; Elias, F.; Graner, F.; Höhler, R.; Pitois, O.; Rouyer, F.; Saint-Jalmes, A. *Foams: Structure and Dynamics*; Oxford University Press; ISBN 978-0-19-176303-8.
37. Langevin, D. Aqueous Foams and Foam Films Stabilised by Surfactants. Gravity-Free Studies. *Comptes Rendus Mécanique* **2017**, *345*, 47–55, doi:10.1016/j.crme.2016.10.009.
38. Bureiko, A.; Trybala, A.; Kovalchuk, N.; Starov, V. Current Applications of Foams Formed from Mixed Surfactant–Polymer Solutions. *Adv. Colloid Interface Sci.* **2015**, *222*, 670–677, doi:10.1016/j.cis.2014.10.001.
39. Klimaszewska, E.; Seweryn, A.; Ogorzałek, M.; Nizioł-Łukaszewska, Z.; Wasilewski, T. Reduction of Irritation Potential Caused by Anionic Surfactants in the Use of Various Forms of Collagen Derived from Marine Sources in Cosmetics for Children. *Tenside Surfactants Deterg.* **2019**, *56*, 180–187, doi:10.3139/113.110616.
40. Lémery, E.; Briançon, S.; Chevalier, Y.; Bordes, C.; Oddos, T.; Gohier, A.; Bolzinger, M.-A. Skin Toxicity of Surfactants: Structure/Toxicity Relationships. *Colloids Surf. Physicochem. Eng. Asp.* **2015**, *469*, 166–179, doi:10.1016/j.colsurfa.2015.01.019.
41. Falusi, F.; Berkó, S.; Kovács, A.; Budai-Szűcs, M. Application of Xanthan Gum and Hyaluronic Acid as Dermal Foam Stabilizers. *Gels* **2022**, *8*, 413, doi:10.3390/gels8070413.
42. Parsa, M.; Trybala, A.; Malik, D.J.; Starov, V. Foam in Pharmaceutical and Medical Applications. *Curr. Opin. Colloid Interface Sci.* **2019**, *44*, 153–167, doi:10.1016/j.cocis.2019.10.007.
43. Cilurzo, F.; Casiraghi, A.; Selmin, F.; Minghetti, P. Supersaturation as a Tool For Skin Penetration Enhancement. *Curr. Pharm. Des. 21*, 2733–2744.
44. Zhao, Y.; Brown, M.B.; Jones, S.A. Pharmaceutical Foams: Are They the Answer to the Dilemma of Topical Nanoparticles? *Nanomedicine Nanotechnol. Biol. Med.* **2010**, *6*, 227–236, doi:10.1016/j.nano.2009.08.002.
45. Kumar, M.; Thakur, A.; Mandal, U.K.; Thakur, A.; Bhatia, A. Foam-Based Drug Delivery: A Newer Approach for Pharmaceutical Dosage Form. *AAPS PharmSciTech* **2022**, *23*, 244, doi:10.1208/s12249-022-02390-x.
46. Maimouni, I.; Cejas, C.M.; Cossy, J.; Tabeling, P.; Russo, M. Microfluidics Mediated Production of Foams for Biomedical Applications. *Micromachines* **2020**, *11*, 83, doi:10.3390/mi11010083.
47. Mantripragada, S. A Lipid Based Depot (DepoFoam Technology) for Sustained Release Drug Delivery. *Prog. Lipid Res.* **2002**, *41*, 392–406, doi:10.1016/s0163-7827(02)00004-8.

48. Mantripragada, S.B.; Howell, S.B. Sustained-Release Drug Delivery with DepoFoam. In *Drug Delivery Systems in Cancer Therapy*; Brown, D.M., Ed.; Cancer Drug Discovery and Development; Humana Press: Totowa, NJ, 2004; pp. 247–262 ISBN 978-1-59259-427-6.
49. Salisbury, A.-M.; Mullin, M.; Foulkes, L.; Chen, R.; Percival, S.L. Controlled-Release Iodine Foam Dressings Demonstrate Broad-Spectrum Biofilm Management in Several in Vitro Models. *Int. Wound J.* **2022**, *19*, 1717–1728, doi:10.1111/iwj.13773.
50. Sivaraman, A.; Banga, A. Quality by Design Approaches for Topical Dermatological Dosage Forms. *Res. Rep. Transdermal Drug Deliv.* **2015**, 9, doi:10.2147/RRTD.S82739.
51. Kovács, A.; Kis, N.; Budai-Szűcs, M.; Gácsi, A.; Csányi, E.; Csóka, I.; Berkó, S. QbD-Based Investigation of Dermal Semisolid in Situ Film-Forming Systems for Local Anaesthesia. *Drug Des. Devel. Ther.* **2020**, *Volume 14*, 5059–5076, doi:10.2147/DDDT.S279727.
52. Radhakrishnan, V.; Davis, P.; Hiebert, D. Scientific Approaches for the Application of QbD Principles in Lyophilization Process Development. In *Challenges in Protein Product Development*; Warne, N.W., Mahler, H.-C., Eds.; AAPS Advances in the Pharmaceutical Sciences Series; Springer International Publishing: Cham, 2018; Vol. 38, pp. 441–471 ISBN 978-3-319-90601-0.
53. Kovács, A.; Berkó, Sz.; Csányi, E.; Csóka, I. Development of Nanostructured Lipid Carriers Containing Salicyclic Acid for Dermal Use Based on the Quality by Design Method. *Eur. J. Pharm. Sci.* **2017**, *99*, 246–257, doi:10.1016/j.ejps.2016.12.020.
54. Visser, J.C.; Dohmen, W.M.C.; Hinrichs, W.L.J.; Breitkreutz, J.; Frijlink, H.W.; Woerdenbag, H.J. Quality by Design Approach for Optimizing the Formulation and Physical Properties of Extemporaneously Prepared Orodispersible Films. *Int. J. Pharm.* **2015**, *485*, 70–76, doi:10.1016/j.ijpharm.2015.03.005.
55. Yu, L.X. Pharmaceutical Quality by Design: Product and Process Development, Understanding, and Control. *Pharm. Res.* **2008**, *25*, 781–791, doi:10.1007/s11095-007-9511-1.
56. Grangeia, H.B.; Silva, C.; Simões, S.P.; Reis, M.S. Quality by Design in Pharmaceutical Manufacturing: A Systematic Review of Current Status, Challenges and Future Perspectives. *Eur. J. Pharm. Biopharm.* **2020**, *147*, 19–37, doi:10.1016/j.ejpb.2019.12.007.
57. Bakonyi, M.; Berkó, S.; Kovács, A.; Budai-Szűcs, M.; Kis, N.; Erős, G.; Csóka, I.; Csányi, E. Application of Quality by Design Principles in the Development and Evaluation of Semisolid Drug Carrier Systems for the Transdermal Delivery of Lidocaine. *J. Drug Deliv. Sci. Technol.* **2018**, *44*, 136–145, doi:10.1016/j.jddst.2017.12.001.
58. Kis, N.; Kovács, A.; Budai-Szűcs, M.; Gácsi, A.; Csányi, E.; Csóka, I.; Berkó, S. Investigation of Silicone-Containing Semisolid in Situ Film-Forming Systems Using QbD Tools. *Pharmaceutics* **2019**, *11*, 660, doi:10.3390/pharmaceutics11120660.
59. Charoo, N.A.; Shamsher, A.A.A.; Zidan, A.S.; Rahman, Z. Quality by Design Approach for Formulation Development: A Case Study of Dispersible Tablets. *Int. J. Pharm.* **2012**, *423*, 167–178, doi:10.1016/j.ijpharm.2011.12.024.
60. Elder, D.; Teasdale, A. ICH Q9 Quality Risk Management. In *ICH Quality Guidelines*; Teasdale, A., Elder, D., Nims, R.W., Eds.; Wiley, 2017; pp. 579–610 ISBN 978-1-118-97111-6.
61. Vandewalle, N.; Caps, H.; Delon, G.; Saint-Jalmes, A.; Rio, E.; Saulnier, L.; Adler, M.; Biance, A.L.; Pitois, O.; Addad, S.C.; et al. Foam Stability in Microgravity. *J. Phys. Conf. Ser.* **2011**, *327*, 012024, doi:10.1088/1742-6596/327/1/012024.
62. Arzhavitina, A.; Steckel, H. Foams for Pharmaceutical and Cosmetic Application. *Int. J. Pharm.* **2010**, *394*, 1–17, doi:10.1016/j.ijpharm.2010.04.028.
63. Mirtič, J.; Papathanasiou, F.; Temova Rakuša, Ž.; GosencaMatjaž, M.; Roškar, R.; Kristl, J. Development of Medicated Foams That Combine Incompatible Hydrophilic and Lipophilic Drugs for Psoriasis Treatment. *Int. J. Pharm.* **2017**, *524*, 65–76, doi:10.1016/j.ijpharm.2017.03.061.
64. Kamal, M. A Novel Approach to Stabilize Foam Using Fluorinated Surfactants. *Energies* **2019**, *12*, 1163, doi:10.3390/en12061163.
65. Eita, A.S.; Makky, A.M.A.; Anter, A.; Khalil, I.A. Atorvastatin-Loaded Emulsomes Foam as a Topical Antifungal Formulation. *Int. J. Pharm. X* **2022**, *4*, 100140, doi:10.1016/j.ijpx.2022.100140.
66. Zhao, Y.; Brown, M.B.; Jones, S.A. Engineering Novel Topical Foams Using Hydrofluroalkane Emulsions Stabilised with Pluronic Surfactants. *Eur. J. Pharm. Sci.* **2009**, *37*, 370–377, doi:10.1016/j.ejps.2009.03.007.
67. Kealy, T.; Abram, A.; Hunt, B.; Buchta, R. The Rheological Properties of Pharmaceutical Foam: Implications for Use. *Int. J. Pharm.* **2008**, *355*, 67–80, doi:10.1016/j.ijpharm.2007.11.057.
68. Bayarri, S.; Carbonell, I.; Costell, E. Viscoelasticity and Texture of Spreadable Cheeses with Different Fat Contents at Refrigeration and Room Temperatures. *J. Dairy Sci.* **2012**, *95*, 6926–6936, doi:10.3168/jds.2012-5711.
69. Falusi, F.; Budai-Szűcs, M.; Csányi, E.; Berkó, S.; Spaits, T.; Csóka, I.; Kovács, A. Investigation of the Effect of Polymers on Dermal Foam Properties Using the QbD Approach. *Eur. J. Pharm. Sci.* **2022**, *173*, 106160, doi:10.1016/j.ejps.2022.106160.

70. Kovács, A.; Falusi, F.; Gácsi, A.; Budai-Szűcs, M.; Csányi, E.; Veréb, Z.; Monostori, T.; Csóka, I.; Berkó, S. Formulation and Investigation of Hydrogels Containing an Increased Level of Diclofenac Sodium Using Risk Assessment Tools. *Eur. J. Pharm. Sci.* **2024**, *193*, 106666, doi:10.1016/j.ejps.2023.106666.
71. Kis, N.; Gunnarsson, M.; Berkó, S.; Sparr, E. The Effects of Glycols on Molecular Mobility, Structure, and Permeability in Stratum Corneum. *J. Controlled Release* **2022**, *343*, 755–764, doi:10.1016/j.jconrel.2022.02.007.
72. Kis, N.; Kovács, A.; Budai-Szűcs, M.; Erős, G.; Csányi, E.; Berkó, S. The Effect of Non-Invasive Dermal Electroporation on Skin Barrier Function and Skin Permeation in Combination with Different Dermal Formulations. *J. Drug Deliv. Sci. Technol.* **2022**, *69*, 103161, doi:10.1016/j.jddst.2022.103161.
73. Jian, L.; Cao, Y.; Zou, Y. Dermal-Epidermal Separation by Heat. *Methods Mol. Biol. Clifton NJ* **2020**, *2109*, 23–25, doi:10.1007/7651_2019_270.
74. Maibach, Y.Z., Howard I. Dermal-Epidermal Separation Methods: Research Implications. In *Percutaneous Absorption*; CRC Press, 2021 ISBN 978-0-429-20297-1.
75. Szoleczky, R.; Budai-Szűcs, M.; Csányi, E.; Berkó, S.; Tonka-Nagy, P.; Csóka, I.; Kovács, A. Analytical Quality by Design (AQbD) Approach to the Development of In Vitro Release Test for Topical Hydrogel. *Pharmaceutics* **2022**, *14*, 707, doi:10.3390/pharmaceutics14040707.
76. Zsikó, S.; Csányi, E.; Kovács, A.; Budai-Szűcs, M.; Gácsi, A.; Berkó, S. Novel In Vitro Investigational Methods for Modeling Skin Permeation: Skin PAMPA, Raman Mapping. *Pharmaceutics* **2020**, *12*, 803, doi:10.3390/pharmaceutics12090803.
77. Berkó, S.; Zsikó, S.; Deák, G.; Gácsi, A.; Kovács, A.; Budai-Szűcs, M.; Pajor, L.; Bajory, Z.; Csányi, E. Papaverine Hydrochloride Containing Nanostructured Lyotropic Liquid Crystal Formulation as a Potential Drug Delivery System for the Treatment of Erectile Dysfunction. *Drug Des. Devel. Ther.* **2018**, *12*, 2923–2931, doi:10.2147/DDDT.S168218.
78. Labedz-Maslowska, A.; Bryniarska, N.; Kubiak, A.; Kaczmarzyk, T.; Sekula-Stryjewska, M.; Noga, S.; Boruczkowski, D.; Madeja, Z.; Zuba-Surma, E. Multilineage Differentiation Potential of Human Dental Pulp Stem Cells—Impact of 3D and Hypoxic Environment on Osteogenesis In Vitro. *Int. J. Mol. Sci.* **2020**, *21*, 6172, doi:10.3390/ijms21176172.
79. Robert, A.W.; Marcon, B.H.; Dallagiovanna, B.; Shigunov, P. Adipogenesis, Osteogenesis, and Chondrogenesis of Human Mesenchymal Stem/Stromal Cells: A Comparative Transcriptome Approach. *Front. Cell Dev. Biol.* **2020**, *8*, doi:10.3389/fcell.2020.00561.
80. Falusi, F.; Berkó, S.; Budai-Szűcs, M.; Veréb, Z.; Kovács, A. Foams Set a New Pace for the Release of Diclofenac Sodium. *Pharmaceutics* **2024**, *16*, 287, doi:10.3390/pharmaceutics16020287.
81. Szűcs, D.; Miklós, V.; Monostori, T.; Guba, M.; Kun-Varga, A.; Póliska, S.; Kis, E.; Bende, B.; Kemény, L.; Veréb, Z. Effect of Inflammatory Microenvironment on the Regenerative Capacity of Adipose-Derived Mesenchymal Stem Cells. *Cells* **2023**, *12*, 1966, doi:10.3390/cells12151966.
82. Lukic, S.; Wegener, J. Impedimetric Monitoring of Cell-Based Assays. In *Encyclopedia of Life Sciences*; Wiley, 2015; pp. 1–8 ISBN 978-0-470-01617-6.
83. Vistejnova, L.; Dvorakova, J.; Hasova, M.; Muthny, T.; Velebny, V.; Soucek, K.; Kubala, L. The Comparison of Impedance-Based Method of Cell Proliferation Monitoring with Commonly Used Metabolic-Based Techniques. *Neuro Endocrinol. Lett.* **2009**, *30 Suppl 1*, 121–127.
84. Hassan, Q.; Ahmadi, S.; Kerman, K. Recent Advances in Monitoring Cell Behavior Using Cell-Based Impedance Spectroscopy. *Micromachines* **2020**, *11*, 590, doi:10.3390/mi11060590.
85. Ghiulai, R.; Avram, S.; Stoian, D.; Pavel, I.Z.; Coricovac, D.; Oprean, C.; Vlase, L.; Farcas, C.; Mioc, M.; Minda, D.; et al. Lemon Balm Extracts Prevent Breast Cancer Progression *In Vitro* and *In Ovo* on Chorioallantoic Membrane Assay. *Evid. Based Complement. Alternat. Med.* **2020**, *2020*, 1–17, doi:10.1155/2020/6489159.
86. Avram, S.; Coricovac, D.-E.; Pavel, I.Z.; Pinzaru, I.; Ghiulai, R.; Baderca, F.; Soica, C.; Muntean, D.; Branisteanu, D.E.; Spandidos, D.A.; et al. Standardization of A375 Human Melanoma Models on Chicken Embryo Chorioallantoic Membrane and Balb/c Nude Mice. *Oncol. Rep.* **2017**, *38*, 89–99, doi:10.3892/or.2017.5658.
87. Ribatti, D. The Chick Embryo Chorioallantoic Membrane (CAM). A Multifaceted Experimental Model. *Mech. Dev.* **2016**, *141*, 70–77, doi:10.1016/j.mod.2016.05.003.
88. Szuhanek, C.A.; Watz, C.G.; Avram, Ștefana; Moacă, E.-A.; Mihali, C.V.; Popa, A.; Campan, A.A.; Nicolov, M.; Dehelean, C.A. Comparative Toxicological In Vitro and In Ovo Screening of Different Orthodontic Implants Currently Used in Dentistry. *Materials* **2020**, *13*, 5690, doi:10.3390/ma13245690.
89. Coricovac, D.; Farcas, C.; Nica, C.; Pinzaru, I.; Simu, S.; Stoian, D.; Soica, C.; Proks, M.; Avram, S.; Navolan, D.; et al. Ethinylestradiol and Levonorgestrel as Active Agents in Normal Skin, and Pathological Conditions Induced by UVB Exposure: In Vitro and In Ovo Assessments. *Int. J. Mol. Sci.* **2018**, *19*, 3600, doi:10.3390/ijms19113600.
90. Ivocular-Hetcam.Pdf.
91. ImageJ Available online: https://imagej.net/ij/index.html (accessed on 13 March 2024).
92. GIMP Available online: https://www.gimp.org/ (accessed on 13 March 2024).

93. Luepke, N.P. Hen's Egg Chorioallantoic Membrane Test for Irritation Potential. *Food Chem. Toxicol.* **1985**, *23*, 287–291, doi:10.1016/0278-6915(85)90030-4.
94. Dollet, B.; Raufaste, C. Rheology of Aqueous Foams. *Comptes Rendus Phys.* **2014**, *15*, 731–747, doi:10.1016/j.crhy.2014.09.008.
95. Thurston, G.B.; Martin, A. Rheology of Pharmaceutical Systems: Oscillatory and Steady Shear of Non-Newtonian Viscoelastic Liquids. *J. Pharm. Sci.* **1978**, *67*, 1499–1506, doi:10.1002/jps.2600671103.
96. Djiobie Tchienou, G.; Tsatsop Tsague, R.; Mbam Pega, T.; Bama, V.; Bamseck, A.; Dongmo Sokeng, S.; Ngassoum, M. Multi-Response Optimization in the Formulation of a Topical Cream from Natural Ingredients. *Cosmetics* **2018**, *5*, 7, doi:10.3390/cosmetics5010007.
97. Ashtikar, M.A.; Verma, D.D.; Fahr, A. Confocal Microscopy for Visualization of Skin Penetration. In *Percutaneous Penetration Enhancers Drug Penetration Into/Through the Skin: Methodology and General Considerations*; Dragicevic, N., I. Maibach, H., Eds.; Springer: Berlin, Heidelberg, 2017; pp. 255–281 ISBN 978-3-662-53270-6.
98. Reinke, J.M.; Sorg, H. Wound Repair and Regeneration. *Eur. Surg. Res. Eur. Chir. Forsch. Rech. Chir. Eur.* **2012**, *49*, 35–43, doi:10.1159/000339613.
99. Childs, D.R.; Murthy, A.S. Overview of Wound Healing and Management. *Surg. Clin. North Am.* **2017**, *97*, 189–207, doi:10.1016/j.suc.2016.08.013.
100. Landén, N.X.; Li, D.; Ståhle, M. Transition from Inflammation to Proliferation: A Critical Step during Wound Healing. *Cell. Mol. Life Sci.* **2016**, *73*, 3861–3885, doi:10.1007/s00018-016-2268-0.
101. Baron, J.M.; Glatz, M.; Proksch, E. Optimal Support of Wound Healing: New Insights. *Dermatology* **2020**, *236*, 593–600, doi:10.1159/000505291.
102. Wessels, Q.; Pretorius, E.; Smith, C.M.; Nel, H. The Potential of a Niacinamide Dominated Cosmeceutical Formulation on Fibroblast Activity and Wound Healing in Vitro. *Int. Wound J.* **2014**, *11*, 152–158, doi:10.1111/j.1742-481X.2012.01052.x.
103. Ashkani Esfahani, S.; Khoshneviszadeh, M.; Namazi, M.R.; Noorafshan, A.; Geramizadeh, B.; Nadimi, E.; Razavipour, S.T. Topical Nicotinamide Improves Tissue Regeneration in Excisional Full-Thickness Skin Wounds: A Stereological and Pathological Study. *Trauma Mon.* **2015**, *20*, e18193, doi:10.5812/traumamon.18193.
104. Tang, S.; Gong, Z.; Wang, Z.; Gao, X.; Zhang, X. Multifunctional Hydrogels for Wound Dressings Using Xanthan Gum and Polyacrylamide. *Int. J. Biol. Macromol.* **2022**, *217*, 944–955, doi:10.1016/j.ijbiomac.2022.07.181.
105. Graça, M.F.P.; Miguel, S.P.; Cabral, C.S.D.; Correia, I.J. Hyaluronic Acid—Based Wound Dressings: A Review. *Carbohydr. Polym.* **2020**, *241*, 116364, doi:10.1016/j.carbpol.2020.116364.
106. Biological Evaluation of Medical Devices —Part 5: Tests for *in Vitro* Cytotoxicity. In *ANSI/AAMI/ISO 10993-5:2009/(R)2014; Biological evaluation of medical devices —Part 5: Tests for in vitro cytotoxicity*; AAMI, 2009 ISBN 978-1-57020-355-8.
107. Pastar, I.; Liang, L.; Sawaya, A.P.; Wikramanayake, T.C.; Glinos, G.D.; Drakulich, S.; Chen, V.; Stojadinovic, O.; Davis, S.C.; Tomic-Canic, M. Preclinical Models for Wound-Healing Studies. In *Skin Tissue Models for Regenerative Medicine*; Elsevier, 2018; pp. 223–253 ISBN 978-0-12-810545-0.
108. Tonello, S.; Bianchetti, A.; Braga, S.; Almici, C.; Marini, M.; Piovani, G.; Guindani, M.; Dey, K.; Sartore, L.; Re, F.; et al. Impedance-Based Monitoring of Mesenchymal Stromal Cell Three-Dimensional Proliferation Using Aerosol Jet Printed Sensors: A Tissue Engineering Application. *Materials* **2020**, *13*, 2231, doi:10.3390/ma13102231.
109. Kudo, C.; Kori, M.; Matsuzaki, K.; Yamai, K.; Nakajima, A.; Shibuya, A.; Niwa, H.; Kamisaki, Y.; Wada, K. Diclofenac Inhibits Proliferation and Differentiation of Neural Stem Cells. *Biochem. Pharmacol.* **2003**, *66*, 289–295, doi:10.1016/S0006-2952(03)00235-1.
110. Fredriksson, M.; Li, Y.; Stålman, A.; Haldosén, L.-A.; Felländer-Tsai, L. Diclofenac and Triamcinolone Acetonide Impair Tenocytic Differentiation and Promote Adipocytic Differentiation of Mesenchymal Stem Cells. *J. Orthop. Surg.* **2013**, *8*, 30, doi:10.1186/1749-799X-8-30.
111. Eid, B.G.; Alhakamy, N.A.; Fahmy, U.A.; Ahmed, O.A.A.; Md, S.; Abdel-Naim, A.B.; Caruso, G.; Caraci, F. Melittin and Diclofenac Synergistically Promote Wound Healing in a Pathway Involving TGF-B1. *Pharmacol. Res.* **2022**, *175*, 105993, doi:10.1016/j.phrs.2021.105993.

ACKNOWLEDGEMENTS

Firstly, I would like to thank **Prof. Dr. Ildikó Csóka**, the head of the Institute of Pharmaceutical Technology and Regulatory Affairs, for allowing me to conduct my research at the institute.

I would like to express my gratitude to my supervisors, **Dr. Anita Kovács** and **Dr. Szilvia Berkó**, who have supported me professionally since my undergraduate years, as well as for their continuous encouragement and emotional support. I am grateful to my former supervisor, **Dr. Erzsébet Csányi**, who has accompanied my scientific work and helped guide my academic career with her advice. I also owe gratitude to **Dr. Mária Budai-Szűcs,** who supported my work with her experience and knowledge.

I am deeply thankful for the countless selfless help and support from **Andrea Szalai**, **Krisztina Tóth**, and **Valéria Varga**.

Special thanks to our cooperative partners, among whom I would like to highlight **Dr. Zoltán Veréb** and **Tamás Monostori** from the University of Szeged, as well as **Dr. Stefana Avram** and **Prof. Dr. Corina Danciu** from Victor Babes University of Medicine and Pharmacy of Timisoara.

I extend my heartfelt appreciation to **Dr. Petra Party** and **Dr. Bence Sipos** for their unwavering support and kindness throughout our journey together. Their presence has brought immense joy and warmth to my life, and I am truly fortunate to have such wonderful friends by my side.

My deepest gratitude goes to my beloved **Parents** and **Grandparents**, who not only raised and supported me every step of the way but also helped shape my life with their love and wise advices. Without them, I would not be who I am today, and I will forever be thankful to them for their support and love. I am especially grateful to my fiancé, **Levente**, who has always been understanding and supportive, even during the difficult times. His presence in my life fills me with gratitude and reassurance, and I am truly blessed to have him by my side.

ANNEX

I.

European Journal of Pharmaceutical Sciences 173 (2022) 106160

Contents lists available at ScienceDirect

European Journal of Pharmaceutical Sciences

journal homepage: www.elsevier.com/locate/ejps

Investigation of the effect of polymers on dermal foam properties using the QbD approach

Fanni Falusi [a], Mária Budai-Szűcs [a], Erzsébet Csányi [a], Szilvia Berkó [a], Tamás Spaits [b], Ildikó Csóka [a], Anita Kovács [a,*]

[a] Institute of Pharmaceutical Technology and Regulatory Affairs, University of Szeged, Faculty of Pharmacy, 6 Eötvös St. Szeged H-6720, Hungary
[b] EGIS Pharmaceuticals PLC, 65 Mátyás király str. Körmend H-9900, Hungary

ARTICLE INFO

Keywords:
Dermal foam
Hyaluronic acid
Foam stability
Quality by design
Rheology

ABSTRACT

Dermal foams are promising drug delivery systems due to their many advantages and ease of application. Foams are also considered a novelty in the field of dermatology. In particular, they are beneficial for the treatment of skin conditions where patients have highly inflamed, swollen, infected and sensitive skin, as the application of the foam to the skin surface to be treated minimizes the need for skin contact. In order to formulate foams, it is necessary to know which material and process parameters influence the quality characteristics of foams and which methods can be used to study foams; this part of the research is assisted by the QbD approach. By using the QbD concept, it contributed during the development process to ensure quality-based development. With initial risk assessment, the critical material attributes (CMAs) and the critical process parameters (CPPs) were identified to ensure the required critical quality attributes (CQAs). During the initial risk assessment, five high-risk CQAs, namely foam volume stability, foam expansion, cross point, the initial values of the number and size of bubbles, and three medium-risk CQAs, namely spreadability, relative foam density and viscosity of the liquid system were identified and investigated. In this research, different types of polymers (xanthan gum, hydroxyethylcellulose, different types of hyaluronic acids) were used to improve the properties of foam formulations. The formulations containing xanthan gum and high molecular weight hyaluronic acid had good foam properties and will be appropriate delivery systems for an active pharmaceutical ingredient. Overall, the polymer content had a great effect on the properties of the foams. Different polymers affect the properties of foams in different ways. When used in combination, the methods reinforce each other and help to select a formula for dermal application.

1. Introduction

Foams are part of our daily lives in the field of cosmetics, as well as in the pharmaceutical and food industries. Pharmaceutical foams are usually applied topically (Zhao et al., 2010) as dermal, vaginal, or rectal administration, but there are other special applications such as parenteral and oral (Farkas et al., 2019; Hoc and Haznar-Garbacz, 2021). It is a preferred delivery system used to improve wound healing and to treat sunburn or skin diseases such as psoriasis and is also used in the pediatric field (Velasco et al., 2019).

Foams have many beneficial properties over conventional carrier systems. Their high rate of expansion allows large skin surfaces to be covered rapidly. It is really advantageous for patients who need to treat highly inflamed, swollen, abraded, infected and sensitive skin because the application of foam minimizes the need for touch, resulting in enhanced patient compliance (Parsa et al., 2019). Dermal foams are used to treat the skin or specific mucosal surfaces in order to exert their effects locally or by absorption through the skin. By applying liquid foams dermally, a local effect can be easily achieved. The transdermal delivery route allows a smaller amount of drugs to be used. It avoids not only the destructive effect of the gastrointestinal tract but also the enterohepatic circulation of the drug, making it less likely to cause systemic side effects. However, the main limitation of using foams is that they are thermodynamically unstable, therefore foams are prone to decay. The composition, both excipients and active ingredients, may affect the stability and quality of foams (Parsa et al., 2019; Cantat and Cohen-Addad, 15 June 2021).

In terms of their structure, foams are produced by dispersing a gaseous substance in a solid or liquid dispersion medium. Before formulation, it is essential to select suitable excipients, which greatly

* Corresponding author.
E-mail address: gasparne.kovacs.anita@szte.hu (A. Kovács).

https://doi.org/10.1016/j.ejps.2022.106160
Received 30 November 2021; Received in revised form 14 February 2022; Accepted 1 March 2022
Available online 4 March 2022

Table 1
Composition of different formulations.

	Foam 1 (F-0polymer)	Foam 2 (F-XANT_0.1)	Foam 3 (F-XANT_0.2)	Foam 4 (F-HEC_0.2)	Foam 5 (F-HEC_0.4)	Foam 6 (F-HA_{LMW}_0.1)	Foam 7 (F-HA_{LMW}_0.2)	Foam 8 (F-HA_{HMW}_0.1)	Foam 9 (F-HA_{HMW}_0.2)	Foam 10 (F-HA_{CL}_0.1)	Foam 11 (F-HA_{CL}_0.2)
Phase A											
Labrasol ALF /surfactant/	+	+	+	+	+	+	+	+	+	+	+
Kolliphor RH40 /surfactant/	+	+	+	+	+	+	+	+	+	+	+
Phase B											
Xanthan gum (Xant.) /polymer/	–	0.1%	0.2%	–	–	–	–	–	–	–	–
Hydroxyethyl-cellulose (HEC) /polymer/	–	–	–	0.2%	0.4%	–	–	–	–	–	–
Low-molecular-weight hyaluronic acid /polymer/	–	–	–	–	–	0.1%	0.2%	–	–	–	–
High-molecular-weight hyaluronic acid /polymer/	–	–	–	–	–	–	–	0.1%	0.2%	–	–
Cross-linked hyaluronic acid /polymer/	–	–	–	–	–	–	–	–	–	0.1%	0.2%
Purified water /solvent/	+	+	+	+	+	+	+	+	+	+	+
Phase C											
Phenoxyethanol /preservative/	+	+	+	+	+	+	+	+	+	+	+

affect foam stability. They usually contain surface-active agents, solvents, foam stabilizers, preservatives and may also include penetration enhancers (Parsa et al., 2019). Aerosols are pressurized in cans. These containers are capable of ex tempore foam formation. Propellant-free liquid foams are produced by adding air to a polymer solution with stirring or a propellant-free pump device. Liquid foams have many unique properties thanks to their ability to exhibit both liquid and solid behavior (Cantat and Cohen-Addad, 15 June 2021).

As noted above, the lifetime and the stability of the foam can be increased by using surfactants and foam stabilizing excipients (Langevin 2017; Bureiko et al., 2015). Increasing the viscosity of the liquid phase with polymers may lead to the stabilization of the foam structure. For instance, polymers used in foams can be naturally occurring polymers such as xanthan gum, agar-agar, tragacanth gum; acidic polymers such as palmitic acid, stearic acid; and semi-synthetic polymers such as cellulose ethers (Parsa et al., 2019). In addition to conventional polymers, there is a lack of literature on the effect of hyaluronic acid on foam stability. Hyaluronic acid plays a crucial role in skin moisture and helps the tissue regeneration process. Furthermore, it has an anti-aging effect and reduces dermatitis (Draelos 2011; Berkó et al., 2013).

There are four different main parallel mechanisms that occur when foam is decaying. These are: drainage, coalescence, disproportionation (Ostwald ripening) and bursting of bubbles. Drainage is when the liquid drains off through the Plateau borders due to gravity. These Plateau borders act as paths for the liquid to flow down through. As this happens, the lamellas of each bubble will get thinner and the foam will dry out. This results in the liquid getting to the bottom, which increases over time. In the case of coalescence, surface tension acts as a driving force when two bubbles get close to each other. Then they will conjoin and form a single bubble. The next way of foam decay is similar to coalescence but the mechanism is slightly different. Both coalescence and Ostwald ripening describe the formation of large masses. Coalescence is the process in which a few smaller masses merge with each other to form a large mass. These small masses can be droplets, bubbles, particles, and so on. When they come in contact, they tend to fuse and form a single drop, particle, or bubble. The main reason for Ostwald ripening is that large particles are thermodynamically more favorable than small particles. For the same reason, the process of Ostwald ripening is a spontaneous process. However, during Ostwald ripening the small particles dissolve in the solution and re-deposit to form large masses. Finally, the bubble form is not a stable state so they burst after a certain time. The bursting of foam lamellas leads to the elimination of air from the foam (Arzhavitina and Steckel, 2010; Karakashev et al., 2012; Guerrero et al., 2013).

Stabilization and thus the right quality is the first and the leading requirement for pharmaceuticals in development (Sivaraman and Banga, 2015; Anita Kovács et al., 2020). Nowadays, the Quality by Design approach in the design stage helps the development in pharmaceutical industry (Radhakrishnan et al., 2018). Generally, QbD aims to improve the efficiency of the design process, reducing costs in different stages of development. Initially, it records the critical quality attributes and critical process parameters that affect the quality of the product. In summary, QbD is science-based and risk-based drug development that begins with predetermined goals. If the design and testing of the active substance and pharmaceutical form are based on the QbD approach in the research phase, the results obtained during the research can be more effectively integrated into the development process. The first step of the QbD approach is to define the Quality Target Product Profile (QTTP), which is the goal of the development. The next step is to identify critical quality attributes (CQA), critical material attributes (CMAs) and critical process parameters (CPPs), and then parameters that potentially affect product quality are selected by risk assessment (A Kovács et al., 2017.; Visser et al., 2015; Yu, 2008). Although, the QbD approach is an innovative method in the field of drug development, its implementation is

Table 2
Quality target product profiles (QTPPs).

QTPP parameters	Target	Justification
Route of administration	Dermal	The dermal delivery of drugs is an opportunity to avoid systemic side effects. It is non-invasive, thus increasing patient compliance.
Dosage form	Foam	The good spreadability of the foams on the skin ensures the immediate release of the active ingredient, no rubbing on the skin is necessary (Parsa et al., 2019).
Site of action	Topical	Most medicated foams contain antiseptic, antifungal, anti-inflammatory, local anesthetic agents, as well as skin moisturizers and emollients (Parsa et al., 2019; Tamarkin et al., 2006). Absorption into the systemic circulation is not the aim of these formulations.
Stability of liquid system	There is no sign of instability, homogenous	Stability is an important parameter of the liquid system as it can affect foaming and foam stability.
Appearance of liquid system	Transparent or white, homogeneous	An esthetic preparation needs to be formulated for good patient adherence.
Stability of foam system	Adequate stability for the dermal route of administration	Adequate stability of the foam system is required for the foam to remain at the site of application.
Appearance of foam system	White	To increase patient compliance.
Polymer content	Increasing foam stability	Increasing the viscosity of the liquid phase with polymers can lead to the stabilization of the foam structure.

Table 3
Critical quality attributes (CQAs) of the foams.

CQA	Target	Justification
Bulk liquid properties		
pH	4–8	Ideal pH of topical formulations for the safety of the product and the skin. (Lambers et al., 2006).
Viscosity	20–200 mPas	Viscosity influences the stability of foam systems and their applicability to the skin.
Surface tension	27–30 mN/m	The surface tension of the initial liquid is important for bubble growth. The lower the surface tension of the initial liquid, the less force is required for the bubbles to blow (Farkas et al., 2021).
Foam properties		
Size of bubbles (initial value)	200–500,000 μm^2	The unique bubble size provides information on the stability and homogeneity of the foam (Farkas et al., 2021).
Number of bubbles (initial values)	100 <	The number of bubbles provides information on the stability of the foam.
Foam volume stability (FVS %)	50% ≤	This parameter indicates the rate of foam collapse. Stability is important to ensure that the active substance has a sufficient contact time (Kamal 2019).
Foam expansion (FE%)	100 ≤	Foam expansion is necessary to make the preparation suitable for treating large surfaces (Bikard et al., 2007).
Relative foam density (RFD)	≤ 0.5	One of the foam stability parameters. It also indicates the firmness of the foam (Mirtič et al., 2017).
Rheology: Cross point	Detectable within the strain value range of 0.1% to 100%	The presence of the cross point ensures that the foam has a coherent structure.
Spreadability	The force required to spread a cream is about 500 mN (Yadav et al., 2014).	In the case of foams, the goal is to spread on their own.

challenging for developers, as the incorporation of elements of the QbD concept varies from one pharmaceutical formulation to another.

The aim of our research was to design stable foam compositions based on the QbD approach and to determine the proper methods to investigate their physicochemical and structural properties and to compare the results of different methods. A further aim was to investigate the effect of different polymers on foam stability as well as on foam structure.

2. Materials and methods

2.1. Materials

Kolliphor RH 40 was obtained from BASF SE Chemtrade GmbH (Ludwigshafen, Germany). Labrasol ALF was from Gattefossé (Saint-Priest Cedex, France), Xantural® 180 was provided by CP Kelco A Huber Company (Atlanta, GA, USA). Verstatil PC was purchased from Biesterfeld GmbH (Hamburg, Germany). Hydroxyethylcellulose (Ph. Eur. 9.) was supplied by Molar Chemicals Ltd. (Budapest, Hungary). Purified and deionized water was used (Milli-Q system, Millipore, Milford, MA, USA). HyaCare50, HyaCare Filler CL and HyaCare Tremella were product samples from Evonik Industries AG (Essen, North Rhine-Westphalia, Germany).

2.2. Methods

2.2.1. Quality by design methodology

2.2.1.1. Definition of quality target product profile (QTPP). The first step in QbD-based development is to define the target product and to summarize the quality characteristics of the product. This determines the efficiency, the delivery route, the dosage form, the packaging, the appearance and therapeutic indication, etc. During development, QTPP parameters form the basis of development (Grangeia et al., 2020; Bakonyi et al., 2018; Kis et al., 2019).

2.2.1.2. Definition of CQA, CMA, CPP. In order to ensure the desired quality of the pharmaceutical product during development and production, the second step is to define the quality attributes. In the case of medicated foam formulations, the pH and viscosity of the bulk liquid, the homogeneity of bubble size and the skin penetration of the active pharmaceutical ingredient (API) etc. can also be critical quality parameters.

As a third step, it is necessary to determine the material and process parameters that can affect the critical quality attributes of the foams. The determination of these parameters helps to find the relationship between material properties and process parameters that are related to critical product quality parameters (Kovács et al., 2017; Charoo et al., 2012).

2.2.1.3. Risk assessment: quality tools. The QbD concept is based on risk assessment. Risk assessment can be used to identify critical parameters that have an impact on critical quality attributes. In our research, we applied quality tools such as the risk estimate matrix (REM), Pareto analysis and Ishikawa diagram. We started the risk assessment with a

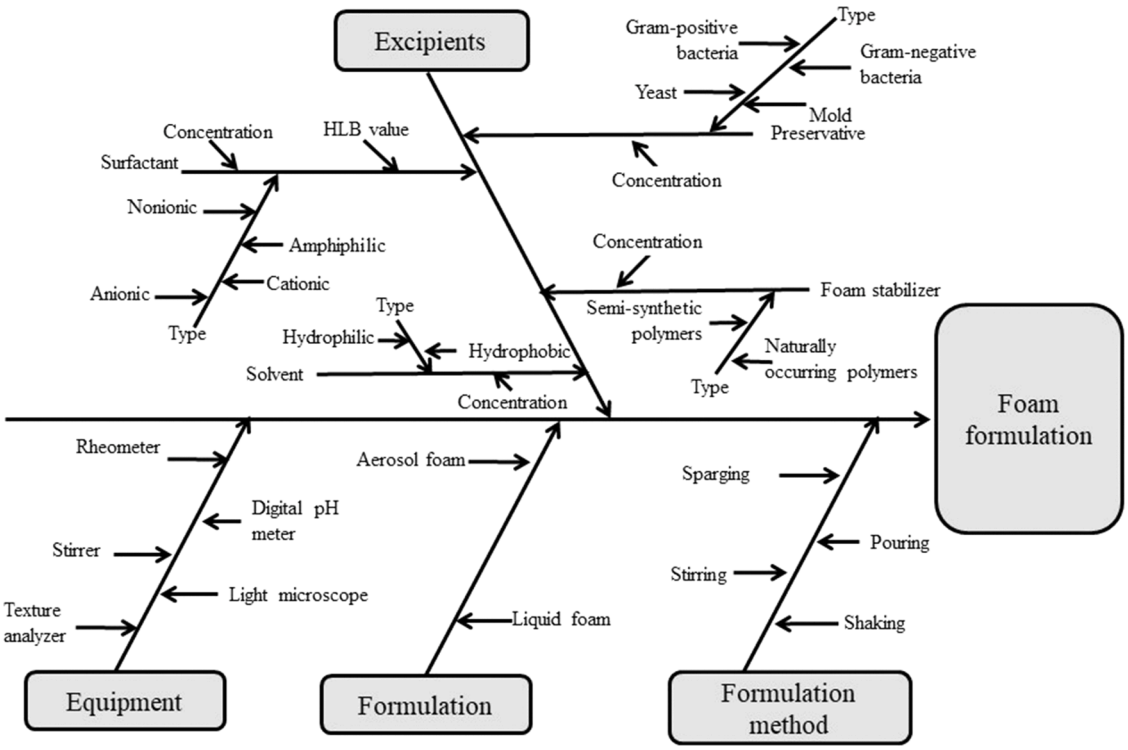

Fig. 1. Ishikawa diagram.

Table 4
Risk estimation matrix of QTPP and CQA parameters (LeanQbD™ Software) Low = low-risk, Medium = medium-risk, High = high-risk parameters during formulation.

	Route of administration (M)	Dosage form (M)	Site of action (M)	Stability of liquid system (M)	Appearance of liquid system (M)	Stability of foam system (M)	Appearance of foam system (M)	Polymer content (M)
pH	Low	Low	Low	Medium	Low	Medium	Low	Low
Viscosity of liquid system	Low	Low	Low	Medium	Medium	Medium	Low	High
Surface tension	Low	Low	Low	Medium	Low	Medium	Low	Medium
Size of bubbles (initial)	Low	High	Low	High	Low	High	Low	Medium
Number of bubbles (initial)	Low	High	Low	High	Low	High	Low	Medium
Foam volume stability	Medium	Medium	Low	High	Low	High	Low	High
Foam expansion	Medium	Medium	Low	High	Low	High	Low	High
Relative foam density	Medium	Medium	Low	Medium	Low	Medium	Low	High
Cross point	High	Medium	Low	Low	Low	High	Medium	High
Spreadability	Medium	High	Low	Medium	Low	High	Low	Medium

popular quality tool method called the Ishikawa diagram. This method helps to collect the possible root causes influencing the quality of foams. The next step was to determine the critical parameters with Pareto analysis, which is also called ABC analysis (Kovács et al., 2017). The items in Category A are the high-risk parameters, in Category B the medium-risk parameters and in Category C the low-risk parameters (ICH Guideline Q9 on Quality Risk Management, 2021). REM was used to define the level of the risk parameters and the connection between quality attributes and CPPs, CMAs. The LeanQbD™ software (QbD Works LLC, Fremont, CA, USA) was used for risk assessment.

2.2.2. Preparation of foams

Different foam compositions (Foam 1-Foam 11) were prepared (Table 1.) The lifetime of the foam can be extended by increasing the viscosity of the liquid phase among the air bubbles. One possible solution is the use of polymers in the composition. Therefore, the formulated foams contain different types of polymers in different concentrations (Phase B) (Vandewalle et al., 2011). The foaming agents are mainly surfactants (Phase A). All formulations contain the same amount of surfactants. Phase C contains the microbiological preservative.

The first step of foam preparation was to prepare Phase B, where the swelling of polymers lasted for 2 h in purified water. Phase C was then added to Phase A. The last step was the addition of Phase B to the mixture of Phases A and C. After the preparation of the samples, the liquids were stored in a well-sealed jar until the start of the examination. Before each investigation, 30 g of bulk liquid was stirred with an IKA stirrer for 5 min at 2000 rpm based on preformulation studies.

2.2.3. Investigation of foam properties

2.2.3.4. Macroscopic characterization of foams. The macroscopic properties of the foams were determined by using the cylinder method

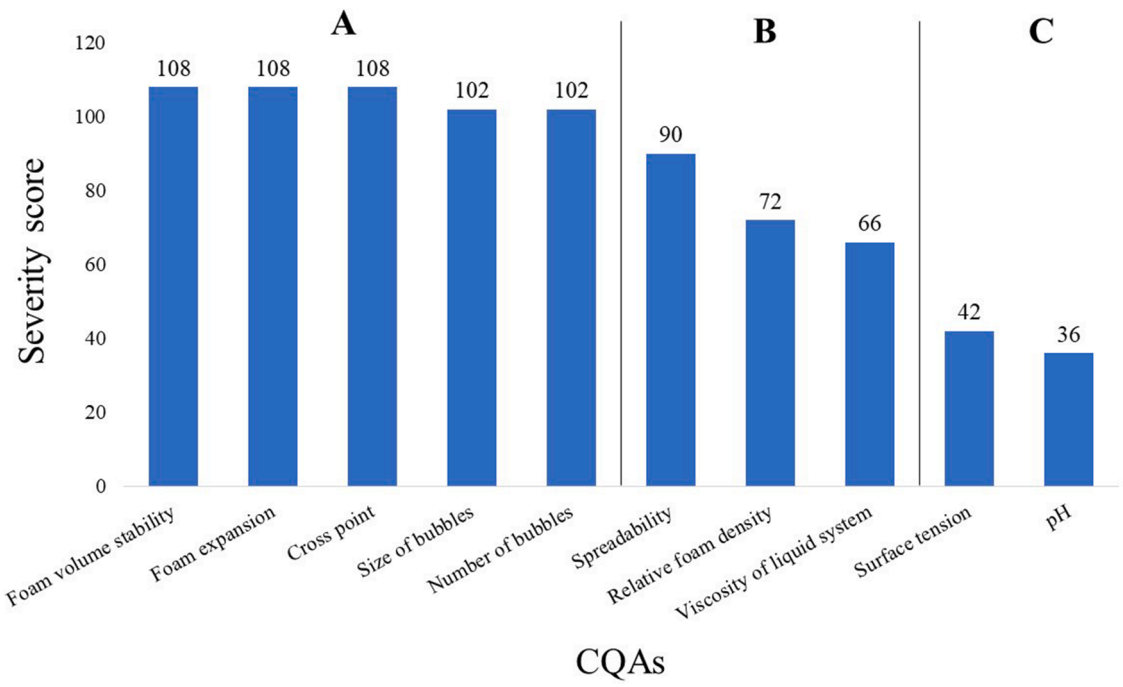

Fig. 2. Pareto chart of CQA parameters.

Table 5
Risk estimation matrix of CPPs/CMAs and CQA parameters (LeanQbD™ Software) Low = low-risk, Medium = medium-risk, High = high-risk parameters during formulation.

	Composition					Production		
	Polymer concentration	Polymer type	Surfactant concentration	Surfactant type	Preservative type	Stirring speed	Stirring time	Stirring temperature
pH	Low	High	Low	Low	Medium	Low	Low	Low
Viscosity of liquid system	High	High	Medium	Medium	Medium	Medium	Medium	Medium
Surface tension	Low	Medium	Low	Low	Low	Low	Low	Low
Size of bubbles (initial)	High	Medium	Medium	Medium	Low	High	High	Low
Number of bubbles (initial)	High	Medium	Medium	Medium	Low	High	High	Low
Foam volume stability	Medium	High	Low	Low	Low	Medium	Medium	Low
Foam expansion	High	Medium	Medium	Medium	Low	High	High	Low
Relative foam density	High	Medium	Medium	Medium	Low	High	High	Low
Cross point	High	High	Medium	Medium	Medium	Medium	Medium	Low
Spreadability	High	High	Medium	Medium	Low	Medium	Medium	Low

(Parsa et al., 2019). After stirring the bulk liquid for 5 min, the foam was filled into a glass measuring cylinder and the initial and the aged volumes of the foam after 30 min were recorded. The following parameters can be determined by macroscopic tests:

- relative foam density (RFD)
- foam expansion (FE,%)
- foam volume stability (FVS,%).

These parameters were calculated using the formula below (Arzhavitina and Steckel, 2010; Mirtič et al., 2017).

$$RFD = \frac{m(foam)}{m(water)} \quad (1)$$

The European Pharmacopoeia describes RFD in the Monograph "Medicated foams". It equals the weight of the test sample of foam compared to the weight of the same volume of water.

$$FE(\%) = \frac{V(foam) - V(formulation)}{V(formulation)} \cdot 100\% \quad (2)$$

where V(formulation) is the volume of the formulation [ml] required to produce V(foam) [ml] (Parsa et al., 2019).

$$FVS(\%) = \frac{V(foam,\ 30\ min)}{V(foam)} \cdot 100\% \quad (3)$$

where V(foam,30 min) is the foam volume after 30 min [ml].

2.2.4. Microscopic examination

The microscopic measurements were performed with Leica DM6 B Fully Automated Upright Microscope System (Leica Biosystems GmbH, Wetzlar, Germany) The structure of the foam from the microscopic images was analyzed after a predetermined time (0, 10, 20, 30 min).

Through microscopic examination, we can determine the structure and bubble size of the foams, providing information about the foam kinetics.

Foam uniformity can also be determined with this method as the homogeneity of air bubbles (Zhao et al., 2009). The size, roundness, and the aspect ratio of incorporated air bubbles as well as bubble amount in a predetermined area are the parameters of interest in foam

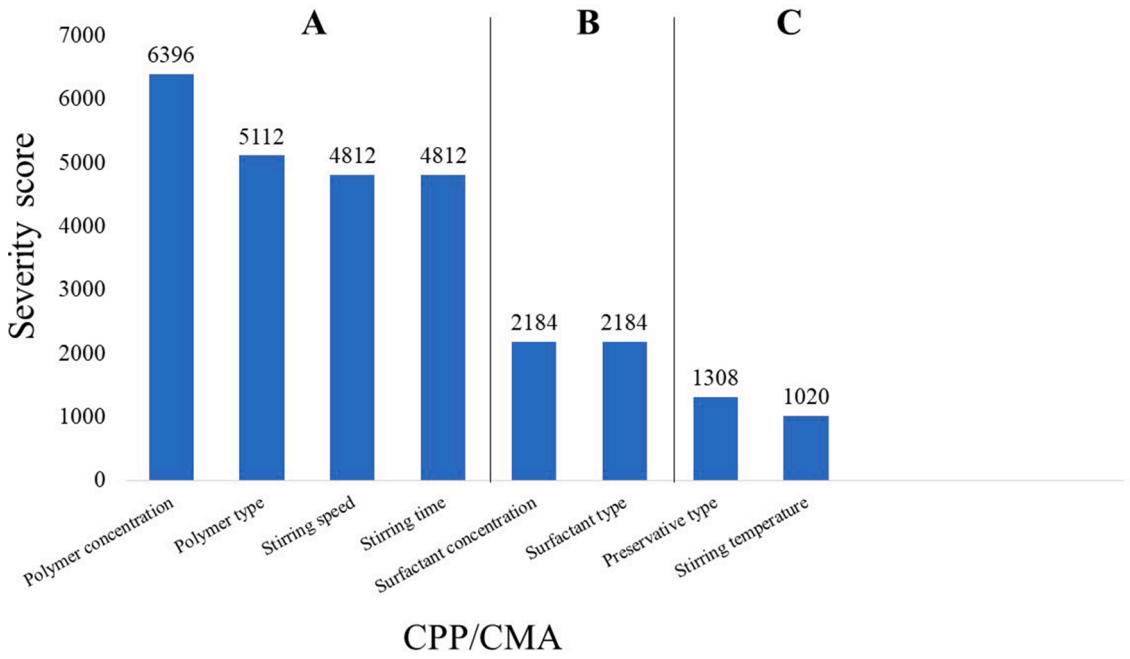

Fig. 3. Pareto chart of CPP/CMA parameters.

characterization.

With the microscopic method, the temporal stability of foams as well as the kinetics of the destabilization mechanism were determined. During the examination, the change in bubble size over time was also observed, which gave information about the stability of the foam samples.

2.2.5. Rheology

The rheological properties were studied with an Anton Paar Physica MCR302 Rheometer (Anton Paar, Graz, Austria). The measuring device was of the parallel plate type (diameter 50 mm, gap height 2 mm). The flow curves were recorded over the shear rate range from 0.1 to 100 and from 100 to 0.1 1/s at 25 °C for the liquid formula.

The foams were analyzed by means of amplitude sweeps, where the strain value was increased from 0.1% to 100%, and the angular frequency was 10 rad/s (Kealy et al., 2008).

2.2.6. Spreadability

The dermal application of any semi-solid dosage forms can be modeled with a texture analyzer. The forces required to spread the product on the skin were measured. The spreadability of the foams was investigated with a TA.XT plus Texture Analyzer (Stable Micro Systems Ltd., Vienna Court, Lammas Road, Godalming, Surrey, UK. GU7 1YL) using a TTC Spreadability Rig, which comprises a male 90° cone probe and a precisely matched female perspex cone-shaped product holder (Bayarri et al., 2012). During the test, the male cone immerses into the sample in the female cone until a gap of 1 mm is reached. The product is forced to flow outward at 45° between the male and female cone surfaces during the test, the ease of which indicates the degree of spreadability. The spreadability of the sample characterized the maximum force (firmness) recorded in the force-distance curve.

3. Results and discussion

3.1. Determination of QTPP and CQAs

The QTPP of the foams containing polymers includes the route of administration, dosage form, site of action, appearance of the drug delivery system, stability of the liquid system and the foam system, appearance of the liquid and the foam system and the polymer content of the foam for stability and skin application. The properties of the liquid system and the foam formed depend on the characteristics of the excipients used. The properties of the foams are influenced by several excipients, from which the polymer content was selected, and the influence of them was investigated. The polymer content can influence the stability of the foams. CQAs are defined from QTPPs. The CQAs were defined with the consideration of the attributes of the liquid system and the formed foam, too. On the one hand, the properties of the liquid systems are, for example, physical properties, viscosity, pH, surface tension. On the other hand, the formed foam system has attributes such as bubble size, foam stability, foam expansion, foam density, rheological properties, spreadability Tables 2. and 3 show the QTPP and CQA parameters with their targets and their justifications.

After the determination of QTPPs and CQAs, the following step is to determine the critical material attributes (CMAs) and the critical process parameters (CPPs) of the foams containing polymer with risk assessment.

3.2. Initial risk assessment

Risk assessment is the determination of the risks related to foams. Risk assessment tools can be utilized to rank and identify parameters based on their risk. An Ishikawa diagram represents the effect of the primary attributes and parameters of foams. It interprets the causes and sub-causes affecting the quality attributes of foam systems (Fig. 1).

The risk estimate matrix (REM) was used to assess the connection between CQAs and QTPPs (Table 4). A three-step scale was applied to rate the link between the CQA and QTPP parameters for the foam formulations: Low (low-risk parameters), Medium (medium-risk parameters), High (high-risk parameters) were the alternative levels. Based on the results of the REM, a Pareto chart (Fig. 2) was created to represent the severity scores of the CQAs

Our results show that five foam properties such as macroscopic foam stability, foam expansion, cross point, size of the bubbles and number of the bubbles are the most critical parameters, called Category A, with the highest severity score (> 100) during development. The next is Category B with a severity score of 60–90, which includes spreadability, relative foam density and viscosity of the liquid system. The third category of

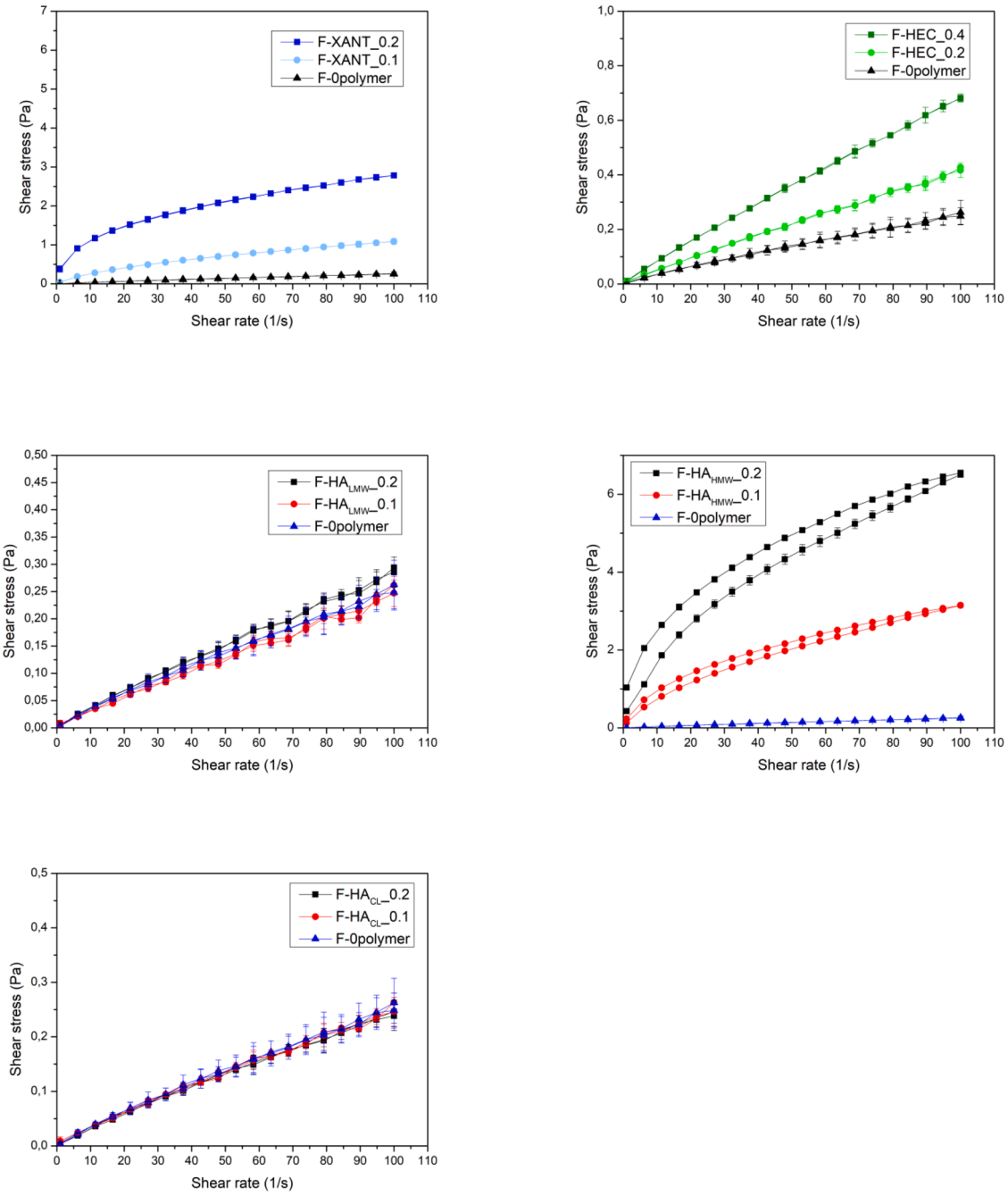

Fig. 4. Flow curves of bulk liquids.

severity scores is Category C (below 60), including parameters which have a low impact on product quality. High (Category A) and medium (Category B) risk parameters indisputably have an effect on the quality of foam systems. Therefore, these parameters were investigated.

The second REM (Table 5) presents the relationship between CQAs, CMAs and CPPs. The same scale was used for assessment (low, medium, high). The critical material attributes are polymer concentration and type, surfactant concentration and type, preservative type. The critical process parameters are the following: stirring speed, time and temperature.

In the light of the results of the initial risk assessment (Fig. 3), there are three groups of parameters regarding the risk level. In Category A, the critical parameters are both material and process parameters: polymer concentration and type, stirring speed and time with the highest severity score (> 4000). Category B includes surfactant concentration and type with a severity score of 2000–4000, which have a medium effect on quality. The parameters considered above are the parameters investigated during the experiment. Category C has the lowest impact (< 2000) on the quality of the foams: preservative type, stirring temperature. Based on the risk assessment, the critical (A) and medium critical (B) quality attributes, defined above, were investigated by varying the critical material and process parameters (A).

Among the QbD tools, the Ishikawa diagram was used to collect from literature and current knowledge all the material and process parameters, affecting the foam properties, from which the critical parameters were selected by REM and Pareto analysis.

According to the results, five CQAs, namely foam volume stability, foam expansion, cross point, the initial size of bubbles and the initial number of bubbles, were found to be critical attributes for the foam system. Moreover, three CQAs, namely spreadability, relative foam

Table 6
Effect of mixing time and speed on foam volume.

F-0polymer	1000 rpm	1500 rpm	2000 rpm
5 mins	×	×	✓
10 mins	×	×	✓
15 mins	×	×	✓
F-XANT_0.2			
5 mins	×	×	✓
10 mins	×	✓	✓
15 mins	×	✓	✓
F-HEC_0.4			
5 mins	×	×	✓
10 mins	×	×	✓
15 mins	×	×	✓
F-$HA_{lmw\_}$ 0.2			
5 mins	×	×	✓
10 mins	×	×	✓
15 mins	×	×	✓
F-$HA_{hmw\_}$ 0.2			
5 mins	×	×	✓
10 mins	×	✓	✓
15 mins	×	✓	✓

density, the viscosity of the liquid system, were found to be attributes of medium influence. These parameters were investigated in the course of the research work. Thus, the number of ten quality attributes of foams, determined based on prior knowledge and literature, was reduced to five with initial risk assessment. Then, test methods were developed to investigate these five critical quality attributes.

Furthermore, the initial risk assessment showed that there were two highly critical material parameters for CQAs that were the concentration and type of polymers, and two highly critical process parameters were found in this development, namely the stirring speed and time. Consequently, the number of eight material and process parameters, influencing the quality attributes of foams, was reduced to four with initial risk assessment and the effect of varying these parameters was investigated.

3.3. Preformulation studies of bulk liquid–Rheological investigation

Based on the results of the risk assessment, the viscosity of the bulk liquids was tested first. Rheological parameters are sensitive indicators of changes within liquid, semi-solid, foam formulations, e.g., they are suitable for characterizing the spreadability, consistency, and stability of the formulation.

The viscosity of the initial liquid preparation can have an effect on the formation of foam. Too high viscosity can hinder foam formation, while too low viscosity can lead to fast destabilization.

Polymer solutions are characterized by a shear-thinning flow due to the shear orientation of the macromolecules. For xanthan gum and HEC-containing solutions, a more significant jump in values can be seen with increasing concentration. The rheological behavior of low molecular weight hyaluronic acid and cross-linked hyaluronic acid-containing solutions was similar to that of the polymer-free solution, no significant increase in rheological parameters was observed with the polymer content. In contrast, high molecular weight hyaluronic acid behaves similarly to xanthan gum, the polymer is characterized by a thinning flow to solution shear, and even slight thixotropy is observed (Fig. 4).

3.4. Preformulation studies of foams of CPPs

Preformulation tests were carried out to select the appropriate mixing time and speed. These were essential to produce a foam with the right consistency. The bulk liquid was stirred at different speeds (1000 rpm, 1500 rpm, 2000 rpm) for different lengths of time (5, 10, 15 min). Our goal was to produce a foam macroscopically suitable for testing purposes. We aimed to have a foam with twice the volume of the liquid to carry out the tests (✓: complies with the criteria, ×: does not comply with the criteria). Based on the results (Table 6), a foam of sufficient consistency for the tests was obtained at 2000 rpm after 5 min.

3.5. Investigation of foam properties

3.5.1. Macroscopic properties

Through the determination of macroscopic properties (cylinder method), we can acquire information on the stability of foam formulations (foam expansion, foam volume stability, relative foam density). Based on the macroscopic tests, polymer-containing foams are more stable formulations than the polymer-free one. In the tested formulations, F-XANT_0.1, F-XANT_0.2, F-HA_{HMW}_0.1 and F-HA_{HMW}_0.2 had the highest stability but the lowest foam expansion values. In general, the results show that the greater the foam expansion, the higher its foamability, and the higher the foam volume stability value, the more stable the resulting foam. From the tested formulations, the well-foaming composition was foams with an expansion above 150%. The most stable formulations are the formulations with foam volume stability above 70%, and in this case these were F-XANT_0.2 and F-HA_{HMW}_0.2 (Table 7).

The macroscopic examinations showed that the polymer-free composition had a high value of foam expansion but a low value of foam stability, which was also apparent because the structure of the foam was broken down quickly. Similarly to the polymer-free formulation, F-HEC_0.2, F-HA_{LMW}_0.1 and F-HA_{LMW}_0.2 showed high foam expansion and low foam stability. F-HA_{CL} showed low foam stability at both concentrations tested, however, its foam expansion was not high either. F-XANT and F-HA_{HMW} formulations showed high foam stability at both concentrations tested.

As the polymer concentration was increased, foam density increased for all polymers used, however, based on the results, it did not correlate with foam stability and foam expansion results.

3.5.2. Microscopic properties

3.5.2.5. Structure and homogeneity. The structure of each foam containing different polymers can be observed with the help of microscopic

Table 7
Results of macroscopic investigations and the viscosity of bulk liquid.

	Viscosity of bulk liquid [mPa•s] (50 1/s)	FE [%]	FVS [%]	RFD
F-0polymer	3.06 ± 0.56	172 ± 15.7	14 ± 1.81	0.2028
F-XANT_0.1	14.32 ± 0.96	158 ± 3.84	95 ± 0.78	0.3879
F-XANT_0.2	42.05 ± 0.22	134 ± 1.92	100 ± 0	0.4265
F-HEC_0.2	4.38 ± 0.19	177 ± 0	15 ± 1.39	0.3614
F-HEC_0.4	7.27 ± 0.22	164 ± 1.92	29 ± 1.28	0.3781
F-HA_{LMW}_0.1	2.67 ± 0.26	179 ± 1.92	14 ± 0.09	0.3585
F-HA_{LMW}_0.2	3.00 ± 0.23	177 ± 0	14 ± 0.35	0.3614
F-HA_{HMW}_0.1	44.22 ± 0.24	130 ± 3.33	77 ± 14.22	0.4348
F-HA_{HMW}_0.2	97.79 ± 1.44	126 ± 3.85	94 ± 0.09	0.4434
F-HA_{CL}_0.1	2.57 ± 0.15	130 ± 3.33	15 ± 0.87	0.4348
F-HA_{CL}_0.2	2.64 ± 0.06	130 ± 3.33	14 ± 0.21	0.4348

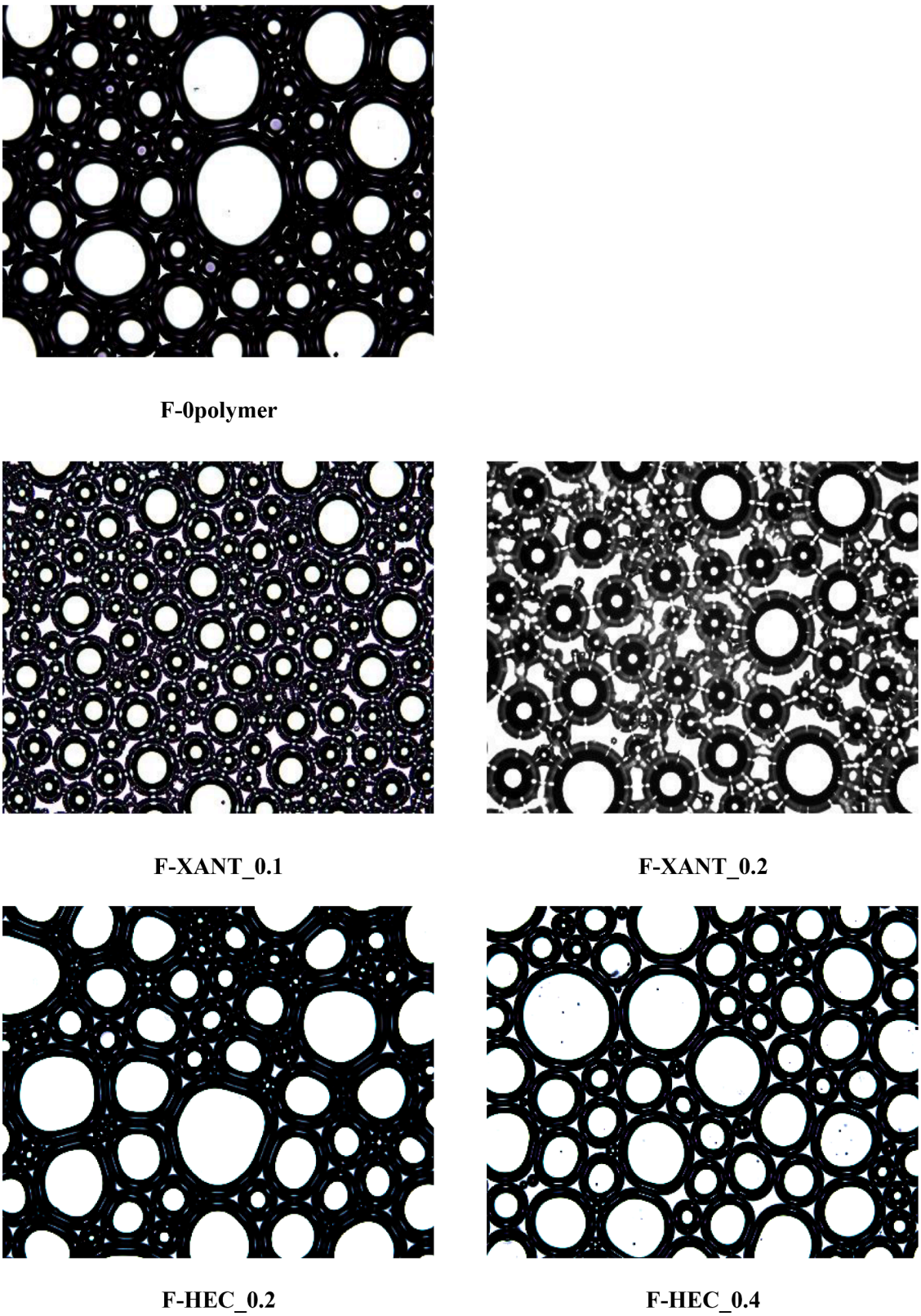

Fig. 5. Microscopic images.

images (Fig. 5). Foams which contain larger bubbles from the beginning are more friable. The size of the bubbles depends on the concentration of the polymer. In the case of F-XANT, F-HA_{HMW}, and F-HA_{CL} with increasing polymer concentration, the initial size of the bubbles was also larger. The lamellas between two bubbles are thinner in F-HEC than in formulations containing xanthan gum and high molecular weight and cross-linked hyaluronic acid.

The homogeneity of formulations can be determined by bubble size

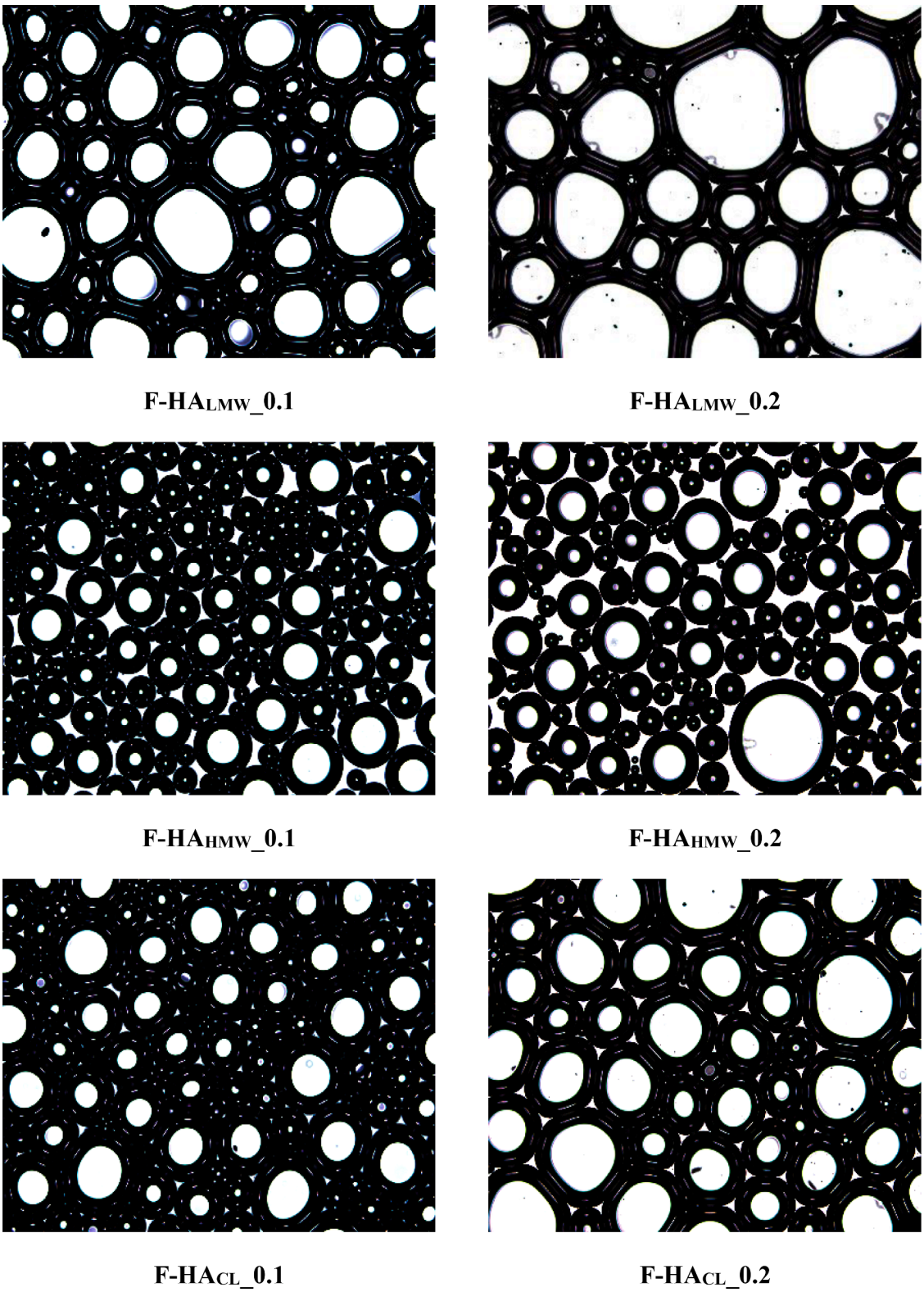

Fig. 5. (*continued*).

analysis (Table 8). An example of bubble size analysis performed by the software is shown in Fig. 6. During editing the bar charts, the data were plotted in the range between the minimum and maximum areas. All foam systems are polydisperse.

3.5.2.6. Kinetics of foam stability. The kinetics of foam destabilization was observed with microscopic examinations. Bubble sizes were detected in microscopic images taken after a predetermined time (0, 10, 20, 30 min). The microscopic pictures showed that the increasing size of the bubbles leads to the destabilization of the foam over time. The stability of the foams could be determined by kinetic analysis Fig. 7. shows the number of bubbles versus time. Foams with an initial bubble count

Table 8
Results of microscopic investigations.

	Minimum area (μm^2)	Maximum area (μm^2)	Mean (μm^2)	Std Dev
F-0polymer				
0 min	**505**	**306 477**	**63 957**	**63 726**
F-XANT_0.1				
0 min	**1339**	**88 659**	**23 718**	**17 973**
F-XANT_0.2				
0 min	**1494**	**174 564**	**26 346**	**31 479**
F-HEC_0.2				
0 min	**3114**	**277 779**	**53 018**	**54 914**
F-HEC_0.4				
0 min	**1015**	**243 753**	**47 054**	**45 447**
F-HA$_{LMW}$_0.1				
0 min	**8574**	**235 000**	**69 631**	**50 716**
F-HA$_{LMW}$_0.2				
0 min	**10 593**	**366 345**	**115 178**	**94 767**
F-HA$_{HMW}$_0.1				
0 min	**456**	**103 582**	**22 721**	**22 420**
F-HA$_{HMW}$_0.2				
0 min	**382**	**286 301**	**23 700**	**31 159**
F-HA$_{CL}$_0.1				
0 min	**5796**	**120 204**	**46 715**	**30 937**
F-HA$_{CL}$_0.2				
0 min	**8281**	**245 578**	**73 323**	**47 835**

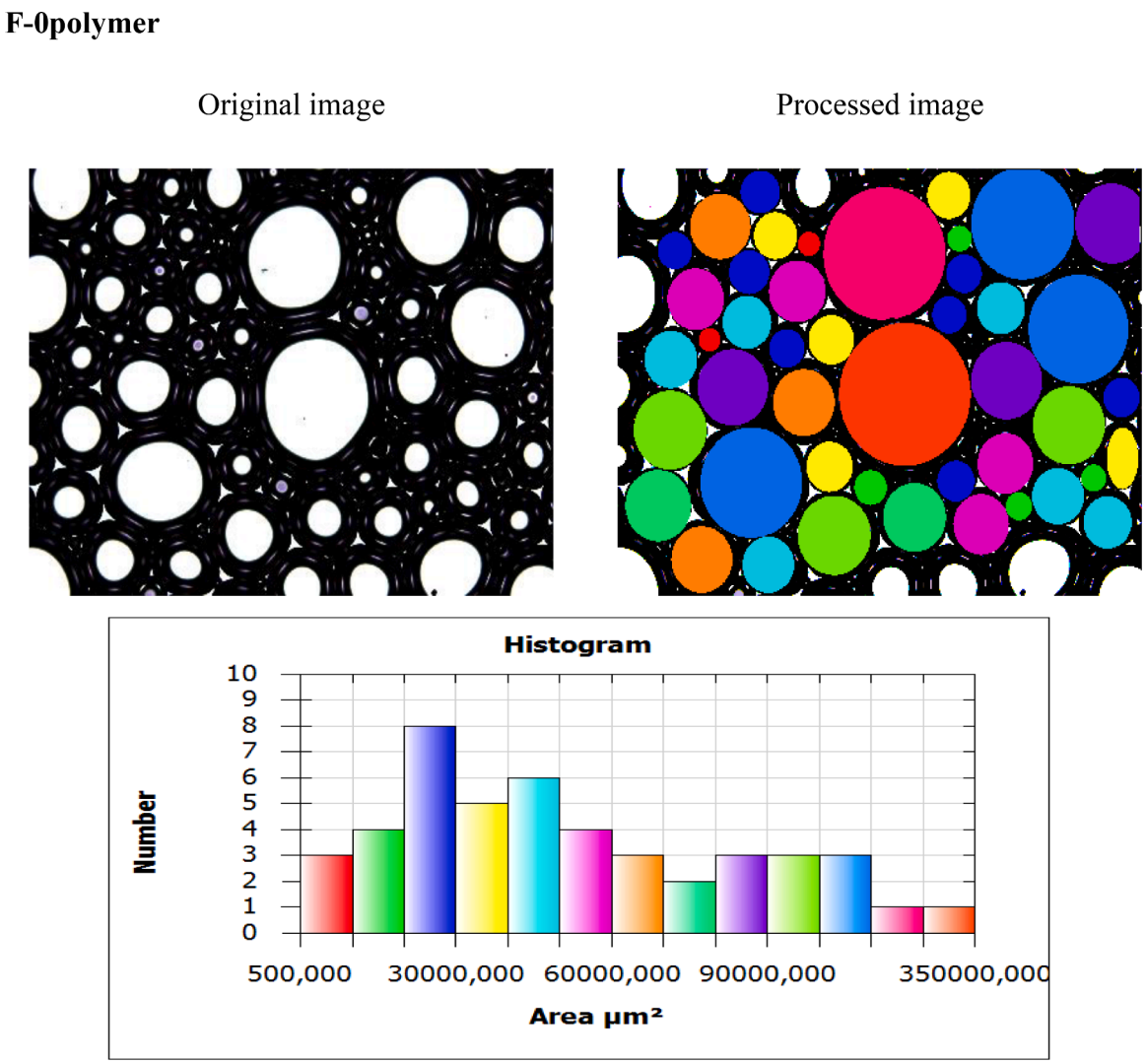

Fig. 6. The method of bubble size analysis in the case of F-0polymer.

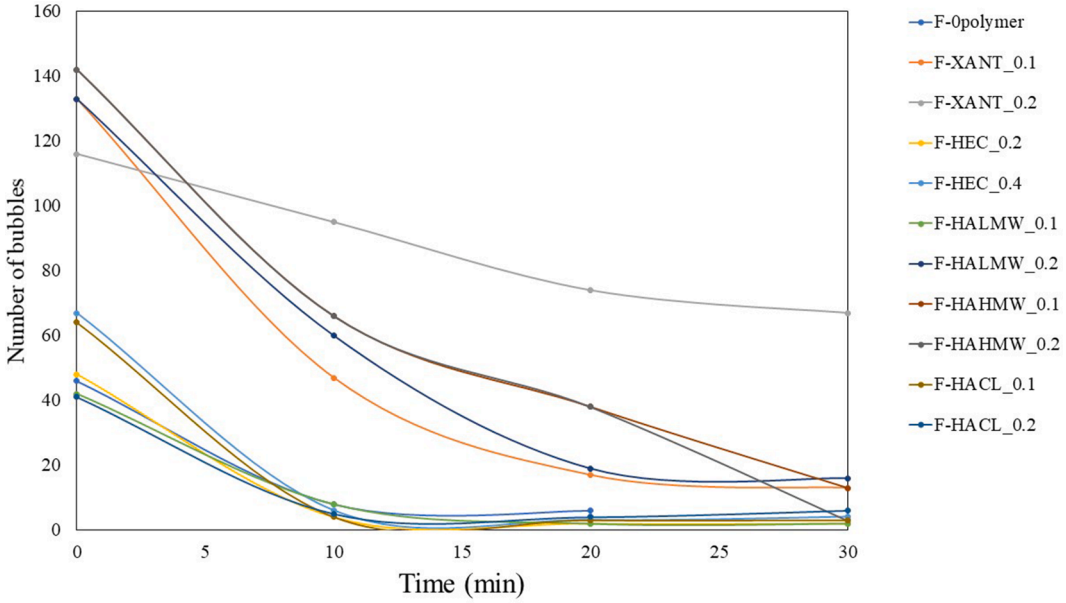

Fig. 7. Kinetics of foam destabilization.

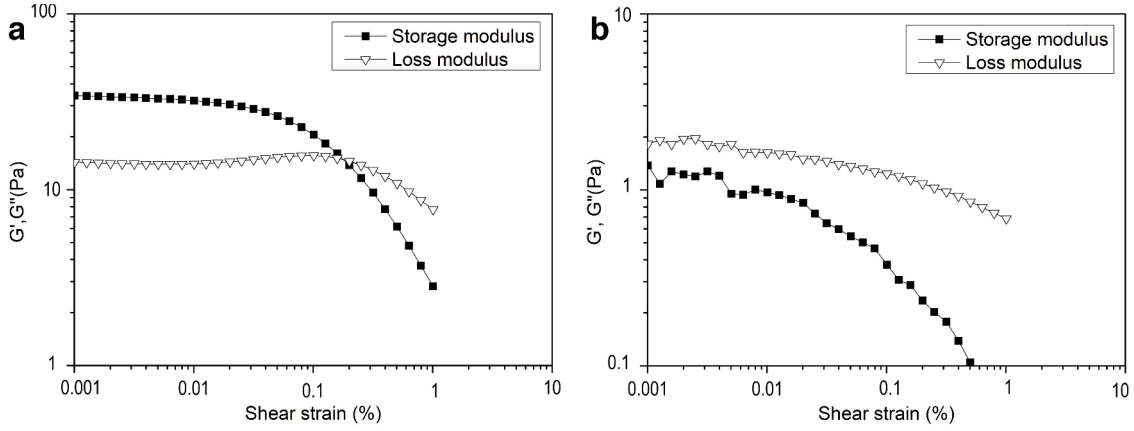

Fig. 8. Typical rheological behavior of the formulated foams; stable (a) and unstable (b) foams.

above 100 were microscopically stable. These are F-XANT_0.1, F-XANT_0.2, F-HA_{LMW}_0.2, F-HA_{HMW}_0.1 and F-HA_{HMW}_0.2, which shows that the results correlated well with the stability determined by the macroscopic FVS% method.

3.5.2.7. Rheology–Oscillometric measurement. The structure of the foam is built up of a network of bubbles. A coherent structure can be formed due to the cohesive dispersion medium formed among the bubbles. This structure can be analysed by oscillatory rheology (Dollet and Raufaste, 2014), (Thurston and Martin, 1978). The viscoelastic property of a material can be expressed by the value of the G' (storage modulus) and G" (loss modulus) parameters and their relationship to each other. In the case of amplitude sweep, the point of intersection of the two curves can be interpreted as a flow point (γ_f). The linear viscoelastic (LVE) range and its limit (yield point, γ_y), which indicate the stability of a coherent structure, can be also determined. In this range, G' and G" are constant, the structure is maintained. The wider this range, the more stable the structure.

Two typical amplitude sweep curves can be distinguished: one which represents a wider LVE range, the elastic modulus is higher than the viscous one, and the moduli are constant up to higher strain values, indicating a more stable coherent structure (Fig. 8.a). The other type of rheological behavior of the foam is when G" dominates over G' in the entire strain range, and a crossover point cannot be detected (Fig. 8.b). These preparations did not form a real coherent foam structure.

The measurable rheological parameters of the foams are summarized in Table 9.

Some foam formulations showed that G" values were higher than G' in the LVE region. These samples had a yield point (detectable limit of LVE range) but no flow point because the structure of these foams did not form a coherent structure, they behaved like liquids. There were other cases where it was not measurable due to foam instability. The polymer-free foam has no flow point, which means it flows from the beginning. The limit of the LVE range was the highest after 10 min due to liquid drainage from the interspace between the bubbles.

F-XANT_0.1 and F-XANT_0.2 have higher γ_y and γ_f values than the polymer-free foam. With increasing concentration, the values of flow point also showed an increase. F-XANT_0.1 was still stable after 30 min, however, higher concentration results in a less stable formulation after 30 min. This can be explained by the fact that too high a polymer content can cause the destabilization of the foam.

The structure of F-HEC_0.2 and F-HEC_0.4 was less coherent than that of F-XANT. Stability decreased over time. Rheological values changed in direct proportion to polymer concentration.

Table 9
Rheological parameters derived from the amplitude sweep curves.

	γ_f (%)	γ_y (%)
F-0polymer		
0 min	×	0.202
10 min	×	0.49
20 min	×	0.205
30 min	not measurable	not measurable
F_XANT_0.1		
0 min	15.9	0.43
10 min	4	0.192
20 min	7.98	0.196
30 min	7.98	0.204
F-XANT_0.2		
0 min	10.1	0.23
10 min	12.7	0.237
20 min	15.9	0.255
30 min	20.1	0.73
F-HEC_0.2		
0 min	×	0.245
10 min	0.318	0.104
20 min	×	101
30 min	not measurable	not measurable
F-HEC_0.4		
0 min	×	0.421
10 min	0.318	0.163
20 min	0.159	0.152
30 min	not measurable	not measurable
F-HA_{LMW}_0.1		
0 min	2.01	0.199
10 min	×	0.311
20 min	×	0.136
30 min	not measurable	not measurable
F-HA_{LMW}_0.2		
0 min	×	0.22
10 min	×	0.112
20 min	×	1.07
30 min	not measurable	not measurable
F-HA_{HMW}_0.1		
0 min	×	0.248
10 min	12.7	0.309
20 min	15.9	0.283
30 min	20.1	0.369
F-HA_{HMW}_0.2		
0 min	0.634	0.157
10 min	25.2	0.79
20 min	31.8	0.69
30 min	31.8	0.658
F-HA_{CL}_0.1		
0 min	0.798	0.206
10 min	×	0.13
20 min	×	0.334
30 min	not measurable	not measurable
F-HA_{CL}_0.2		
0 min	×	0.221
10 min	×	0.331
20 min	not measurable	not measurable
30 min	not measurable	not measurable

x: no cross point.
not measurable: the foam sample was immeasurable due to destabilization.

F-HA_{LMW} formulations were measurable for 20 min. The foam containing the lower concentration of polymer started to lose its coherent structure after 10 min. The increase in the amount of polymer made it more stable after 20 min.

F-HA_{HMW} had the best rheological properties among our formulations. Both concentrations had a decrease in the rheological values after 20 min. However, after 30 min, F-HA_{HMW}_0.1 proved to be more coherent. As with the xanthan gum-containing foam, higher polymer concentration caused the breakage of the coherent structure of the foam.

Cross-linked hyaluronic acid also caused the early breakage of the structure of the foam. The higher the polymer concentration, the earlier the breakage of the coherent structure occurs.

The long-term stability of the foam is insufficient for possible application to the skin. Our results indicate that xanthan gum-containing and high molecular weight hyaluronic acid foams met this requirement. These results correlated well with FVS% values.

3.5.2.8. Spreadability. Spreadability is the ability of foam to spread on the skin. If spreadability values decrease, the application of the foam is easier (Djiobie Tchienou et al., 2018).

The force is applied with a male cone probe, which penetrates through the foam to a certain depth. During penetration, the force gradually increases to the maximum penetration depth. The maximum force (firmness) is obtained during the measurement. Primarily, the factors that affect the firmness of the foam are the viscosity of the bulk liquid, the interactions between the bubbles, the distribution of the bubbles and the geometry of the bubbles. The results show that the lower the detected force, the easier for the foam to spread. Secondly, the greater the force required to spread, the more stable the foam.

The spreadability of the polymer-free foam is not-compliant, it starts to flow very quickly. On the basis of the results, in general, the polymer content improved the firmness of the foam (Fig. 9), which would prevent the formulation from flowing off the skin. As the concentration increases, the force required to spread the foam is also greater. In the case of high molecular weight hyaluronic acid-containing foams, the greatest force was required to spread the foam formulation. Our results indicate that xanthan gum-containing and high molecular weight hyaluronic acid foams met this requirement and correlated with the macroscopic investigations.

4. Conclusions

The aim of our study was to find, develop and compare the test methods that are suitable for the investigation of foam compositions, and with their help to select the appropriate composition during the development of a foam formula. The application of the QbD concept, including risk assessment, was of great help in the development of methods for testing foams.

The purpose of this research work was to acquire a better knowledge of the properties of API free foams as a delivery system and to establish control methods suitable for testing the foams.

Considering the results of initial risk assessment, eleven compositions were formed and investigated.

During the initial risk assessment, five CQAs, namely foam volume stability, foam expansion, cross point, size of bubbles and number of bubbles were found to be highly critical attributes, and three CQAs, namely spreadability, foam density and the viscosity of the liquid system were found to be medium critical attributes in the development of foam formulations. These parameters were investigated. The initial risk assessment also showed that there are two material parameters, polymer concentration and polymer type, which were highly critical parameters for CQAs, while surfactant had a medium impact on CQAs.

In summary, the polymer content has a great effect on the properties of the foams. Different polymers affect the properties of foams in different ways Table 10. summarizes and compares the results obtained on the basis of the previously established requirements (Table 3). When used in combination, the methods reinforce each other and help to select a formula for dermal application. Based on our results, formulations F-XANT_0.1, F-XANT_0.2, F-HA_{HMW}_0.1 and F-HA_{HMW}_0.2 have good foam properties and will be appropriate delivery systems for an active pharmaceutical ingredient. The results of the different methods showed good correlation and can be used in preformulation studies. The appropriate formula can be selected by using macroscopic method of foam stability (FVS), the investigation of the number of bubbles with a light microscope, and the oscillometric measurement methods of cross-point determination. While previous research papers have used these test methods separately, the selection protocol of an appropriate foam formula has been developed based on the results of the present research

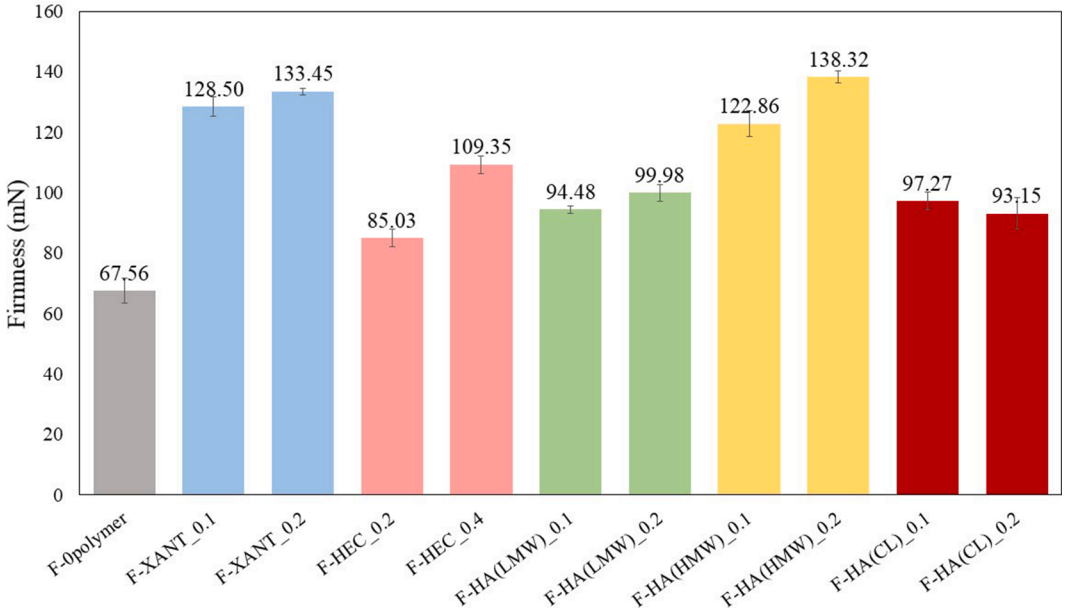

Fig. 9. Foam firmness.

Table 10
Summary of the investigation of foams; ✓✓: Exceptionally good result, ✓: The result meets the target requirement, ×: The result does not meet the target requirement.

Investigation	Target	F-0polymer	F-XANT_0.1	F-XANT_0.2	F-HEC_0.2	F-HEC_0.4	F-HA_{LMW}_0.1	F-HA_{LMW}_0.2	F-HA_{HMW}_0.1	F-HA_{HMW}_0.2	F-HA_{CL}_0.1	F-HA_{CL}_0.2
Foam expansion	100% ≤	✓✓	✓✓	✓	✓✓	✓✓	✓✓	✓✓	✓	✓	✓	✓
Foam density	≤ 0.5	✓	✓	✓	✓	✓	✓	✓	✓	✓	✓	✓
Number of bubbles (Initial values)	100 <	×	✓	✓	×	×	×	✓	✓	✓	×	×
Spreadability	< 500 mN	✓	✓	✓	✓	✓	✓	✓	✓	✓	✓	✓
Cross point	Detectable	×	✓	✓	×	×	✓	×	×	✓	✓	×
Foam volume stability	50% ≤	×	✓✓	✓✓	×	×	×	×	✓✓	✓✓	×	×
Viscosity of liquid system	20–200 mPas	×	×	✓	×	×	×	×	✓	✓	×	×

and these results assist in the development of pharmaceutical foams to determine the control strategy. Furthermore, the results of the present research on foams have expanded the knowledge space. Based on the results, we plan to develop an experimental design for API-containing foams in the future.

Funding

The publication was supported by The University of Szeged Open Access Fund (FundRef, Grant No. 5579).

Project no. TKP2021-EGA-32 has been implemented with the support provided by the Ministry of Innovation and Technology of Hungary from the National Research, Development and Innovation Fund, financed under the TKP2021-EGA funding scheme

CRediT authorship contribution statement

Fanni Falusi: Writing – original draft, Methodology, Investigation, Visualization. **Mária Budai-Szűcs:** Software, Methodology. **Erzsébet Csányi:** Supervision, Writing – review & editing. **Szilvia Berkó:** Methodology, Writing – review & editing. **Tamás Spaits:** Methodology. **Ildikó Csóka:** Conceptualization. **Anita Kovács:** Supervision, Conceptualization, Writing – review & editing.

References

Arzhavitina, A., Steckel, H., 2010. Foams for pharmaceutical and cosmetic application. Int. J. Pharm. 394 (1–2), 1–17. https://doi.org/10.1016/j.ijpharm.2010.04.028.

Bakonyi, Mónika, Berkó, Szilvia, Kovács, Anita, Budai-Szűcs, Mária, Kis, Nikolett, Erős, Gábor, Csóka, Ildikó, Csányi, Erzsébet, 2018. Application of quality by design principles in the development and evaluation of semisolid drug carrier systems for the transdermal delivery of lidocaine. J. Drug Deliv. Sci. Technol. 44 (April), 136–145. https://doi.org/10.1016/j.jddst.2017.12.001.

Bayarri, S., Carbonell, I., Costell, E., 2012. Viscoelasticity and texture of spreadable cheeses with different fat contents at refrigeration and room temperatures. J. Dairy Sci. 95 (12), 6926–6936. https://doi.org/10.3168/jds.2012-5711.

Berkó, Szilvia, Maroda, Mónika, Bodnár, Magdolna, Erős, Gábor, Hartmann, Petra, Szentner, Kinga, Szabó-Révész, Piroska, Kemény, Lajos, Borbély, János, Csányi, Erzsébet, 2013. Advantages of cross-linked versus linear hyaluronic acid for semisolid skin delivery systems. Eur. Polym. J. 49 (9), 2511–2517. https://doi.org/10.1016/j.eurpolymj.2013.04.001.

Bikard, J., Bruchon, J., Coupez, T., Silva, L., 2007. Numerical simulation of 3D polyurethane expansion during manufacturing process. Colloids Surf. A 309 (1–3), 49–63. https://doi.org/10.1016/j.colsurfa.2007.04.025.

Bureiko, Andrei, Trybala, Anna, Kovalchuk, Nina, Starov, Victor, 2015. Current applications of foams formed from mixed surfactant–polymer solutions. Adv. Colloid Interface Sci. 222 (August), 670–677. https://doi.org/10.1016/j.cis.2014.10.001.

Cantat, Isabelle, Cohen-Addad, Sylvie, 2021. *Foams: Structure and Dynamics. Foams.* FlorenceElias, FrançoisGraner, ReinhardHöhler, OlivierPitois, Florence Rouyer, and Arnaud Saint-Jalmes. n.d. Oxford University Press. Accessed. https://oxford.universitypressscholarship.com/view/10.1093/acprof:oso/9780199662890.001.0001/acprof-9780199662890.

Charoo, Naseem A., Shamsher, Areeg A.A., Zidan, Ahmed S., Rahman, Ziyaur, 2012. Quality by design approach for formulation development: a case study of dispersible tablets. Int. J. Pharm. 423 (2), 167–178. https://doi.org/10.1016/j.ijpharm.2011.12.024.

Djiobie Tchienou, Gertrude, Roli Tsatsop, Tsague, Therese Mbam, Pega, Vera, Bama, Albert, Bamseck, Selestin Dongmo, Sokeng, Ngassoum, Martin, 2018. Multi-response

optimization in the formulation of a topical cream from natural ingredients. Cosmetics 5 (1), 7. https://doi.org/10.3390/cosmetics5010007.
Dollet, Benjamin, Raufaste, Christophe, 2014. Rheology of aqueous foams. C.R. Phys. 15 (8–9), 731–747. https://doi.org/10.1016/j.crhy.2014.09.008.
Draelos, Zoe Diana, 2011. A clinical evaluation of the comparable efficacy of hyaluronic acid-based foam and ceramide-containing emulsion cream in the treatment of mild-to-moderate atopic dermatitis: barrier restoration therapy in atopic dermatitis. J. Cosmet. Dermatol. 10 (3), 185–188. https://doi.org/10.1111/j.1473-2165.2011.00568.x.
Farkas, Dóra, Kállai-Szabó, Nikolett, Antal, István, 2019. Foams as carrier systems for pharmaceuticals and cosmetics. Acta Pharm. Hung. 89 (1), 5–15. https://doi.org/10.33892/aph.2019.89.5-15.
Farkas, Dóra, Kállai-Szabó, Nikolett, Sárádi-Kesztyűs, Ágnes, Lengyel, Miléna, Magramane, Sabrina, Kiss, Éva, Antal, István, 2021. Investigation of propellant-free aqueous foams as pharmaceutical carrier systems. Pharm. Dev. Technol. 26 (3), 253–261. https://doi.org/10.1080/10837450.2020.1863426.
Grangeia, Helena Bigares, Silva, Cláudia, Simões, Sérgio Paulo, Reis, Marco S., 2020. Quality by design in pharmaceutical manufacturing: a systematic review of current status, challenges and future perspectives. Eur. J. Pharm. Biopharm. 147 (February), 19–37. https://doi.org/10.1016/j.ejpb.2019.12.007.
Guerrero, Jáder, Mejia-Ospino, Enrique, Cabanzo, Rafael, 2013. Monitoring foam coarsening using a computer optical mouse as a dynamic laser speckle measurement sensor. Pramana 81 (6), 987–994. https://doi.org/10.1007/s12043-013-0617-1.
Hoc, Dagmara, Haznar-Garbacz, Dorota, 2021. Foams as unique drug delivery systems. Eur. J. Pharm. Biopharm. 167 (October), 73–82. https://doi.org/10.1016/j.ejpb.2021.07.012.
'ICH Guideline Q9 on quality risk management. n.d., 20. 2021.
Kamal, Muhammad., 2019. A novel approach to stabilize foam using fluorinated surfactants. Energies 12 (6), 1163. https://doi.org/10.3390/en12061163.
Karakashev, Stoyan I., Georgiev, Petyr, Balashev, Konstantin, 2012. Foam production–ratio between foaminess and rate of foam decay. J. Colloid Interface Sci. 379 (1), 144–147. https://doi.org/10.1016/j.jcis.2012.04.048.
Kealy, Tim, Abram, Alby, Hunt, Barry, Buchta, Richard, 2008. The rheological properties of pharmaceutical foam: implications for use. Int. J. Pharm. 355 (1–2), 67–80. https://doi.org/10.1016/j.ijpharm.2007.11.057.
Kis, Nikolett, Kovács, Anita, Budai-Szűcs, Mária, Gácsi, Attila, Csányi, Erzsébet, Csóka, Ildikó, Berkó, Szilvia, 2019. Investigation of silicone-containing semisolid in situ film-forming systems using QbD tools. Pharmaceutics 11 (12), 660. https://doi.org/10.3390/pharmaceutics11120660.
Kovács, A., Berkó, Sz., Csányi, E., Csóka, I., 2017. Development of nanostructured lipid carriers containing salicyclic acid for dermal use based on the quality by design method. Eur. J. Pharm. Sci. 99 (March), 246–257. https://doi.org/10.1016/j.ejps.2016.12.020.
Kovács, Anita, Kis, Nikolett, Budai-Szűcs, Mária, Gácsi, Attila, Csányi, Erzsébet, 2020. QbD-based investigation of dermal semisolid in situ film-forming systems for local anaesthesia. Drug Des. Devel. Ther. 14 (November), 5059–5076. https://doi.org/10.2147/DDDT.S279727.
Lambers, H., Piessens, S., Bloem, A., Pronk, H., Finkel, P., 2006. Natural skin surface PH Is on average below 5, which is beneficial for its resident flora. Int. J. Cosmet. Sci. 28 (5), 359–370. https://doi.org/10.1111/j.1467-2494.2006.00344.x.
Langevin, Dominique., 2017. Aqueous foams and foam films stabilised by surfactants. gravity-free studies. Comptes Rendus Mécanique 345 (1), 47–55. https://doi.org/10.1016/j.crme.2016.10.009.
Mirtič, Janja, Papathanasiou, Foteini, Temova Rakuša, Žane, GosencaMatjaž, Mirjam, Roškar, Robert, Kristl, Julijana, 2017. Development of medicated foams that combine incompatible hydrophilic and lipophilic drugs for psoriasis treatment. Int. J. Pharm. 524 (1–2), 65–76. https://doi.org/10.1016/j.ijpharm.2017.03.061.
Parsa, Maryam, Trybala, Anna, Malik, Danish Javed, Starov, Victor, 2019. Foam in pharmaceutical and medical applications. Curr. Opin. Colloid Interface Sci. 44 (December), 153–167. https://doi.org/10.1016/j.cocis.2019.10.007.
Radhakrishnan, Vinay, Davis, Penny, Hiebert, David, 2018. Scientific approaches for the application of QbD principles in lyophilization process development. In: Warne, Nicholas W., Mahler, Hanns-Christian (Eds.), Challenges in Protein Product Development. Springer International Publishing, Cham. https://doi.org/10.1007/978-3-319-90603-4_20, 38:441–71. AAPS Advances in the Pharmaceutical Sciences Series.
Sivaraman, Arunprasad, Banga, Ajay, 2015. Quality by design approaches for topical dermatological dosage forms. Res. Rep. Transdermal Drug Deliv. (July), 9. https://doi.org/10.2147/RRTD.S82739.
Tamarkin, Dov, Friedman, Doron, Shemer, Avner, 2006. Emollient foam in topical drug delivery. Expert Opin. Drug Deliv. 3 (6), 799–807. https://doi.org/10.1517/17425247.3.6.799.
Thurston, George B., Martin, Alfred, 1978. Rheology of pharmaceutical systems: oscillatory and steady shear of non-Newtonian viscoelastic liquids. J. Pharm. Sci. 67 (11), 1499–1506. https://doi.org/10.1002/jps.2600671103.
Vandewalle, N., Caps, H., Delon, G., Saint-Jalmes, A., Rio, E., Saulnier, L., Adler, M., et al., 2011. Foam stability in microgravity. J. Phys. Conf. Ser. 327 (December), 012024 https://doi.org/10.1088/1742-6596/327/1/012024.
Velasco, M., González-Fernández, D., Rodriguez-Martín, M., Sánchez-Regaña, M., Pérez-Barrio, S., 2019. Patient and physician satisfaction with calcipotriol and betamethasone dipropionate aerosol foam in the treatment of plaque psoriasis on the body. Actas Dermo-Sifiliogr. 110 (9), 752–758. https://doi.org/10.1016/j.adengl.2019.07.022.
Visser, J.Carolina, Dohmen, Willem M.C., Hinrichs, Wouter L.J., Breitkreutz, Jörg, Frijlink, Henderik W., Woerdenbag, Herman J., 2015. Quality by design approach for optimizing the formulation and physical properties of extemporaneously prepared orodispersible films. Int. J. Pharm. 485 (1–2), 70–76. https://doi.org/10.1016/j.ijpharm.2015.03.005.
Yadav, Narayan Prasad, Rai, Vineet Kumar, Mishra, Nidhi, Sinha, Priyam, Bawankule, Dnyaneshwar Umrao, Pal, Anirban, Tripathi, Arun Kumar, Chanotiya, Chandan Singh, 2014. A novel approach for development and characterization of effective mosquito repellent cream formulation containing citronella oil. Biomed. Res. Int. 2014, 1–11. https://doi.org/10.1155/2014/786084.
Yu, Lawrence X., 2008. Pharmaceutical quality by design: product and process development, understanding, and control. Pharm. Res. 25 (4), 781–791. https://doi.org/10.1007/s11095-007-9511-1.
Zhao, Yanjun, Brown, Marc B., Jones, Stuart A., 2009. Engineering novel topical foams using hydrofluroalkane emulsions stabilised with pluronic surfactants. Eur. J. Pharm. Sci. 37 (3–4), 370–377. https://doi.org/10.1016/j.ejps.2009.03.007.
Zhao, Yanjun, Jones, Stuart A., Brown, Marc B., 2010. Dynamic foams in topical drug delivery. J. Pharm. Pharmacol. 62 (6), 678–684. https://doi.org/10.1211/jpp.62.06.0003.

II.

gels

MDPI

Article

Application of Xanthan Gum and Hyaluronic Acid as Dermal Foam Stabilizers

Fanni Falusi, Szilvia Berkó, Anita Kovács and Mária Budai-Szűcs *

Institute of Pharmaceutical Technology and Regulatory Affairs, Faculty of Pharmacy, University of Szeged, Eötvös u. 6, 6720 Szeged, Hungary; falusi.fanni@szte.hu (F.F.); berko.szilvia@szte.hu (S.B.); gasparne.kovacs.anita@szte.hu (A.K.)

* Correspondence: budai-szucs.maria@szte.hu; Tel.: +36-6254-5573

Abstract: Foams are increasingly popular in the field of dermatology due to their many advantages such as easy spreading, good skin sensation, and applicability in special skin conditions. One of the critical points of foam formulation is the choice of the appropriate stabilizing ingredients. One of the stability-increasing strategies is retarding the liquid drainage of liquid films from the foam structure. Therefore, our aim was the application of different hydrogel-forming polymers in order to retain the stabilizing liquid film. Dexpanthenol and niacinamide-containing foams were formulated, where xanthan gum and hyaluronic acid were used as foam-stabilizing polymers. Amplitude (LVE range) and frequency sweep (G′, G″, tanδ, and frequency dependency) were applied as structure- and stability-indicating rheological parameters. The rheological data were compared with the results of the cylinder method, microscopical images, and the spreadability measurements. The application of the gel-forming polymers increased the stability of the dermal foams (increased LVE range, G′ values, and decreased frequency dependency). These results were in correlation with the results of the cylinder and spreadability tests. It was concluded that in terms of both foam formation and stability, the combination of xanthan gum and dexpanthenol can be ideal.

Keywords: foam stability; hyaluronic acid; xanthan gum; spreadability; rheology

Citation: Falusi, F.; Berkó, S.; Kovács, A.; Budai-Szűcs, M. Application of Xanthan Gum and Hyaluronic Acid as Dermal Foam Stabilizers. *Gels* **2022**, *8*, 413. https://doi.org/10.3390/gels8070413

Academic Editors: Miao Du and Qiang Wu

Received: 30 May 2022
Accepted: 29 June 2022
Published: 30 June 2022

1. Introduction

The use of dermal foams has become widespread in both the pharmaceutical and cosmetic fields. Foams are colloidal systems in which gas bubbles are dispersed in a solid or liquid dispersion medium and the two phases are separated by a solid wall (solid foams) or a liquid lamella (liquid foams). The lamellae can adhere to each other to form a foam. Dermal foams are liquid foams and preferred pharmaceutical products which are used to improve wound healing and treat chronic dermatological diseases and are also used in the pediatric field. They can be considered as special delivery systems due to their many advantages, such as convenient application on extensive or hairy skin surfaces [1]. In addition, their high rate of expansion allows large skin surfaces to be covered rapidly. The bulk liquid, which is stored in a container, is unsaturated or saturated for the active substance used. With the use of an appropriate foaming pump head, foams are produced by adding air to the bulk liquid. The volatile components are rapidly eliminated from the applied foam, resulting in supersaturation. For the active substance, after the foam starts to decay, a supersaturated thin liquid film (lamella) is formed, from which penetration starts at high speed due to the propulsive forces in the system. The fields of application require that the foam remains stable for a sufficient period of time to achieve a good spreading and the desired therapeutic effect, which is also beneficial for improving patient compliance.

In order to find the most suitable components and formulation strategies to ensure the foam stability, the main mechanisms that cause the foam decay must be clarified. The four main mechanisms are drainage, coalescence, Ostwald ripening, and bursting of bubbles [2]. Briefly, drainage is when the liquid drains off owing to gravity. The Plateau

borders between the bubbles allow the liquid to flow down through. Foams with a high liquid content can show very round bubbles. As the liquid starts to go through the foam, the bubbles take a polyhedral shape. As a result, the foam becomes unstable because the liquid is crucial to stabilize the lamellas of each bubble. The occurrence of coalescence is the result of surface tension (SFT). The bubbles get close to each other; afterwards, they conjoin and form a single bubble. Ostwald ripening is a consequence of thermodynamical instability between bubbles. In bigger bubbles, the pressure is lower and the small bubbles can dissolve in the solution and re-deposit to form large bubbles. Finally, bursting causes the air to eliminate from the foam bubbles as the liquid film is ruptured.

Foam formation involves three main stages [3], which are represented in Figure 1.

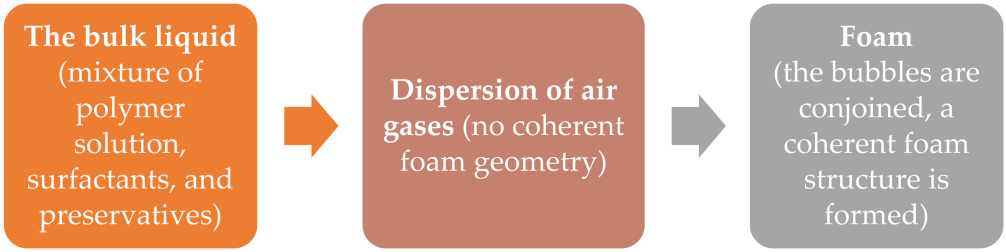

Figure 1. Stages of the foam formation.

Foaming techniques can be grouped into physical, chemical, and biological foaming [4]. The physical foaming techniques of mixing and foam formation by foam pumps are discussed in our article. These two techniques are the easiest and the most environmentally friendly methods. During the use of the mechanical stirrer, the turbulence causes air to diffuse into the liquid medium, thus allowing the foam to form. Among dermal foams, the propellant-free pump formulations are more favored. The propellant-free foam pump is easy for patients to use, and it is an environmentally friendly method as the liquid is mixed with the air, resulting in foam generation. The bulk liquid is contained in a liquid dosing chamber. The foam pump device also includes an air dosing chamber. The air from the air dosing chamber and the bulk liquid from the dosing chamber are moved through an uptake tube.

Foam stability is determined by a combination of dynamic and static factors. Forces between the interfaces of two bubbles determine the stability of the liquid film that separates them [4]. The key objective when stabilizing foams is to stop destabilizing mechanisms. Studies over the past decade indicate that many strategies can be used to stabilize foams. These methods may include the use of surfactants, photosurfactants [5], proteins [6], polyelectrolytes [7], and other gel-forming polymers. They can be usually used in combination to achieve the desired stability. The most common combination is the simultaneous use of polymer and surfactant, which are commonly used as foaming agents [8,9]. On the one hand, if higher elasticity can be reached by adding a high concentration of the foaming agent, then the bubbles have to work against the increased interfacial viscoelasticity. This mechanism can provide an energy barrier that could prevent the early shrinkage of the bubbles [10]. Moreover, polymers can increase the viscosity and elasticity of the liquid films, which can greatly contribute to delaying the break-up of lamellae. On the other hand, surfactants can reduce the mobility of the bubbles when adhering to the liquid–gas interface, which delays bubble formation fluctuations. In our research, we used surfactants and gel-forming polymers whose effects on the skin are already recognized, but their effects on foam stability are not known. Regarding surfactants, although ionic surfactants are effective foam stabilizers, they are known to be skin irritants [11] and the use of non-ionic surfactants is therefore recommended, especially when inflamed areas need to be treated. Our research has been conducted to investigate the effect of two popular polymers on foam stability: xanthan gum (XANT) and hyaluronic acid (HA). Xanthan gum is a widely used excipient in pharmaceutics [12,13]. It is one of the only naturally derived thickeners commonly used in dermal preparations. Accordingly, it has the ability to lock in water to

help maintain skin hydration. The hyaluronic acid used in the formulae is derived from natural sources and has moisturizing and water-retaining properties. Hyaluronic acid not only promotes skin hydration but also plays a crucial role in wound healing because it has an anti-inflammatory effect and aids tissue regeneration [14,15].

Our work aimed to formulate stable foam formulations containing two potential dermatological active ingredients (API) (dexpanthenol, DEX and niacinamide, NIA), for which two different liquid film stabilizing polymers (namely xanthan gum and hyaluronic acid) were chosen. The formation of foam was analyzed by rheological amplitude sweep test (linear viscoelastic (LVE) range), surface tension, microscopical investigation, and cylinder test. The stability of the foams was investigated through the rheological frequency sweep test and the spreadability test.

The application of the gel-forming polymers improved the stability of dermal foams (wider LVE range, higher G' values, and decreased frequency dependency). The rheological results were in correlation with the results of the cylinder and spreadability tests. With the applied methods, the ideal combination and composition can be selected.

2. Results and Discussion

In the first part of the work, the foam formation ability of the composition was analyzed using surface tension measurement, macroscopic foam stability (foam expansion, FE; foam volume stability FVS), microscopical, and rheological investigations. In this section, two physical foam-forming techniques were compared. Mechanical stirring represents the foam formation more realistically, the duration of the foam formation is more traceable, while the propellant-free pump devices imitate the real conditions of the application.

In the second part of the work, the structure and the applicability of the foams formed by the pump (Figure S1) were evaluated using rheological and texture analyzer technics.

2.1. Foam Formation Ability

The surface tension of liquids significantly affects the dispersibility of air, the size [16,17], and the stability of the bubbles formed [18]. The surface tension of the bulk liquids was determined using the pendant drop method. The surface tension of the API-free (AF) and the polymer-free (PF) solution was 27.54 mN/m; compared to this, the addition of polymers caused an increase, i.e., their surfactant inactivity prevailed (Table 1). When dexpanthenol was added to the formulation, a decrease in surface tension was observed in the polymer-free and xanthan gum-containing formulations, suggesting that dexpanthenol may be contributing to the interfacial formation, whereas niacinamide only altered the polymer-free formulations and increased the surface tension in a similar way to polymer-containing formulations. The results suggest (Table 1) that dexpanthenol-containing formulations have the most favorable surface tension for foam formation, even with xanthan gum which increases the surface tension, lower surface tension can be measured to compensate for its surface inactivity.

Table 1. The results of the surface tension, foam expansion, and foam volume stability measurements.

Sample	SFT (mN/m)	FE (%)	FVS (%)
PF-AF	27.54 ± 0.11	172.2 ± 15.8	14.3 ± 1.8
XANT-AF	29.20 ± 0.06	134.4 ± 1.9	100.0 ± 0.0
HA-AF	28.78 ± 0.33	125.6 ± 3.8	94.6 ± 0.1
PF-DEX	24.32 ± 1.18	180.0 ± 0.0	15.1 ± 0.7
XANT-DEX	24.00 ± 3.85	114.4 ± 1.9	100.0 ± 0.0
HA-DEX	28.40 ±0.30	144.4 ± 1.9	88.2 ± 0.7
PF-NIA	29.20 ± 0.22	183.3 ± 0.0	11.8 ± 0.0
XANT-NIA	29.49 ± 0.08	126.7 ± 3.3	100.0 ± 0.0
HA-NIA	29.31 ± 0.01	113.3 ± 3.3	91.9 ± 1.3

The lower surface tension may lead to a significantly higher foam expansion (FE). However, the FE-values are more significant in polymer-free compositions, with values above 170%, while in polymer-containing compositions, it is usually below 150%. This is due to the fact that the amount of air emulsified in the foam with mechanical stirring depends significantly on the viscosity of the mixed bulk liquid, and in our case, polymer-containing bulk liquids are considered to be more viscous. Comparing the effect of the two polymer-containing foams on expansion, no distinct correlation can be found.

Regarding foam volume stability, the macroscopic tests confirmed that polymer-free systems collapsed rapidly (FVS values ranging from 11 to 15%), while for polymer-containing systems, xanthan-containing foams maintained their foam volume after 30 min, although a 5–10% volume decrease was observed for HA-containing compositions. Although the addition of the polymer to the bulk liquid increases the viscosity and elasticity, which leads to a more difficult foam formation, the thickness and stability of the lamellae surrounding the bubbles after foam formation are increased [19]. A common example is the polymer-free and xanthan gum samples containing dexpanthenol, where due to the favorable surface tension, the foam formation is the greatest in the case of the polymer-free sample (FE = 180%), while the polymer-containing foam has a much lower value (FE = 114%). By contrast, the parameter indicating their stability (FVS) is much more favorable in the sample containing xanthan gum (100% vs. 15%).

During rheological investigations, the linear viscoelastic range of the formed foams (Figure 2) was determined, and measurements were performed with pump-formed foams, and also foams prepared with mechanical stirrer after preparation (0 min) and 10, 20, and 30 min. With amplitude sweep, the mechanical resistance of the foams can be determined and the formation of the foam, namely the formation of the foam structure can be identified. The interfacial interactions between bubbles and lamellae induced a coherent structure, which can be characterized by the storage (G′) and loss (G″) moduli on the rheological curves for the elastic and viscous properties.

In our case, for compositions defined as real foam, when the coherent structure is formed, the G′ modulus was higher than the G″ modulus, and it was constant up to a given strain value, depending on the strength of the foam structure. The end of linearity, and the associated strain value, represent the resistance of the structure to deformation; the higher the strain value, the more resistant the structure is. The coherent foam structure is weak, and the viscoelastic range of our formulated foams ends under 1% strain (Figure 2). These results are similar to values indicated in previous literature on topically applied foams [20]. We could also observe that samples from the aged foams were rheologically divergent (Table S1). In some cases, water leaking out of the lamellae means a decrease in the fluidity of the lamellae, so the viscoelastic range is extended. This behavior could be observed in most foams; however, it should be added that in polymer-free formulations, the measurements were performed on a foam that had already shrunk significantly (below 15% FVS-value). In several cases, the coherent structure was no longer measurable, and the classical foam structure disappeared (PF-AF at 30 min; DEX-PF at 30 min). In these cases, the G″ modulus was higher than the G′ modulus, and no linearity was observed, so the end of the viscoelastic range in the investigated range was not detectable.

The foams formed with mechanical stirrer and the foams formed with pumps were also compared throughout the rheological studies. The linear viscoelastic range of the foams generated by the mechanical stirrer is most similar to the initial rheological values of the non-aging foam, showing a highly rapid structural breakdown ($\gamma_{LVER} < 0.3\%$). In general, the viscoelastic range of polymer-free systems breaks down earlier, resulting in a more fragile structure when produced by both mechanical stirrer and pump.

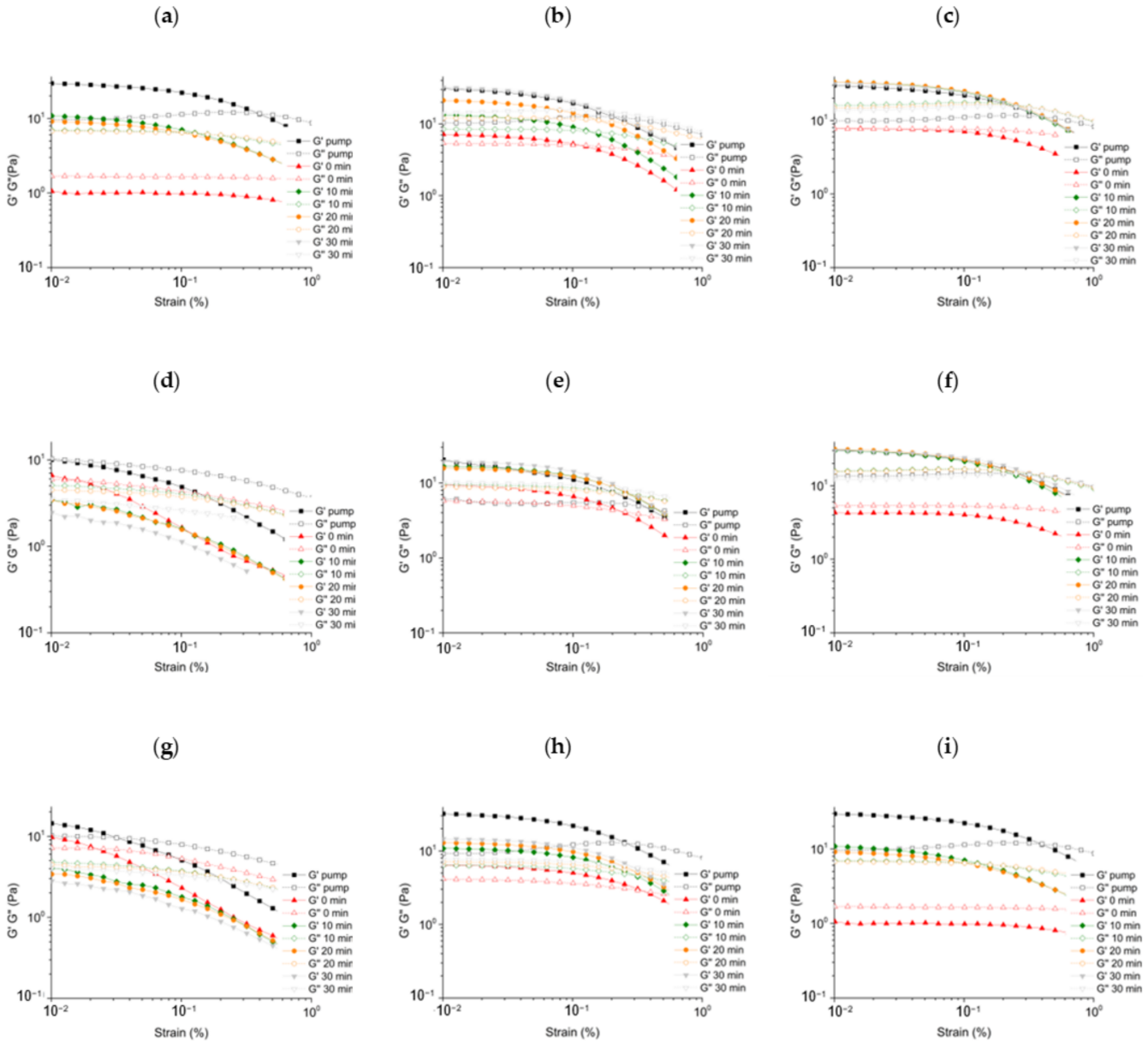

Figure 2. The amplitude sweep of the formed foams (**a**) without polymer; (**b**) with XANT; (**c**) with HA.; (**d**) DEX: without polymer; (**e**) DEX with XANT; (**f**) DEX with HA; (**g**) NIA without polymer; (**h**) NIA with XANT; (**i**) NIA with HA.

The structure of foams produced by mechanical stirrer and pump is illustrated by microscopic images (Figure 3). Foams produced with a pump exhibit a more heterogeneous structure, meaning that there is a variety of smaller and larger bubbles, whereas the size of the bubbles was smaller and more uniform in systems produced with a mechanical stirrer.

Microscopic images provide the opportunity to study the film or lamellae that bound the bubbles. In general, a thicker wall structure was observed in polymer-containing foam systems, which was more noticeable in pump-formed foams. When comparing the two polymers, the film thickness may have been greater for xanthan gum-containing compositions, and the amount of liquid bound by the polymer in the interfacial layer may have been more significant.

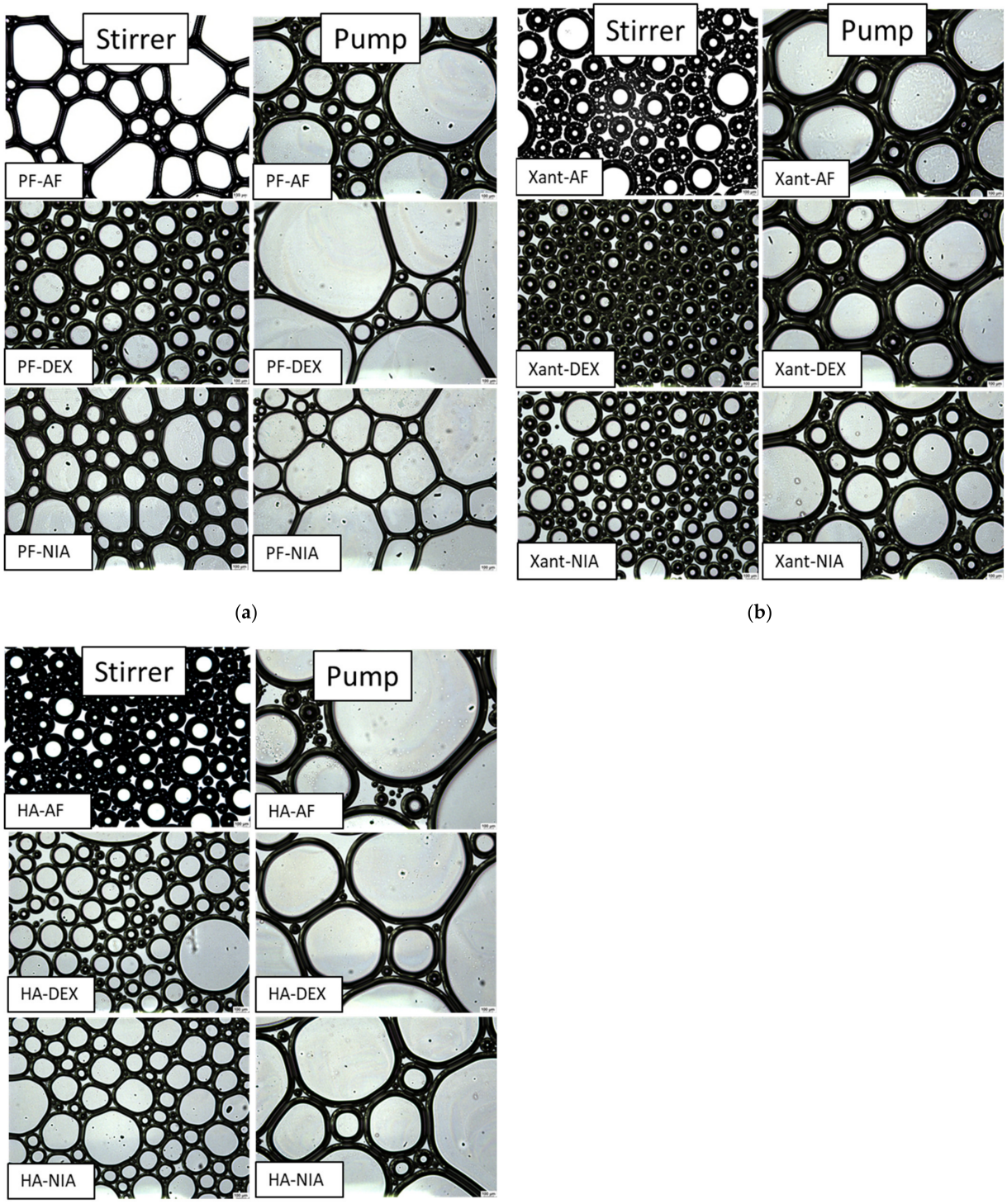

Figure 3. The comparison of the structure of foams produced by the pump and mechanical stirring: (**a**) polymer-free foams; (**b**) xanthan gum-containing foams; (**c**) hyaluronic acid.

Microscopic images enable the determination of the bubble sizes as well as the characterization of the wall thickness of the lamellae around the bubbles. However, several authors [21,22] and our own experience point out that conventional microscopic sectioning is difficult due to the dynamic behavior of foams and their weak structure; therefore, occasionally no conclusions can be drawn. In order to avoid this, our work compared only the differences in bubble size (monodisperse or heterodisperse) and wall thicknesses for

microscopic evaluations, without detailed statistical measurements. For a more accurate characterization of the structure, we therefore subsequently used methods that provide well-reproduced information on a large sample volume (rheology and texture analyzer)

2.2. Characterization of the Structure of Foams Generated by Pumps

Dermal foams are usually formed using propellent-free pump devices, and therefore it was considered necessary to investigate the structure of these foam systems in more detail.

The formed coherent gel structure was investigated with frequency sweep (Figure 4). The value of the G′ and G″ moduli, their relationship to each other (tanδ), and their frequency dependence provided information about the strength and stability of the formed foam structure (Table 2). For polymer-free systems, the moduli showed much lower values, the storage modulus was lower than the loss modulus, and the tanδ values were below 1, which means that the coherent structure did not characterize the formed foam. The significant frequency dependence (high slope value) of the polymer-free samples also indicated instability. The addition of polymer in the system showed an increase in elasticity, an increase in G′ modulus values, and an increase in tanδ and frequency dependence. The addition of the polymer referred to the strengthening of the coherent structure. In the API-free systems, the two polymers resulted in similar changes in rheological parameters, with no significant difference. However, it is remarkable that dexpanthenol together with xanthan gum significantly increased the elasticity and stability of the foam. The G′ modulus increased from 11.2 Pa to 20.3 Pa after the addition of dexpanthenol, while tanδ decreased from 0.30 to 0.26, similarly, the frequency-dependent slope decreased from 0.50 to 0.33. This formulation had a very low surface tension value which indicates the xanthan gum and the dexpanthenol together can modify the bubble-liquid film interface. This modification may change the mechanical behavior of the foam based on the results presented earlier, which also suggests that the combination of polymer and dexpanthenol strengthens the effect of each other.

Table 2. Results of the frequency sweep measurement and the spreadability of the foam formed by the pump.

Sample	Rheology				Spreadability
	G′ at 10 rad/s (Pa)	G″ at 10 rad/s (Pa)	tanδ at 10 rad/s (-)	Slope	Firmness (mN)
PF-AF	3.86 ± 0.61	6.60 ± 0.87	1.76 ± 0.46	1.89 ± 0.33	120.9 ± 5.0
XANT-AF	29.09 ± 3.81	8.71 ± 1.24	0.30 ± 0.03	0.51 ± 0.09	229 ± 6.7
HA-AF	29.73 ± 6.29	9.83 ± 2.38	0.33 ± 0.01	0.53 ± 0.03	291.9 ± 5.8
PF-DEX	8.51 ± 2.32	9.38 ± 0.69	1.14 ± 0.23	0.85 ± 0.08	127.9 ± 11.3
XANT-DEX	40.35 ± 0.74	10.63 ± 0.38	0.26 ± 0.01	0.34 ± 0.03	275.8 ± 4.9
HA-DEX	30.60 ± 1.27	15.62 ± 3.76	0.45 ± 0.02	0.56 ± 0.04	271.0 ± 8.9
PF-NIA	9.32 ± 1.65	11.04 ± 1.35	1.19 ± 0.06	1.30 ± 0.46	145.9 ± 8.5
XANT-NIA	38.02 ± 2.58	11.13 ± 0.49	0.29 ± 0.01	0.42 ± 0.03	254.2 ± 6.3
HA-NIA	30.96 ± 0.26	11.29 ± 0.62	0.36 ± 0.02	0.47 ± 0.07	258.6 ± 14.4

Commercially available dermally applied foams can have very different rheological properties [20]. In our research, the rheological parameters were used to optimize the composition in order to select the appropriate formulation with the most favorable stability and structure. The combination of dexpanthenol and xanthan gum is also indicated as the optimal formulation in this respect.

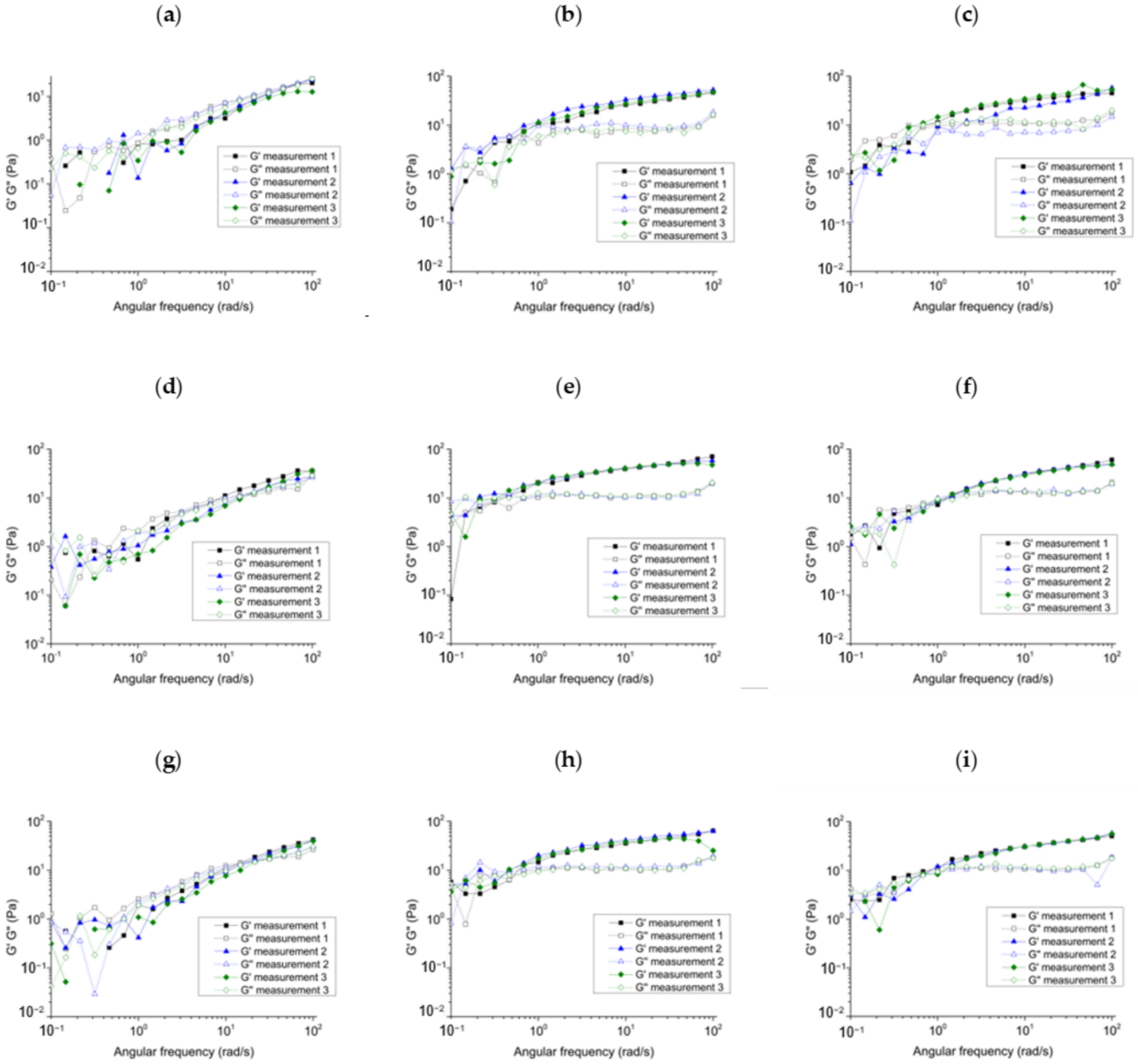

Figure 4. The frequency sweep of the formed foams (**a**) without polymer; (**b**) with XANT; (**c**) with HA.; (**d**) DEX: without polymer; (**e**) DEX with XANT; (**f**) DEX with HA; (**g**) NIA without polymer; (**h**) NIA with XANT; (**i**) NIA with HA. Three parallel measurements are presented.

The spreadability of the foams can appear to be critical for application and for this purpose, a texture analyzer was used to determine the firmness values, which are characterized by the maximum strength of the force-distance curve required to spread the foam to a thickness of 1 mm (firmness). The results suggest that polymer-free foams with no elastic properties could be spread with much lower forces, as predicted from the rheological properties. No clear correlation was observed between the two foam systems containing different polymers in terms of spreading. In the absence of a similar study of foams in previous literature, we compared the values obtained with the rheological parameters in our research. With the texture analyzer, the foams did not show as much difference as with the rheological parameters, which means that the rheological parameters can provide a more accurate indication of the effect of both polymers and active ingredients on the structure.

3. Conclusions

The purpose of our work was to formulate a dermal foam in which the ingredients are present in quality and quantity that results in a foam structure with adequate mechanical strength and stability. Two potential dermal agents (dexpanthenol, niacinamide) were used with the aim of selecting an ideal polymer.

The results proved that the addition of the polymer resulted in a much more stable and better structured foam. The xanthan gum provided more favorable rheological properties and more stable foam systems. In terms of both foam formation and stability, the combination of xanthan gum and dexpanthenol proved to have the most beneficial properties, making it an ideal combination.

4. Materials and Methods

4.1. Materials

Kolliphor RH 40 was provided by BTC Europe GmbH-A BASF Group Company (Burgbemheim, Germany). Labrasol ALF was supplied by Azelis Hungary Ltd. (Budapest, Hungary), Xantural® 180 was obtained from Biesterfeld GmbH (Budapest, Hungary). Verstatil PC was purchased from Biesterfeld GmbH (Budapest, Hungary). Purified and deionized water was used (Milli-Q system, Millipore, Milford, MA, USA). HyaCare Tremella (1240 kDa) was a product sample from Finecon-Evonik Industries AG (Essen, North Rhine-Westphalia, Germany). Niacinamide was kindly supplied by Biesterfeld GmbH (Budapest, Hungary). D-Panthenol was by DSM Nutritional Products Ltd. (Basel, Switzerland).

4.2. Methods

4.2.1. Composition and Preparation of Foam Samples

The exact composition of different foam formulations is shown in Table 3. The type and the concentration of the surfactants and preservative were chosen based on our earlier study [23].

Table 3. Composition of the investigated formulations.

	Polymer Free Compositions			**Xanthan Gum-Containing Compositions**			**Hyaluronic Acid-Containing Compositions**		
Components	**PF-AF**	**PF-DEX**	**PF-NIA**	**XANT-AF**	**XANT-DEX**	**XANT-NIA**	**HA-AF**	**HA-DEX**	**HA-NIA**
Phase A									
Labrasol ALF /surfactant/	+	+	+	+	+	+	+	+	+
Kolliphor RH40 /surfactant/	+	+	+	+	+	+	+	+	+
Phase B									
Xanthan gum (Xant.) /polymer/	-	-	-	0.2%	0.2%	0.2%	-	-	-
Hyaluronic acid (HA) /polymer/	-	-	-	-	-	-	0.2%	0.2%	0.2%
Purified water /solvent/	+	+	+	+	+	+	+	+	+
Dexpanthenol /active ingredient/	-	5%	-	-	5%	-	-	5%	-
Niacinamide /active ingredient/	-	-	5%	-	-	5%	-	-	5%
Phase C									
Phenoxyethanol /preservative/	+	+	+	+	+	+	+	+	+

+ the component is in the formulation, - the component is not in the formulation.

Each formulation contains the same amount of surfactants, preservatives, and solvents. The difference between the formulations is the contained polymer and active ingredient. As the aim is to develop an appropriate foam formula for dermatological use, we were looking

for a suitable polymer for transdermal application. Niacinamide and dexpanthenol are the active ingredients used as they contribute to the improvement of the skin's barrier function.

Phase A contains a mixture of surfactants, which are the main foaming agents of the formulation. Phase B contains the chosen polymers, the solvent, and one of the active ingredients. When preparing Phase B, the polymer was swollen in half the amount of purified water for 1.5 h. In the remaining water, a solution was made with the active ingredient. After the complete dissolution of the active ingredient and swelling of the polymer, the two solutions were then mixed. The first step was the addition of Phase C to Phase A. Lastly, Phase B was mixed with the mixture of Phases A and C. After the preparation of bulk liquids, the samples were kept in well-sealed jars and propellant-free foam pumps until the start of the investigations. To compare the effect of the two production methods, the tested foams were generated with a propellant-free foam pump. In the other method of preparation, 30 g of bulk liquid was stirred with the IKA stirrer for 5 min at 2000 rpm, before each investigation.

4.2.2. Macroscopic Characterization of Foams

In order to develop appropriate compositions, it is important to identify test methods for investigating the stability of foams. Foam stability is the parameter that indicates the period of time until which the foam can maintain its initial properties. These can be tested to provide data on foamability and foam stability. This method has only been performed with foams produced with mechanical stirring. First, 30 g bulk liquid was stirred for 5 min, then a glass graduated cylinder was filled up with the foam. The initial foam volumes were recorded, and after 30 min the aged foam volumes.

The parameters can be calculated using the following formulae [24]:

$$\mathrm{FVS}(\%) = \frac{\mathrm{V(foam,\ 30\ min)}}{\mathrm{V(foam)}} \cdot 100\% \quad (1)$$

where V(foam,30 min) is the foam volume after 30 min (mL).

$$\mathrm{FE}(\%) = \frac{\mathrm{V(foam)} - \mathrm{V(formulation)}}{\mathrm{V(formulation)}} \cdot 100\% \quad (2)$$

where V(formulation) is the volume of the formulation (mL) required to produce V(foam) (mL) [24].

The cylinder method can be used to determine the foam volume stability (FVS, %) and foam expansion (FE, %), as it is an easy and convenient method [24].

4.2.3. Spreadability (Texture Analyzer)

With texture analyzer, dermal application of any semi-solid dosage forms can be modeled. The instrument measures the forces required to spread the product on the skin.

The spreadability of the foams was examined with a TA.XT plus Texture Analyzer (Stable Micro Systems Ltd., Vienna Court, Lammas Road, Godalming, Surrey, UK. GU7 1YL) using a TTC Spreadability Rig, which includes a 90° cone-shaped male probe and a precisely fitting female cone-shaped, Perspex product holder. When a trigger force of 1 g was achieved, the male probe proceeded to penetrate the sample at a test speed of 10 mm/s until a gap of 1 mm. The force to penetrate the sample increased during this time. The tested foam flowed outward at 45° between the surfaces of male and female cones and the ease of spreading indicated the degree of spreadability. The maximum force value in the force-distance graph is a measure of firmness that characterizes the spreadability of the sample.

4.2.4. Microscopic Characterization of Foams and Image Analysis

The investigation of the microscopically observable properties of foams was carried out with Leica DM6 B Fully Automated Upright Microscope System (Leica Biosystems GmbH,

Wetzlar, Germany). The structure of the foams can be observed with microscopic images. The roundness, size, size distribution of bubbles, and the thickness of lamellae between two bubbles can provide paramount information on foam stability. The structure of the foam was analyzed immediately after the generation of foams through the light microscope.

4.2.5. Determination of the Surface Tension

The surface tension affects the foam stability. Measuring the surface tension is of major importance because the lower surface tension assists the bubble formation and the higher surface elasticity helps to maintain the stability of the foam lamellae [25]. The surface tension of bulk liquids was measured with OCA 20 Contact Angle System (Dataphysics Instruments GmbH, Filderstadt, Germany) by analyzing the shape of the pendant drop. The pendant drop was created at the end of a needle with a predefined inner and outer diameter in a vertical position. The contour of the droplet was detected by the SCA20/22 software V.5.0.41 module using the Young–Laplace equation. The camera was rotated by 90° for a better resolution, which allowed the software to get a larger screenshot and a more accurate contour analysis, in which case the camera image detected the hanging droplet from left to right. As the instrument detected the contour of the pendant drop, it calculated the surface tension from it. The average of 5 parallel measurements was used for the evaluation.

4.2.6. Oscillometric Measurements

Studying the structure of foams has always been problematic, as the structure of foams is easily friable and often contains large bubbles. Oscillometric methods (amplitude sweep, frequency sweep) can be used to gain more insight into the mechanical properties of foams such as the elasticity of the film, and thus the stability of the foam. The rheological properties of foams were studied at 25 °C with an Anton Paar Physica MCR302 Rheometer (Anton Paar, Graz, Austria). The measuring device was of the parallel plate type (diameter 50 mm, gap height 2 mm). Each measurement was performed immediately after the generation of foam samples or after a given storage time (10, 20, and 30 min).

4.2.7. Amplitude Sweep

The foams were analyzed through amplitude sweeps [20], at an increase of the strain value from 0.1% to 100%, and at a constant angular frequency of 10 rad/s. The linear viscoelastic (LVE) range was determined by the RheoCompass™ software v.1.25 (Anton Paar, Graz, Austria). We selected a 3% tolerance range of deviation for G′ around the plateau value for the determination of the LVE range. The results of the measurement of the LVE range were used for the setting of the frequency sweep tests, and the LVE range can give information on the formation of foam structure.

4.2.8. Frequency Sweep

Storage modulus (G′), loss modulus (G″), loss factor (tanδ), and the slope of the curve (frequency-dependency) were determined [20] over the angular frequency range from 0.1 to 100 rad/s. The applied strain value (0.1%) was in the range of the linear viscoelasticity of the foams. Three parallel measurements were carried out.

Supplementary Materials: The following supporting information can be downloaded at: https://www.mdpi.com/article/10.3390/gels8070413/s1, Table S1: Calculated LVE range of the foams; Figure S1: Photos of the different foams. (a) PF-AF, XANT-AF, HA-AF; (b) PF-DEX, XANT-DEX, HA-DEX, and (c) PF-NIA, XANT-NIA, HA-NIA.

Author Contributions: Conceptualization, S.B. and A.K.; formal analysis, F.F. and M.B.-S.; investigation, F.F.; methodology, M.B.-S.; supervision, S.B. and A.K.; visualization, F.F.; writing—original draft, F.F. and M.B.-S.; writing—review and editing, S.B. and A.K. All authors have read and agreed to the published version of the manuscript.

Funding: Project no. TKP2021-EGA-32 was implemented with the support provided by the Ministry of Innovation and Technology of Hungary from the National Research, Development, and Innovation Fund, financed under the TKP2021-EGA funding scheme.

Institutional Review Board Statement: Not applicable.

Informed Consent Statement: Not applicable.

Data Availability Statement: Data are contained within the article or Supplementary Materials.

Acknowledgments: The authors are grateful for the gift samples from Finecon-Evonik, Azelis Hungary, Biesterfeld Hungary.

Conflicts of Interest: The authors declare no conflict of interest. The funders had no role in the design of the study; in the collection, analyses, or interpretation of data; in the writing of the manuscript, or in the decision to publish the results.

Abbreviations

AF	API-free
API	active ingredient
DEX	dexpanthenol
FE	foam expansion
FVS	foam volume stability
HA	hyaluronic acid
NIA	niacinamide
PF	polymer-free
STF	surface tension
XANT	xanthan gum

References

1. Parsa, M.; Trybala, A.; Malik, D.J.; Starov, V. Foam in Pharmaceutical and Medical Applications. *Curr. Opin. Colloid Interface Sci.* **2019**, *44*, 153–167. [CrossRef]
2. Yanagisawa, N.; Tani, M.; Kurita, R. Dynamics and Mechanism of Liquid Film Collapse in a Foam. *Soft Matter* **2021**, *17*, 1738–1745. [CrossRef] [PubMed]
3. Arzhavitina, A.; Steckel, H. Foams for Pharmaceutical and Cosmetic Application. *Int. J. Pharm.* **2010**, *394*, 1–17. [CrossRef] [PubMed]
4. Wang, J.; Nguyen, A.V.; Farrokhpay, S. A Critical Review of the Growth, Drainage and Collapse of Foams. *Adv. Colloid Interface Sci.* **2016**, *228*, 55–70. [CrossRef]
5. Anazadehsayed, A.; Rezaee, N.; Naser, J.; Nguyen, A.V. A Review of Aqueous Foam in Microscale. *Adv. Colloid Interface Sci.* **2018**, *256*, 203–229. [CrossRef]
6. Oetjen, K.; Bilke-Krause, C.; Madani, M.; Willers, T. Temperature Effect on Foamability, Foam Stability, and Foam Structure of Milk. *Colloids Surf. Physicochem. Eng. Asp.* **2014**, *460*, 280–285. [CrossRef]
7. Kristen, N.; Von Klitzing, R. Effect of Polyelectrolyte/Surfactant Combinations on the Stability of Foam Films. *Soft Matter* **2010**, *6*, 849. [CrossRef]
8. Bureiko, A.; Trybala, A.; Kovalchuk, N.; Starov, V. Current Applications of Foams Formed from Mixed Surfactant–Polymer Solutions. *Adv. Colloid Interface Sci.* **2015**, *222*, 670–677. [CrossRef]
9. Langevin, D. Aqueous Foams and Foam Films Stabilised by Surfactants. Gravity-Free Studies. *Comptes Rendus Mécanique* **2017**, *345*, 47–55. [CrossRef]
10. Murray, B.S.; Ettelaie, R. Foam Stability: Proteins and Nanoparticles. *Curr. Opin. Colloid Interface Sci.* **2004**, *9*, 314–320. [CrossRef]
11. Lémery, E.; Briançon, S.; Chevalier, Y.; Bordes, C.; Oddos, T.; Gohier, A.; Bolzinger, M.-A. Skin Toxicity of Surfactants: Structure/Toxicity Relationships. *Colloids Surf. Physicochem. Eng. Asp.* **2015**, *469*, 166–179. [CrossRef]
12. Shawan, M.M.A.K.; Islam, N.; Aziz, S.; Khatun, N.; Sarker, S.R.; Hossain, M.; Hossan, T.; Morshed, M.; Sarkar, M.; Shakil, S.; et al. Fabrication of Xanthan Gum: Gelatin (Xnt:Gel) Hybrid Composite Hydrogels for Evaluating Skin Wound Healing Efficacy. *Mod. Appl. Sci.* **2019**, *13*, 101. [CrossRef]
13. Singhvi, G.; Hans, N.; Shiva, N.; Kumar Dubey, S. Xanthan Gum in Drug Delivery Applications. In *Natural Polysaccharides in Drug Delivery and Biomedical Applications*; Elsevier: Amsterdam, The Netherlands, 2019; pp. 121–144. ISBN 978-0-12-817055-7.
14. Berkó, S.; Maroda, M.; Bodnár, M.; Erős, G.; Hartmann, P.; Szentner, K.; Szabó-Révész, P.; Kemény, L.; Borbély, J.; Csányi, E. Advantages of Cross-Linked versus Linear Hyaluronic Acid for Semisolid Skin Delivery Systems. *Eur. Polym. J.* **2013**, *49*, 2511–2517. [CrossRef]

15. Draelos, Z.D. A Clinical Evaluation of the Comparable Efficacy of Hyaluronic Acid-Based Foam and Ceramide-Containing Emulsion Cream in the Treatment of Mild-to-Moderate Atopic Dermatitis: Barrier Restoration Therapy in Atopic Dermatitis. *J. Cosmet. Dermatol.* **2011**, *10*, 185–188. [CrossRef]
16. Loubière, K.; Hébrard, G. Influence of Liquid Surface Tension (Surfactants) on Bubble Formation at Rigid and Flexible Orifices. *Chem. Eng. Process. Process Intensif.* **2004**, *43*, 1361–1369. [CrossRef]
17. Hsu, S.-H.; Lee, W.-H.; Yang, Y.-M.; Chang, C.-H.; Maa, J.-R. Bubble Formation at an Orifice in Surfactant Solutions under Constant-Flow Conditions. *Ind. Eng. Chem. Res.* **2000**, *39*, 1473–1479. [CrossRef]
18. Walstra, P. Principles of Foam Formation and Stability. In *Foams: Physics, Chemistry and Structure*; Wilson, A., Ed.; Springer Series in Applied Biology; Springer: London, UK, 1989; pp. 1–15. ISBN 978-1-4471-3809-9.
19. Zhao, G.; Dai, C.; Zhang, Y.; Chen, A.; Yan, Z.; Zhao, M. Enhanced Foam Stability by Adding Comb Polymer Gel for In-Depth Profile Control in High Temperature Reservoirs. *Colloids Surf. Physicochem. Eng. Asp.* **2015**, *482*, 115–124. [CrossRef]
20. Kealy, T.; Abram, A.; Hunt, B.; Buchta, R. The Rheological Properties of Pharmaceutical Foam: Implications for Use. *Int. J. Pharm.* **2008**, *355*, 67–80. [CrossRef]
21. Zhao, Y.; Brown, M.B.; Jones, S.A. Pharmaceutical Foams: Are They the Answer to the Dilemma of Topical Nanoparticles? *Nanomed. Nanotechnol. Biol. Med.* **2010**, *6*, 227–236. [CrossRef]
22. Postema, M.; Abraham, H.; Krejcar, O.; Assefa, D. Size Determination of Microbubbles in Optical Microscopy: A Best-Case Scenario. *Opt. Express* **2017**, *25*, 33588–33601. [CrossRef]
23. Falusi, F.; Budai-Szűcs, M.; Csányi, E.; Berkó, S.; Spaits, T.; Csóka, I.; Kovács, A. Investigation of the Effect of Polymers on Dermal Foam Properties Using the QbD Approach. *Eur. J. Pharm. Sci.* **2022**, *173*, 106160. [CrossRef]
24. Mirtič, J.; Papathanasiou, F.; Temova Rakuša, Ž.; GosencaMatjaž, M.; Roškar, R.; Kristl, J. Development of Medicated Foams That Combine Incompatible Hydrophilic and Lipophilic Drugs for Psoriasis Treatment. *Int. J. Pharm.* **2017**, *524*, 65–76. [CrossRef]
25. Tiwari, S.P.; Steckel, J.A.; Sarma, M.; Bryant, J.; Lippert, C.A.; Widger, L.R.; Thompson, J.; Liu, K.; Siefert, N.; Hopkinson, D.; et al. Foaming Dependence on the Interface Affinities of Surfactant-like Molecules. *Ind. Eng. Chem. Res.* **2019**, *58*, 19877–19889. [CrossRef]

III.

pharmaceutics

MDPI

Article

Foams Set a New Pace for the Release of Diclofenac Sodium

Fanni Falusi [1], Szilvia Berkó [1], Mária Budai-Szűcs [1], Zoltán Veréb [2,3,4] and Anita Kovács [1,*]

[1] Institute of Pharmaceutical Technology and Regulatory Affairs, Faculty of Pharmacy, University of Szeged, 6 Eötvös St., 6720 Szeged, Hungary; falusi.fanni@szte.hu (F.F.); berko.szilvia@szte.hu (S.B.); budai-szucs.maria@szte.hu (M.B.-S.)
[2] Regenerative Medicine and Cellular Pharmacology Laboratory, Department of Dermatology and Allergology, University of Szeged, 6720 Szeged, Hungary; vereb.zoltan@med.u-szeged.hu
[3] Centre of Excellence for Interdisciplinary Research, Development and Innovation, University of Szeged, 6720 Szeged, Hungary
[4] Hungarian Centre of Excellence for Molecular Medicine-USz Skin Research Group, University of Szeged, 6720 Szeged, Hungary
* Correspondence: gasparne.kovacs.anita@szte.hu

Abstract: Medicated foams have emerged as promising alternatives to traditional carrier systems in pharmaceutical research. Their rapid and convenient application allows for effective treatment of extensive or hirsute areas, as well as sensitive or inflamed skin surfaces. Foams possess excellent spreading capabilities on the skin, ensuring immediate drug absorption without the need for intense rubbing. Our research focuses on the comparison of physicochemical and biopharmaceutical properties of three drug delivery systems: foam, the foam bulk liquid, and a conventional hydrogel. During the development of the composition, widely used diclofenac sodium was employed. The safety of the formulae was confirmed through an in vitro cytotoxicity assay. Subsequently, the closed Franz diffusion cell was used to determine drug release and permeation in vitro. Ex vivo Raman spectroscopy was employed to investigate the presence of diclofenac sodium in various skin layers. The obtained results of the foam were compared to the bulk liquid and to a conventional hydrogel. In terms of drug release, the foam showed a rapid release, with 80% of diclofenac released within 30 min. In summary, the investigated foam holds promising potential as an alternative to traditional dermal carrier systems, offering faster drug release and permeation.

Keywords: dermal foam; diclofenac sodium; Raman mapping; in vitro permeation test; in vitro release test

Citation: Falusi, F.; Berkó, S.; Budai-Szűcs, M.; Veréb, Z.; Kovács, A. Foams Set a New Pace for the Release of Diclofenac Sodium. *Pharmaceutics* **2024**, *16*, 287. https://doi.org/10.3390/pharmaceutics16020287

Academic Editors: Anna Czajkowska-Kośnik and Magdalena Wróblewska

Received: 18 January 2024
Revised: 5 February 2024
Accepted: 15 February 2024
Published: 18 February 2024

1. Introduction

Dermal drug delivery is a critical field of study in pharmaceutical research, with the goal of successfully administering therapeutic agents through the skin for localized or systemic effects.

A wide range of dermal preparations are available for use in product development. Within the traditional forms, solid, semi-solid, and liquid preparations are distinguished. Powders and patches are associated with the solid form applied dermally, while ointments, creams, gels, and pastes represent the semi-solid form. Solutions, emulsions, suspensions, and aerosols belong to the liquid form [1,2].

Only a few of the active ingredients are capable of achieving adequate transdermal penetration on their own since they need to possess suitable solubility and permeability [3]. To achieve a systemic effect, it is necessary to develop a formulation that is capable of crossing this protective barrier by temporarily disrupting the skin barrier before it quickly returns to its original structure. Among the methods for enhancing penetration, we distinguish between passive and active approaches. Passive methods involve reducing the barrier function of the stratum corneum through the use of chemical penetration

enhancers [4,5], increasing hydration [6], and employing various nanostructured systems (NLC, liposome) [7].

In addition, an increasing number of new, innovative forms are being encountered in both the pharmaceutical and cosmetic industries [8]. In the field of dermatology, foams have gained attention [9,10], particularly in the treatment of sunburns, wounds, and ulcers. They are used in numerous areas, and the development of environmentally friendly designs has become paramount to reducing the environmental footprint [11]. This has led to the gradual replacement of propellant-containing systems with propellant-free systems. The therapeutic use of dermal foams is becoming increasingly appealing to the population because of its ease of application [12]. Foams are often utilized as a topical formulation, which allows for easier distribution and consistent covering of the affected region. Their appearance is aesthetic, non-greasy, and non-sticky, yet easily removable from the skin, thereby improving patient adherence. Foams also have good spreadability on the skin [13], ensuring the immediate absorption of the active ingredient, and eliminating the need for vigorous rubbing [14].

Foams have specific physical properties and a distinct structure that set them apart from other conventional drug delivery systems, such as hydrogels. Understanding the physical characteristics and structure of foams is critical for comprehending their benefits in dermal drug delivery. Foams are distinguished by their porous structure, which is formed during the foaming process [15]. These pores are bare spots or holes inside the foam matrix that contribute to its spongy appearance. The presence of pores in foams is essential for their drug delivery capabilities. The porous nature enables the incorporation and entrapment of drugs within the foam structure, allowing for sustained release upon [16–18] application to the skin. Additionally, this porous nature increases the accessible surface area for drug absorption, allowing for faster (immediate) drug diffusion. During formulation, it is essential to ensure the perfect dissolution of the active ingredient in the carrier excipient. Upon application, volatile components quickly evaporate from the foam applied to the skin, leading to supersaturation [19,20]. Consequently, a supersaturated layer forms on the epidermis in terms of the active ingredient, from which penetration initiates at a high speed due to the tremendous driving force within the system. If this process occurs rapidly, there is no opportunity for the active ingredient to crystallize since the rapid penetration causes a decrease in the concentration of the active ingredient in the foam layer. Furthermore, the linked network of foams allows for effective medication transportation across the epidermal layers, resulting in improved absorption and bioavailability [21].

Despite numerous advantages, formulating dermal foams presents significant challenges. When designing their compositions, it is crucial for the formulation to remain on the skin for a sufficient duration. It should quickly spread to meet user preferences and provide a pleasant skin sensation. In terms of shelf life, they are stored in sealed containers, minimizing microbiological contamination. However, despite the aforementioned advantages of foams, the number of available topical foam preparations in the market remains relatively low compared to traditional formulations such as creams and gels.

In our study, diclofenac sodium was used as an active pharmaceutical ingredient (API). Among the NSAIDs, diclofenac sodium is the only API approved by the FDA for topical use in the treatment of pain associated with osteoarthritis. Being an organic acid, diclofenac exhibits lipophilic characteristics, whereas its salts readily dissolve in water under neutral pH conditions. The mix of these two attributes enables diclofenac to effectively permeate cell membranes, encompassing the synovial lining of diarthrodial joints as well as the skin [22]. Furthermore, the occurrence of adverse effects is minimal compared to oral administration, especially those topical formulations that contain diclofenac [23,24]. Various concentrations of hydrogels, creams, and other products with this API are available on the market.

Foams and hydrogels are two significant rivals within the dermal field that have been widely researched. However, it is becoming increasingly clear that foams have triumphed, outperforming hydrogels in many ways and changing dermal drug delivery [21,25].

Foams possess excellent stability and a prolonged shelf life due to their ability to maintain structural integrity during storage and application. Unlike hydrogels, foams are less prone to leakage or drying out, ensuring a consistent and effective drug delivery performance over an extended period.

In summary, achieving transdermal permeation is challenging, requiring the development of formulations that can temporarily disrupt the skin barrier for systemic effects. Foams, gaining attention in dermatology, offer advantages such as an easy application, aesthetic appearance, and better patient adherence. Despite their numerous benefits, formulating dermal foams poses challenges, with considerations for duration on the skin, user preferences, and shelf life. In our study, diclofenac sodium served as an active substance, showcasing its effectiveness in topical formulations. In many ways, foams are superior to hydrogels in terms of stability and extended shelf life, making them a promising dosage form in dermal drug delivery research.

Our research focused on comparing the physicochemical and biopharmaceutical properties of three drug delivery systems: foam, foam bulk liquid (a polymer solution), and a conventional hydrogel. Addressing the limited studies on medicated foams, our goal was to develop comprehensive investigational methods covering aspects such as foam stability, viscosity, pH, in vitro drug release, and ex vivo skin permeation. This includes examining the potential differences in properties between the preparations, as well as investigating the impact of diclofenac sodium (DS) at a concentration of 1% on the foam system.

2. Materials and Methods

2.1. Materials

Diclofenac sodium (DS) and fluorescein sodium were handled by Sigma-Aldrich (Budapest, Hungary). Isopropanol (IPA) was obtained from Avantor (Radnor, PA, USA). Hydroxypropyl methylcellulose (HPMC) was provided by Colorcon (Budapest, Hungary). Polyethylene glycol 200 (PEG 200) was purchased from Merck KGaA (Darmstadt, Germany). Phenoxyethanol and Caprylyl Glycol were from Biesterfeld GmbH (Hamburg, Germany). Polyoxyl castor oil was kindly supplied by BASF SE Chemtrade GmbH (Ludwigshafen, Germany). Gattefossé (Saint-Priest Cedex, France) provided Caprylocaproyl Polyoxyl-8 glycerides and CP Kelco A Huber Company (Atlanta, GA, USA) provided xanthan gum. Deionized and purified water was used (Milli-Q system, Millipore, Milford, MA, USA) during the research. The cellulose acetate filter (Porafil membrane filter, cellulose acetate, pore diameter: 0.45 μm) was acquired from Macherey-Nagel GmbH & Co. KG (Düren, Germany). Additionally, 70% sodium laureth sulfate (SLES) was provided by Kao Chemicals Europe S.L. (Barcelona, Spain).

2.2. Methods

2.2.1. Preparation of the Formulations

In terms of the examined formulations, both the foam and hydrogel contained the same non-ionic emulsifiers and preservatives at the same concentration. The difference lies in the type of the solvents and the type and the concentration of the polymer. In our preliminary research, we investigated several polymers. Among the foams, formulations containing xanthan gum exhibited the most stable and superior physicochemical properties [26], while for the hydrogels, those containing HPMC showed the best results.

The initial stage of hydrogel preparation involved the hydration of HPMC, which was carried out in purified water for a duration of 2 h. Simultaneously, a mixture of polyethylene glycol 200 and isopropanol was prepared. Following the swelling of the polymer, a predetermined quantity of DS was dissolved in the solvent mixture. The DS solution was then added incrementally to the hydrated polymer. The final homogenization of the formulation was carried out using a mechanical stirrer (Velp DLH Digital Overhead Stirrer, Italy). Ultimately, the uniform preparation was preserved.

The first stage of foam preparation was to prepare a polymer solution, with the polymers undergoing a 2 h swelling process in purified water. Subsequently, the preservative

solution was blended with the emulsifiers. The final step involved incorporating the swelled polymer into the mixture of emulsifiers and preservative solution. Following the preparation and homogenization with a mechanical stirrer, the liquid was stored in a well-sealed container until the start of the examination. The process of preparing the bulk liquid and its composition in this study is identical to that of the foam.

The exact compositions are illustrated in Table 1.

Table 1. Composition of the formulated foam, foam bulk liquid, and hydrogel ('+' indicates that the formulation contains the excipient, '−' indicates that the formulation does not contain the excipient).

	Hydrogel	**Foam/Foam Bulk Liquid**
Diclofenac sodium (g)	1	1
PEG 200	+	−
IPA	+	−
HPMC	+	−
Xanthan gum	−	+
Caprylocaproyl Polyoxyl-8 glycerides	+	+
Polyoxyl castor oil	+	+
Blend of Phenoxyethanol and Caprylyl Glycol	+	+
Purified water	up to 100 g	up to 100 g

2.2.2. Citotoxicity Assay

The impact of the utilized components on cell toxicity was assessed through MTT assays following the manufacturer's guidelines. Human-adipose-tissue-derived mesenchymal stem cells (AD-MSCs) were distributed into 96-well plates, with each well initially containing 5×10^3 cells. These cells were then exposed to a solution containing the components, in the same concentrations as used in the formulations, for 24 h in triplicate. Absorbance was measured using the Synergy HTX multi-plate reader (Agilent/BioTek, Santa Clara, CA, USA) at 550 nm, with a reference wavelength set at 650 nm.

2.2.3. Preformulation Studies of Foam Formula

In order to examine a foam formulation effectively, it is crucial to analyze the physicochemical properties of the foam formula. This analysis allows us to assess the impact of each component on the foam structure.

2.2.3.1. Macroscopic Characterization of Foam Formula

The macroscopic characteristics of the foam formula were evaluated using the cylinder method [9]. After 5 min (min) of mechanical stirring of the bulk liquid, the foam was poured into a glass measuring cylinder, and the initial volume as well as the volume after 30 min of aging were measured. Macroscopic tests enable the determination of various parameters, including foam expansion (FE, %); foam volume stability (FVS, %); and foam liquid stability (FLS, %).

The parameters can be calculated using the following equations:

$$\mathrm{FE}(\%) = \frac{\mathrm{V(foam)} - \mathrm{V(formulation)}}{\mathrm{V(formulation)}} \times 100\% \quad (1)$$

where V(formulation) represents the volume of the formulation [mL] required to generate V(foam) [mL]. A direct correlation can be observed between FE (foam expansion) and good foamability.

$$\mathrm{FVS}(\%) = \frac{\mathrm{V(foam,\ 30\ min)}}{\mathrm{V(foam)}} \times 100\% \quad (2)$$

where V(foam, 30 min) represents the volume of the foam after 30 min [mL].

$$\mathrm{FLS}(\%) = \frac{\mathrm{V(liquid,\ 30\ min)}}{\mathrm{V(foam)}} \times 100\% \quad (3)$$

where V(liquid, 30 min) is the drained volume after 30 min [mL].

2.2.3.2. Microscopic Characterization of Foam Formula

The microscopic measurements were conducted using the Leica DM6 B Fully Automated Upright Microscope System (Leica Biosystems GmbH in Wetzlar, Germany). The structure of foams and the relative bubble sizes provide information on the differences between foam generation techniques and their stability. The images were captured at 50× magnification.

2.2.3.3. Ex Vivo Permeation through the Skin Using Fluorescent Microscope

To model whether the formulation can permeate the stratum corneum, fluorescent microscopy was employed. During the investigation, the permeation capacity of the blank foam (without API) was examined. Experiments involving ex vivo skin permeation were carried out using excised human skin obtained from a Caucasian female patient who had undergone routine plastic surgery at the Department of Dermatology and Allergology, University of Szeged (Ethical Permission: BMEÜ/2339-3/2022/EKU). Following the plastic surgery, the skin surface underwent a gentle cleansing process using cotton swabs and was subsequently stored at a temperature of −20 °C for a maximum period of 6 months before being used.

Fluorescein sodium water-soluble dye was used to visualize the permeation of the foam system. At room temperature, full-thickness subcutaneous fat-free human abdominal skin was used in the experiment. The skin samples were defrosted and kept on filter papers soaked in a phosphate-buffered solution to preserve their hydration. To ensure the permeation of formulations, 0.2 g of each formulation was applied to the skin surface, and observation times of 10 and 30 min were employed. Following the treatment, any excess preparation remaining on the skin was carefully wiped off. Subsequently, a section of the treated skin was frozen and sliced using a Leica CM1950 Cryostat (Leica Biosystems GmbH, Wetzlar, Germany). Cross-sections with a thickness of 10 µm were placed on slides and examined using a light microscope (LEICA DM6 B, Leica Microsystems GmbH, Wetzlar, Germany) at room temperature. A red fluorescence filter (580–660 nm) was utilized to prevent interference from skin autofluorescence during the analysis. The examination was conducted at a magnification of 200× [4].

Images of the untreated skin were captured as a negative control, while skin pretreated with a solution containing sodium laureth sulfate (SLES) was used as a positive control. Images of the treatments were taken and visually compared to the control groups. ImageJ1 software was employed to assess the color intensity of the images, representing the distribution of color intensity within each image. The increase in intensity is indicated as relative intensity (RI), signifying how many times the increase in intensity compares to the negative control (untreated skin) [27].

2.2.4. Comparison of Physicochemical Properties of Foam Formula, Bulk Liquid, and Hydrogel

2.2.4.1. Rheological Measurements

The viscosity of the bulk liquid, foam, and hydrogel was examined using an Anton Paar Physica MCR302 Rheometer (Anton Paar, Graz, Austria) at a temperature of 25 °C. A cone-plate-type measuring device was applied with a diameter of 50 mm, and the gap height in the middle of the cone was 0.045 mm. The RheoCompass™ software v.1.25 (Anton Paar, Graz, Austria) of the instrument was utilized to calculate the viscosity of the preparations at a shear rate of 50 1/s through interpolation. The process involved conducting three measurements in parallel. Flow curves of the investigated formulations were plotted from a 0.1 to 100 1/s shear rate.

2.2.4.2. Investigation of pH

Each 5 g sample was placed in a beaker, and the pH was measured using a Testo 206 pH meter (Testo SE & Co. KGaA, Lenzkirch, Germany), at room temperature. Three

measurements were performed in parallel. The pH values were evaluated to assess the basicity/acidity of the preparations since the normal pH of the skin varies from 4 to 6 [28–30].

2.2.5. Comparison of Biopharmaceutical Properties of Foam Formula, Bulk Liquid, and Hydrogel

2.2.5.1. In Vitro Drug Release and Permeation Tests (IVRT and IVPT) Using Franz Diffusion Cell System

The drug release through the synthetic membrane from the bulk liquid, foam, and hydrogel, as well as its permeation through the human heat-separated epidermis, were modeled using the Vertical Franz diffusion cell (Hanson Microette TM Topical & Transdermal Diffusion Cell System, Hanson Research Corporation, Chatsworth, CA, USA). The excised human skin, just like in the case of the fluorescent microscope method, was obtained through plastic surgery.

For in vitro release tests, as a donor phase, 0.3 g of the sample (in the case of the hydrogel and bulk liquid) was applied onto a synthetic membrane filter. In the case of foam (due to its large volume), 0.085 g was placed onto the membrane (Porafil cellulose acetate membrane with a pore diameter of 0.45 µm, Macherey-Nagel GmbH & Co. KG, Düren, Germany). In contrast, for the in vitro permeation test, a heat-separated human epidermis [31,32] was employed as the membrane. Both the drug release and permeation tests lasted 6 h and the sampling dates were 10, 20, and 30 min, and 1, 2, 4, and 6 h. The amount of the active pharmaceutical ingredient released from the formulation and transported through the skin was determined by using UHPLC (Shimadzu Nexera ×2, Shimadzu, Kyoto, Japan, ultra high-performance liquid chromatography system).

The UHPLC was equipped with a Phenomenex Kinetex XB-C18 (50 × 2.1 mm, 2.6 µm) column, which was used as a stationary phase. Separation was achieved through isocratic elution, employing a 36:64 mixture of a 0.136 g/L KH_2PO_4 solution and methanol as the eluent. The separation procedure occurred at 40 °C with a flow rate of 0.5 mL/min, spanning a 3 min analysis time. The retention time for DS was noted at 1.5 min. A sample volume of 3 µL was injected for the analysis. Detection was carried out using a diode array UV-VIS detector at a wavelength of 247 nm [33].

To study the release mechanism of the investigated formulations, we applied the Korsmeyer–Peppas model by fitting it to the release curve until reaching the plateau phase, providing information about the mechanism of drug release [34].

The calculation of in vitro permeation was based on the cumulative amount of DS that permeated through the epidermis, considering the diffusion area. These findings were graphed over time, and the steady-state flux (J) was calculated from the slope of the permeation curve, quantified in terms of µg cm^{-2} h^{-1}. For this analysis, the incubation period ranged from 1 to 6 h, during which the flux data for DS were determined.

2.2.5.2. Investigation of Ex Vivo Drug Permeation Using Raman Spectroscopy

Raman spectroscopy is an emerging spectroscopic approach grounded in identifying the characteristic vibrational energy states of a molecule when exposed to laser irradiation. It offers insights into the molecular arrangement of tissue constituents devoid of the necessity for fluorescent markers or chemical dyes [35,36]. The confocal Raman microscopy can be employed to investigate topical formulations, for determining both permeation and permeation depth. In our research, Raman microscopy was utilized to capture images depicting the spatial distribution of DS within ex vivo human skin.

The preparation and sectioning of the skin were conducted in the same manner as for fluorescence microscopy examination, with the only difference being the incubation time of 3 h. Subsequently, the cross-sectional skin samples, with a thickness of approximately 15 micrometers, were positioned onto slides coated with aluminum. Raman spectroscopic assessments were conducted using a Thermo Fisher DXR Dispersive Raman Spectrometer (Thermo Fisher Scientific Inc., Waltham, MA, USA) fitted with a CCD camera and a diode laser. A laser light emitting at a wavelength of 780 nm was employed, reaching a peak power of 24 mW. This wavelength is optimal for studying biological specimens as it provides

enough energy for the vibrations of protein constituents within the skin. Using this specific laser source reduced the impact of fluorescence. For the measurements, a microscopic lens with a magnification of 50× was employed, and the pinhole aperture had a diameter of 25 µm [37]. While conducting the mapping procedure, an area of 100 × 500 µm on the skin was visualized, using both vertical and horizontal step sizes of 50 µm. Throughout the measurement, the map of the untreated skin was used as a control.

The spectra of DS in the bulk liquid and hydrogel were employed as a basis for comparing treated and untreated skin samples. To capture the spectra of DS, a 780 nm laser source was utilized. A total of 33 scans were recorded for each spectrum with an exposure time of 6 s. The Raman microscope featured 10× optical magnification with a 25 µm slit aperture.

The data collection and analysis were carried out using the Dispersive Raman software package OMNICTM 8.2 (ThermoFisher Scientific Inc., Waltham, MA, USA).

2.2.6. Statistical Analysis

The results of the in vitro drug release tests underwent statistical evaluation using the two-way ANOVA analysis of variance test (Bonferroni's multiple comparison) with Prism 5.0 for Windows 10 software (GraphPad Software Inc., La Jolla, CA, USA). The data represent the mean values derived from six experiments, along with the standard deviations, and significant differences from the foam formulation were observed at the levels of * $p \leq 0.05$ and *** $p \leq 0.001$.

3. Results

3.1. Cytotoxicity Assay

The MTT test was conducted for the components of all three examined preparations (Figure 1). The findings indicated that the applied components enhanced cell viability, although diclofenac sodium had a minor reducing effect, as determined by the MTT assay. All examined components exhibited a viability of over 70%, indicating that, in accordance with the ISO 10993-5 standard [38], these substances are not cytotoxic to mesenchymal cells. The control group demonstrated 100% viability (measured in triplicate, N = 3).

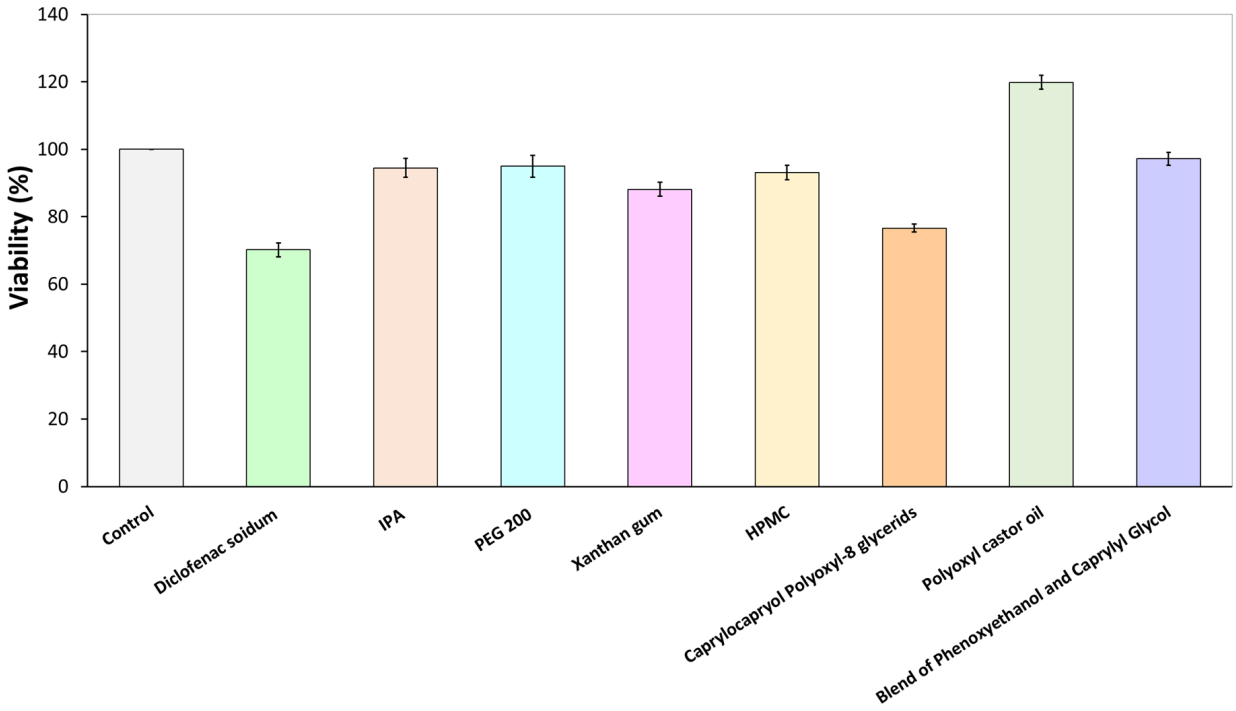

Figure 1. Effect of components on the viability of AD-MSCs.

3.2. Preformulation Studies of Foam Formula

A preformulation study was carried out to ensure that our foam formula meets the physicochemical and biopharmaceutical properties required for dermal application.

3.2.1. Macroscopic Characterization of Foam Formula

In order to determine the effect of the polymer and the active pharmaceutical ingredient (API) on foam expansion, foam volume, and foam liquid stability, a comparison was made between a polymer-and-active-ingredient-free formulation, a xanthan-gum-containing, active-ingredient-free formulation, and the foam system containing DS and xanthan gum together (Table 2).

Table 2. Result of the macroscopic examination.

	Polymer-and-API-Free Foam	Xanthan-Gum-Containing Foam	Xanthan-Gum-and-DS-Containing Foam
Foam expansion (FE, %)	172 ±15.8	134 ± 1.9	120 ± 0.7
Foam volume stability (FVS, %)	14 ± 1.8	100 ±0.0	98 ± 0.0
Foam liquid stability (FLS, %)	36 ± 2.0	0 ± 0.0	1.5 ± 0.2

The API and the polymer content had a negative effect on foam expansion, possibly due to the initial increase in the viscosity of the bulk liquid. However, each foam formulation met the criterion for well-foaming preparations, exhibiting over 100% foam expansion [26].

Regarding foam volume stability, macroscopic observations clearly supported that the polymer-and-API-free systems collapsed quickly, while the xanthan-gum-containing system maintained its foam volume even after 30 min. The foam system containing DS, which also included xanthan gum as a polymer, also preserved its original volume at nearly 100%.

The FLS value also indicates macroscopic foam stability and a lower FLS value refers to better stability. In this case as well, it was observed that the polymer-free foam had lower stability, compared to the other two formulations.

3.2.2. Microscopic Characterization of Foam Formula

The structure of foams can be analyzed directly after their formation using a light microscope. The examination of the microscopic structure of foams can be conducted most conveniently with a fully automated microscopic system. Microscopic images provide the opportunity to study the connections between bubbles and liquid films, known as lamellae, that enclose the bubbles. Additionally, the changes in bubble size and number over time can be observed.

The foams were produced using two different foam formation techniques, which were compared during the investigation (Figure 2). Mechanical stirring provides a more realistic representation of foam formation, and the duration of foam formation can be better tracked, while the foams produced with a propellant-free pump simulate real application conditions.

The bubbles produced with a propeller stirrer are smaller and more uniform in size in the case of xanthan-gum- and diclofenac-containing formulations. The smaller bubbles contribute to the formation of a coherent foam structure, making these systems more stable than the polymer- and API-free formulation. The results, therefore, correlate with the results of macroscopic foam stability. For the formulations produced with the pump, the film thickness was greater in the case of xanthan-gum-containing compositions, and the amount of liquid bound by the polymer in the boundary layer could be more significant.

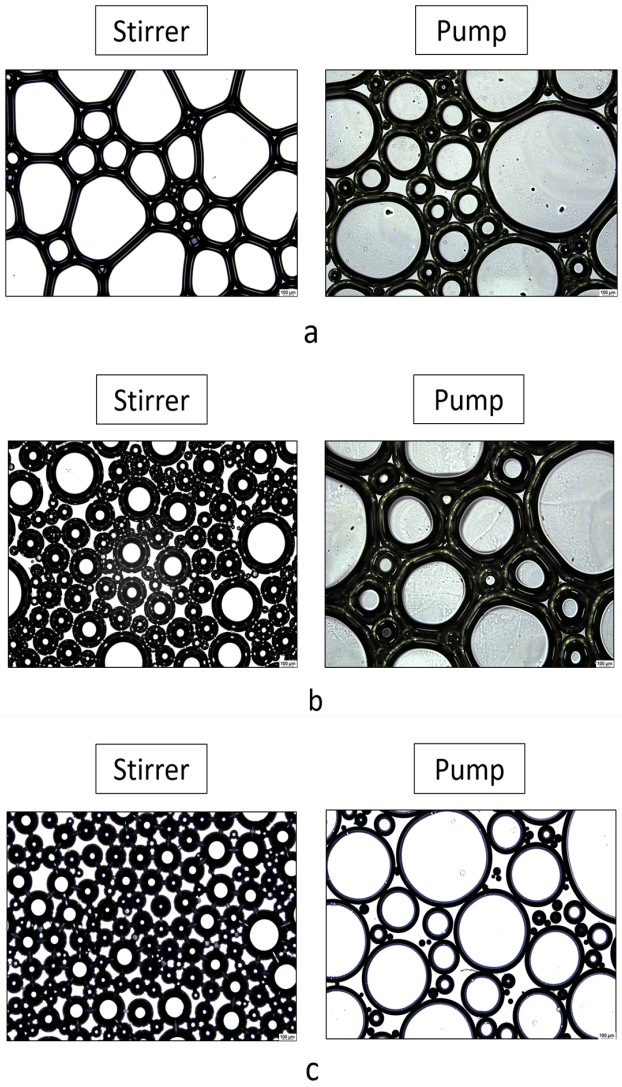

Figure 2. Microscopic images of the structure of foams produced by the pump and mechanical stirrer: (**a**) polymer- and DS-free foams; (**b**) xanthan-gum-containing, DS-free foam; (**c**) xanthan-gum- and DS-containing foam. The images were captured at 50× magnification.

3.2.3. Ex Vivo Permeation through Fluorescent Microscope

The foam was compared to the negative and positive controls throughout the investigation. The negative control involved assessing the appearance of untreated skin under a fluorescent microscope. The microscopical images revealed that the stratum corneum exhibited a high fluorescence intensity (Figure 3A). This characteristic of untreated skin has already been documented in previous literature, which indicates the physiological appearance of the structure of the stratum corneum [39]. To determine the permeation of the formulation marked with the fluorescent dye, lower epidermal and dermal layers need to be examined since these layers only appear with low intensity under the fluorescent filter, and the autofluorescence of the skin does not interfere with the evaluation (Figure 3B).

In the case of the positive control, the skin was pretreated with an SLES solution, which facilitated permeation. Alkyl sulfates have the capacity to disrupt the barrier structure and allow a fluorescein dye solution to pass through the stratum corneum. Based on these evaluations, the increase in intensity (relative intensity) was assessed compared to the untreated skin (negative control).

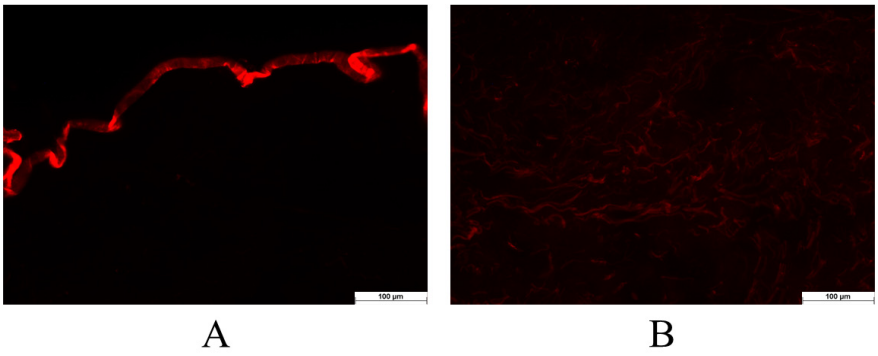

Figure 3. The untreated skin was used as a negative control. The stratum corneum with the upper skin layers (**A**) and the lower skin layers (**B**). The examination was conducted at a magnification of 200×.

The findings indicated (seen in Figure 4) that the light intensity of the skin significantly increased following the SLES pretreatment. SLES reduced the protective function of the stratum corneum, allowing the fluorescent dye solution to reach deeper layers of the skin. After 10 min of treatment, the intensity increased by 7.51 times, while after 30 min of treatment, it only increased by 6.41 times compared to the negative control.

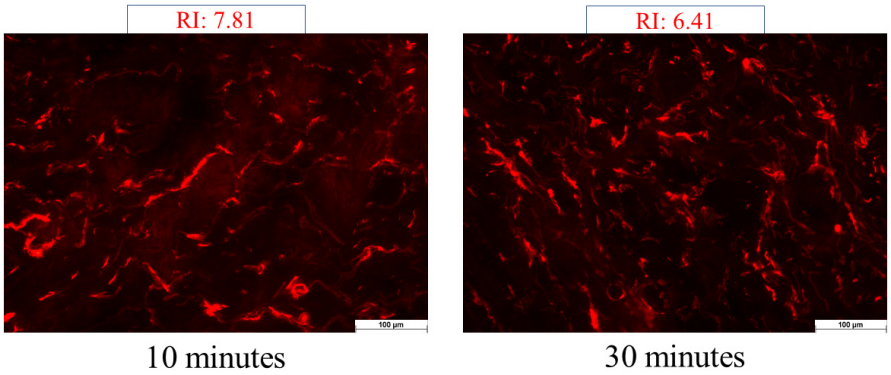

Figure 4. Images of the positive control: Relative Intensity Values at 10 and 30 min. The examination was conducted at a magnification of 200×.

In the case of the foam, as the observation time increased, there was a noticeable increase in fluorescence intensity. After 10 min, there was a 3.76-fold increase in permeation, but after 30 min, this value increased by 6.68-fold (Figure 5). In the case of foam preparation, the intensity of permeation was low at 10 min, but after 30 min, it reached almost the same relative intensity compared to the positive control. Without irritation, deeper permeation similar to the positive control can be achieved with the foam formulation.

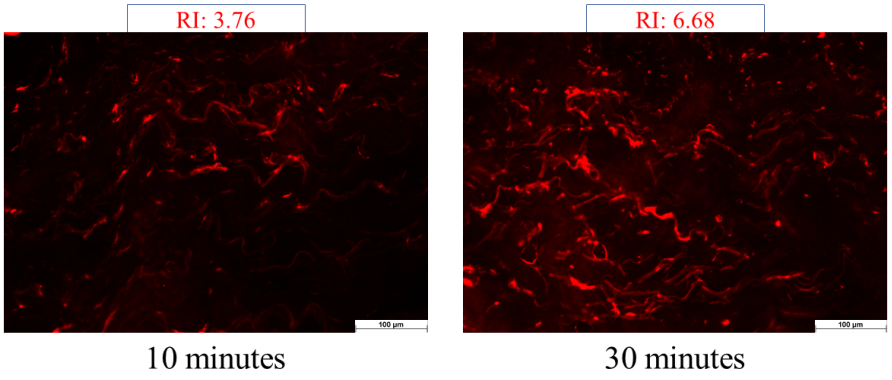

Figure 5. Images of the skin treated with the foam formulation: Relative Intensity Values at 10 and 30 min. The examination was conducted at a magnification of 200×.

3.3. Comparison of Physicochemical Properties of Foam Formula, Bulk Liquid, and Hydrogel

3.3.1. Rheological Measurements

The consistency of the systems was investigated with rheological measurements.

The viscosities of the bulk liquid and the liquid film, remaining after the breakdown of the foam, were compared to each other and the reference hydrogel formulation (Table 3).

Table 3. The viscosity of the formulated preparations at 50 1/s shear rate.

	Viscosity (mPas)
Bulk liquid	46.99 ± 0.80
Liquid film (after the foam decay)	58.68 ± 1.07
Hydrogel	378.78 ± 4.39

The foam was formed from the bulk liquid (initial polymer solution), during which the propellant-free foam pump mixed it with the ambient air. After a certain period of time, as the foam decayed, it transformed into a liquid film through the effects of binding forces and interactions between chains, causing the polymer chains to form a more orderly network or structure than what exists among the polymers in the initial liquid. This ordered structure can result in reduced volume filling and density, increasing the viscosity of the liquid film. The viscosity of the formulated hydrogel was much higher, found to be typical of semi-solid formulations.

According to the rheological results (Figure S1), all three systems exhibit the characteristic shear-thinning behavior typical of polymer solutions, where viscosity decreases under the influence of shear. Clearly, in the case of the hydrogel, the viscosity value is high due to the higher polymer content. The viscosity of the remaining liquid film was greater than that of the initial liquid. The increase in viscosity may be due to the ordered structure of the polymer liquid film, making it less liquid and more resistant to deformation. This could potentially cause a slight delay in skin permeation due to the more orderly network formed between polymer chains.

3.3.2. Investigation of pH

Testing and adjusting the pH of dermal formulations can be key to ensuring the efficacy of the formulation and the barrier function of the skin. The pH values of the bulk liquid/foam and the hydrogel were in the range of 7–8, revealing the suitability of them for topical application, as it is reported in Table 4. In addition, the surface of the stratum corneum is slightly acidic, although it tends toward more neutral values (pH 7–7.4) in the vital layers [40]. Moreover, in the short term, a higher pH value may be tolerated. Human skin has a certain degree of buffer capacity and may tolerate a slight pH change in the skin.

Table 4. The pH values of the formulated preparations.

	pH
Bulk liquid/Foam	7.86 ± 0.11
Hydrogel	7.29 ± 0.37

3.4. Comparison of Biopharmaceutical Properties of Foam Formula, Bulk Liquid, and Hydrogel

3.4.1. In Vitro Drug Release and Permeation Tests (IVRT and IVPT) Using Franz Diffusion Cell System

The release of the active substance may depend on a number of factors that can influence how much and at what rate it is released from a given formulation into the surrounding medium or onto the treated surface. The drug release curves of the three forms are shown in Figure 6.

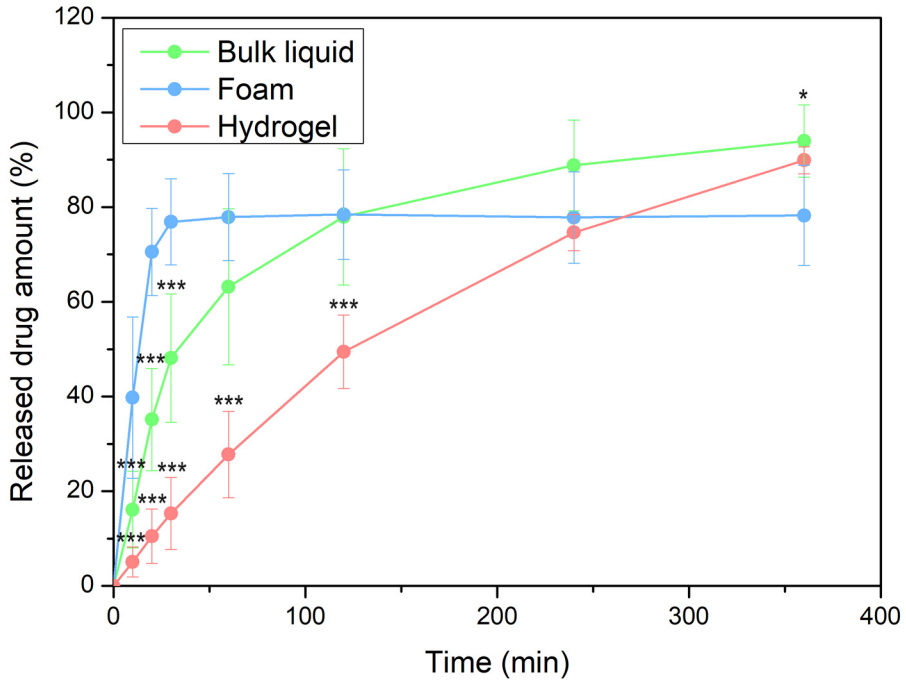

Figure 6. The release profile of DS in different dosage forms (*** $p \leq 0.001$ vs. foam, * $p \leq 0.05$ vs. foam).

The results suggested that most of the DS was released from the foam within a relatively brief duration. Around 80% of the active ingredient was released in just 30 min when using the foam, whereas it took approximately 5 h for the hydrogel to achieve the same outcome. This quantity of DS was released from the bulk liquid after approximately 2 h.

The results could be due to the porous structure of the foam; it consists of many pores, channels, or air bubbles in which the active substances are more easily dispersed. This porous structure allows the active ingredients to move and reach their target site more quickly. The kinetics of release exhibited a resemblance between the bulk liquid and the hydrogel; however, DS demonstrated a slightly more rapid diffusion from the bulk liquid. On the one hand, polymer solutions (bulk liquid) generally have a lower viscosity than hydrogels. The lower viscosity allows the active molecules to diffuse more easily from the polymer solution into the surrounding medium or onto the skin. Conversely, hydrogels have a higher viscosity, which may limit the diffusion and release of the active substance.

On the other hand, the release may be affected by the polymer network and structure. Hydrogels typically possess a more organized, interconnected structure, which may result in a slower release as the drug has more difficulty diffusing through the polymer network.

In the investigation, the release of the drug is comprehensively studied and explained through the application of the Korsmeyer–Peppas model. This model allows for a detailed analysis and understanding of the drug release kinetics, providing valuable insights into the release mechanism (Table 5).

Table 5. Korsmeyer–Peppas model for the mechanism of drug release kinetics of the investigated formulations.

Formulation	R^2	n	k
Bulk liquid	0.9094	0.6105	4.9352
Foam	0.9372	0.6243	9.8115
Hydrogel	0.9880	0.8033	0.9284

In the case of all systems, the observed *n* values are between 0.5 and 1.0, indicating that the mechanism of drug transport involves both diffusion and relaxation (erosion). Based on the k value, the fastest release rate was observed in the case of foam formulation [34].

The permeation rate values (Table 6) suggested that, in the case of foam, quick drug release resulted in rapid drug permeation. The foam can come into contact with the skin over a large surface area and the active ingredient can be absorbed quickly. This facilitates the swift delivery of active ingredients to the skin, expediting their effectiveness. The liquid film that emerges after the foam decaying may become supersaturated, resulting in accelerated permeation compared to hydrogel and bulk liquid.

Table 6. The flux values of DS through the human epidermis.

	J (μg/cm^2/h)	R^2
Bulk liquid	0.866	0.9811
Foam	5.838	0.9921
Hydrogel	1.65	0.9173

3.4.2. Investigation of Ex Vivo Drug Permeation Using Raman Spectroscopy

The correlation maps depicted the distribution of DS, employing suitable spectra for accurate fitting with the spectra of the treated skin. Figures 6–8 exhibit the qualitative distribution of DS within human skin samples following the application of foam, bulk liquid, and hydrogel. Our objective was to ascertain whether the permeation of DS remains confined to the stratum corneum or if it can permeate into the epidermis or dermis. On the maps, the warmer color indicates a higher presence of DS.

For the bulk liquid, DS became detectable in the deeper skin layers within 10 min and exhibited a more pronounced presence in these layers by 30 min (Figure 7). In contrast, in the case of skin sections treated with foam, the DS was concentrated in the upper layers of the epidermis after 10 min, and the presence of the active substance was detected in deeper layers as time progressed (Figure 8). Due to the gradual decay of the foam, liquid between the bubbles began to leak onto the skin after 10 min, forming a supersaturated liquid layer. Consequently, the intense presence of DS in the foam became more prominent, with higher concentrations of the active substance observed between 20 and 30 min.

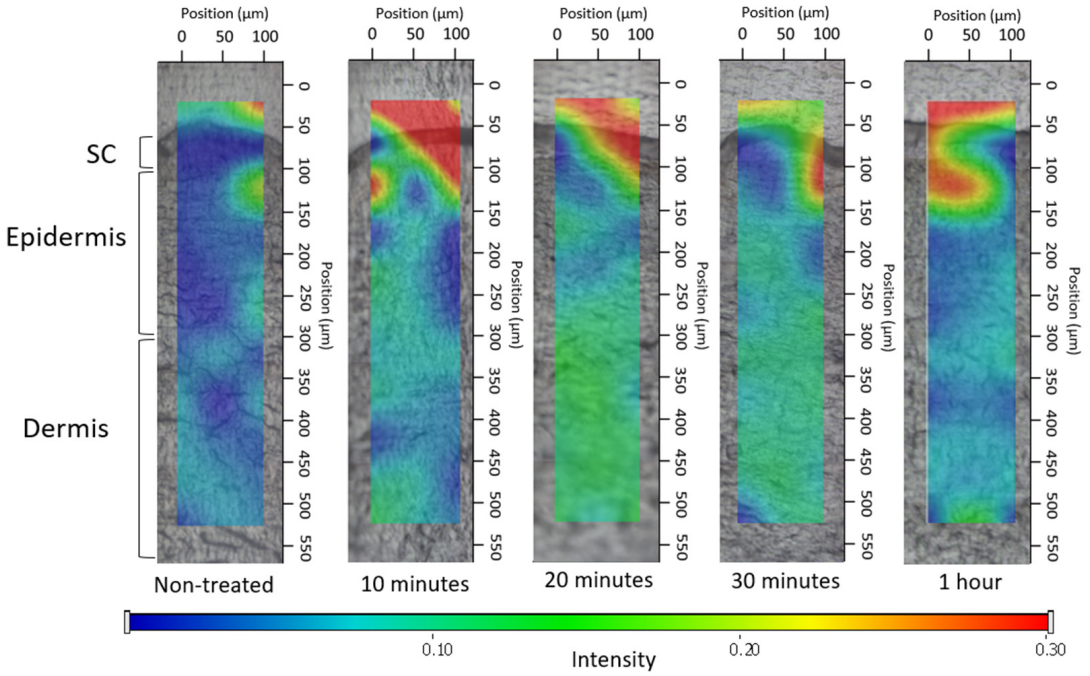

Figure 7. Kinetics of ex vivo drug permeation of bulk liquid.

Regarding the hydrogel (Figure 9), the observation indicated that DS managed to permeate solely into the uppermost epidermal layer throughout the study duration. After 1 h, higher concentrations were achieved in the stratum corneum.

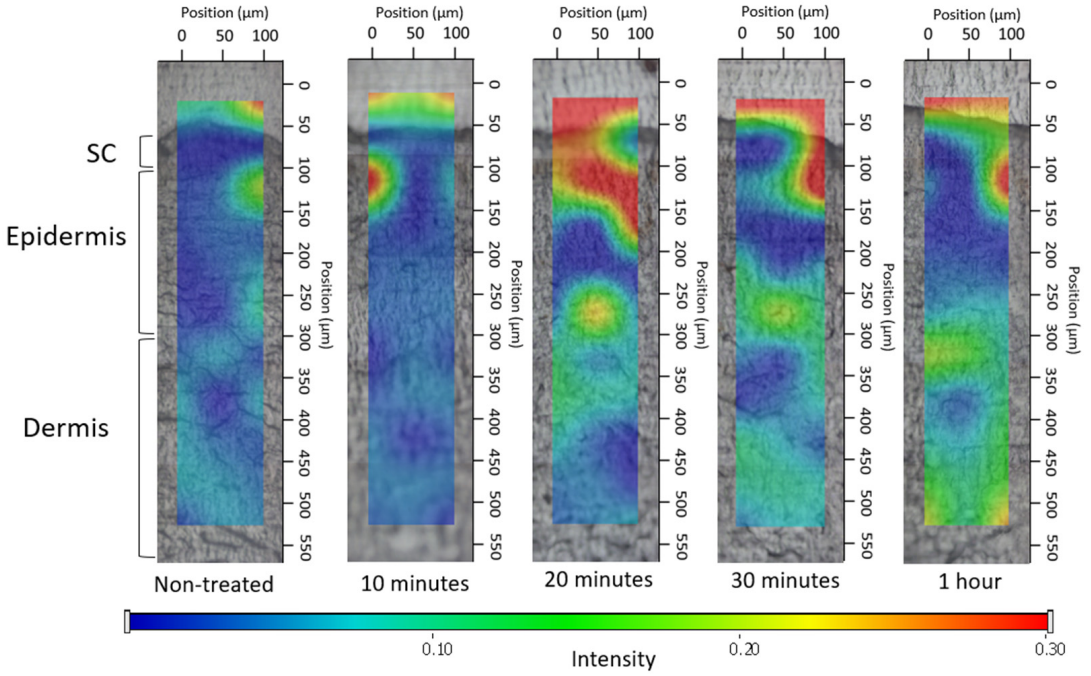

Figure 8. Kinetics of ex vivo drug permeation of foam.

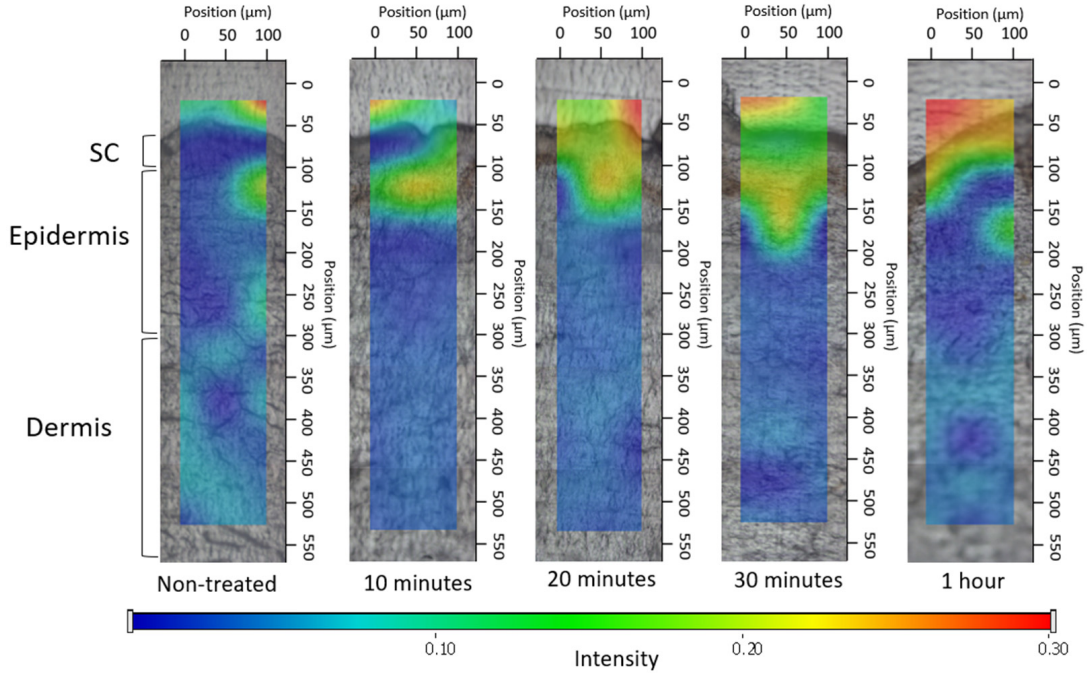

Figure 9. Kinetics of ex vivo drug permeation of hydrogel.

To conclude, the Raman maps highlighted the impact of viscosity on permeation. The composition of the foam and bulk liquid is the same; however, in the case of the foam formula, there is a higher permeation of the active ingredient after 20 min, which is visible as an intense red color on the Raman map. When compared to the hydrogel, possessing the greatest viscosity, it hindered the permeation of DS; therefore, it did not permeate the deeper layers of the skin even after 1 h. This higher viscosity prevents the active ingredient from permeating into the deeper layers of the skin even after 1 h. Meanwhile, the bulk liquid, with the lowest viscosity, exhibited swift and intense permeation into the deeper layers. The formation of a supersaturated liquid film during foam aging was evident after 20 min and its effects were still detectable after 1 h. The supersaturated liquid film formed

during the aging of the foam could be formed after 20 min and its effect was still detectable after 1 h.

4. Discussion

In this work, we compared the physicochemical and biopharmaceutical properties of foams with those of traditional hydrogel and polymer solutions.

According to the cytotoxicity assessment, the components in the formulations did not exhibit any cytotoxic impact on mesenchymal cells at the concentrations used. Therefore, we found these components to be suitable for the formulation of dermally applied preparations.

In terms of preformulation studies of foams, the presence of DS reduced foam expansion based on macroscopic observations but did not negatively impact foam stability, as confirmed by microscopic results, since it had no adverse effects on the foam structure. The pH values of both the bulk liquid/foam and the hydrogel ranged from 7 to 8, making them suitable for topical application.

Biopharmaceutical examinations revealed that the foam, as a drug delivery system, can achieve rapid drug release and deeper skin permeation compared to the hydrogel. Approximately 80% of the active ingredient was released in just 30 min using the foam, while it took approximately 5 h for the hydrogel to achieve the same outcome.

The drug release from the formulations was studied and explained using the Korsmeyer–Peppas model. The fastest release rate was observed in the case of foam formulation, which correlates with the result of drug permeation.

Results from Raman skin permeation studies demonstrated that within just 10 min, the foam concentrated in the upper layers of the epidermis and gradually permeated even deeper layers over time. The supersaturated liquid film formed during the aging of the foam could be observed after 20 min, and its effect was still detectable after 1 h. The Raman mapping results exhibited a strong correlation with the fluorescent microscopic examination, as the foam formulation maintained high light intensity even after 10 min, providing additional evidence for the system's rapid permeation. In comparison, the hydrogel, with the greatest viscosity, hindered the permeation of DS. Therefore, it did not permeate the deeper layers of the skin even after 1 h.

The applied test methods were suitable for the complex investigation of the foam formula, including the physicochemical and biopharmaceutical properties, as well as for the detection of the potential differences between the preparations. Furthermore, it can be concluded that diclofenac sodium (DS) at a concentration of 1% did not negatively affect the stability of the foam.

5. Conclusions

Overall, foaming systems have great potential through rapid drug release and deeper skin permeation, not only for the pharmaceutical industry but also for the cosmetic industry. Among our future plans is the assessment of the developed formulations' effects on keratinocytes and mesenchymal stem cells in vitro. Additionally, we aim to conduct in vivo studies using animal models.

Supplementary Materials: The following supporting information can be downloaded at: https://www.mdpi.com/article/10.3390/pharmaceutics16020287/s1, Figure S1: Flow curves of the investigated systems.

Author Contributions: Conceptualization, A.K. and S.B.; methodology, F.F., A.K. and Z.V.; formal analysis, F.F. and M.B.-S.; investigation, F.F., Z.V. and M.B.-S.; resources, M.B.-S.; writing—original draft preparation, F.F.; writing—review and editing, A.K. and S.B.; visualization, F.F.; supervision, A.K.; project administration, S.B.; funding acquisition, S.B. All authors have read and agreed to the published version of the manuscript.

Funding: Supported by the ÚNKP-22-3—SZTE-149 New National Excellence Program of the Ministry for Culture and Innovation from the source of the National Research, Development and Innovation Fund. Project no. TKP2021-EGA-32 has been implemented with the support provided by the Ministry

of Innovation and Technology of Hungary from the National Research, Development and Innovation Fund, financed under the TKP2021-EGA funding scheme.

Institutional Review Board Statement: Not applicable.

Informed Consent Statement: Not applicable.

Data Availability Statement: The data presented in this study are available on request from the corresponding author.

Acknowledgments: The authors would like to thank Tamás Monostori for his valuable help in conducting cytotoxicity measurements. The authors wish to thank Azelis Hungary Ltd., BASF SE Chemtrade GmbH, and Biesterfeld GmbH for providing the samples for formulations.

Conflicts of Interest: The authors declare no conflicts of interest.

References

1. Barnes, T.M.; Mijaljica, D.; Townley, J.P.; Spada, F.; Harrison, I.P. Vehicles for Drug Delivery and Cosmetic Moisturizers: Review and Comparison. *Pharmaceutics* **2021**, *13*, 2012. [CrossRef]
2. Daniels, R.; Knie, U. Galenics of Dermal Products—Vehicles, Properties and Drug Release. *JDDG J. Dtsch. Dermatol. Ges.* **2007**, *5*, 367–383. [CrossRef]
3. Wang, M.; Marepally, S.K.; Vemula, P.K.; Xu, C. Chapter 5—Inorganic Nanoparticles for Transdermal Drug Delivery and Topical Application. In *Nanoscience in Dermatology*; Hamblin, M.R., Avci, P., Prow, T.W., Eds.; Academic Press: Boston, MA, USA, 2016; pp. 57–72, ISBN 978-0-12-802926-8.
4. Kis, N.; Gunnarsson, M.; Berkó, S.; Sparr, E. The Effects of Glycols on Molecular Mobility, Structure, and Permeability in Stratum Corneum. *J. Control. Release* **2022**, *343*, 755–764. [CrossRef]
5. Zaid Alkilani, A.; McCrudden, M.T.C.; Donnelly, R.F. Transdermal Drug Delivery: Innovative Pharmaceutical Developments Based on Disruption of the Barrier Properties of the Stratum Corneum. *Pharmaceutics* **2015**, *7*, 438–470. [CrossRef]
6. Karande, P.; Mitragotri, S. Enhancement of Transdermal Drug Delivery via Synergistic Action of Chemicals. *Biochim. Biophys. Acta BBA Biomembr.* **2009**, *1788*, 2362–2373. [CrossRef]
7. Alexander, A.; Dwivedi, S.; Ajazuddin; Giri, T.K.; Saraf, S.; Saraf, S.; Tripathi, D.K. Approaches for Breaking the Barriers of Drug Permeation through Transdermal Drug Delivery. *J. Control. Release* **2012**, *164*, 26–40. [CrossRef]
8. Chaturvedi, S.; Garg, A. An Insight of Techniques for the Assessment of Permeation Flux across the Skin for Optimization of Topical and Transdermal Drug Delivery Systems. *J. Drug Deliv. Sci. Technol.* **2021**, *62*, 102355. [CrossRef]
9. Parsa, M.; Trybala, A.; Malik, D.J.; Starov, V. Foam in Pharmaceutical and Medical Applications. *Curr. Opin. Colloid Interface Sci.* **2019**, *44*, 153–167. [CrossRef]
10. Trybala, A.; Koursari, N.; Johnson, P.; Arjmandi-Tash, O.; Starov, V. Interaction of Liquid Foams with Porous Substrates. *Curr. Opin. Colloid Interface Sci.* **2019**, *39*, 212–219. [CrossRef]
11. Singh, A.; Sharma, P.K.; Malviya, R. Eco Friendly Pharmaceutical Packaging Material. *World Appl. Sci. J.* **2011**, *14*, 1703–1716.
12. Gennari, C.G.M.; Selmin, F.; Minghetti, P.; Cilurzo, F. Medicated Foams and Film Forming Dosage Forms as Tools to Improve the Thermodynamic Activity of Drugs to Be Administered Through the Skin. *Curr. Drug Deliv.* **2019**, *16*, 461–471. [CrossRef]
13. Farkas, D.; Kállai-Szabó, N.; Sárádi-Kesztyűs, Á.; Lengyel, M.; Magramane, S.; Kiss, É.; Antal, I. Investigation of Propellant-Free Aqueous Foams as Pharmaceutical Carrier Systems. *Pharm. Dev. Technol.* **2021**, *26*, 253–261. [CrossRef]
14. Purdon, C.H.; Haigh, J.M.; Surber, C.; Smith, E.W. Foam Drug Delivery in Dermatology: Beyond the Scalp. *Am. J. Drug Deliv.* **2003**, *1*, 71–75. [CrossRef]
15. Maimouni, I.; Cejas, C.M.; Cossy, J.; Tabeling, P.; Russo, M. Microfluidics Mediated Production of Foams for Biomedical Applications. *Micromachines* **2020**, *11*, 83. [CrossRef]
16. Mantripragada, S. A Lipid Based Depot (DepoFoam Technology) for Sustained Release Drug Delivery. *Prog. Lipid Res.* **2002**, *41*, 392–406. [CrossRef] [PubMed]
17. Mantripragada, S.B.; Howell, S.B. Sustained-Release Drug Delivery with DepoFoam. In *Drug Delivery Systems in Cancer Therapy*; Brown, D.M., Ed.; Cancer Drug Discovery and Development; Humana Press: Totowa, NJ, USA, 2004; pp. 247–262. ISBN 978-1-59259-427-6.
18. Salisbury, A.-M.; Mullin, M.; Foulkes, L.; Chen, R.; Percival, S.L. Controlled-Release Iodine Foam Dressings Demonstrate Broad-Spectrum Biofilm Management in Several in Vitro Models. *Int. Wound J.* **2022**, *19*, 1717–1728. [CrossRef] [PubMed]
19. Cilurzo, F.; Casiraghi, A.; Selmin, F.; Minghetti, P. Supersaturation as a Tool for Skin Penetration Enhancement. *Curr. Pharm. Des.* **2015**, *21*, 2733–2744. [CrossRef]
20. Zhao, Y.; Brown, M.B.; Jones, S.A. Pharmaceutical Foams: Are They the Answer to the Dilemma of Topical Nanoparticles? *Nanomedicine Nanotechnol. Biol. Med.* **2010**, *6*, 227–236. [CrossRef]
21. Kumar, M.; Thakur, A.; Mandal, U.K.; Thakur, A.; Bhatia, A. Foam-Based Drug Delivery: A Newer Approach for Pharmaceutical Dosage Form. *AAPS PharmSciTech* **2022**, *23*, 244. [CrossRef]

22. Altman, R.; Bosch, B.; Brune, K.; Patrignani, P.; Young, C. Advances in NSAID Development: Evolution of Diclofenac Products Using Pharmaceutical Technology. *Drugs* **2015**, *75*, 859–877. [CrossRef]
23. Balmaceda, C.M. Evolving Guidelines in the Use of Topical Nonsteroidal Anti-Inflammatory Drugs in the Treatment of Osteoarthritis. *BMC Musculoskelet. Disord.* **2014**, *15*, 27. [CrossRef]
24. Heyneman, C.A.; Lawless-Liday, C.; Wall, G.C. Oral versus Topical NSAIDs in Rheumatic Diseases. *Drugs* **2000**, *60*, 555–574. [CrossRef]
25. Hoc, D.; Haznar-Garbacz, D. Foams as Unique Drug Delivery Systems. *Eur. J. Pharm. Biopharm.* **2021**, *167*, 73–82. [CrossRef]
26. Falusi, F.; Budai-Szűcs, M.; Csányi, E.; Berkó, S.; Spaits, T.; Csóka, I.; Kovács, A. Investigation of the Effect of Polymers on Dermal Foam Properties Using the QbD Approach. *Eur. J. Pharm. Sci.* **2022**, *173*, 106160. [CrossRef]
27. Kis, N.; Kovács, A.; Budai-Szűcs, M.; Erős, G.; Csányi, E.; Berkó, S. The Effect of Non-Invasive Dermal Electroporation on Skin Barrier Function and Skin Permeation in Combination with Different Dermal Formulations. *J. Drug Deliv. Sci. Technol.* **2022**, *69*, 103161. [CrossRef]
28. Ali, S.M.; Yosipovitch, G. Skin pH: From Basic Science to Basic Skin Care. *Acta Derm. Venereol.* **2013**, *93*, 261–267. [CrossRef] [PubMed]
29. Honari, G.; Andersen, R.; Maibach, H.L. *Sensitive Skin Syndrome*; CRC Press: Boca Raton, FL, USA, 2017; ISBN 978-1-4987-3735-7.
30. Schneider, L.A.; Korber, A.; Grabbe, S.; Dissemond, J. Influence of pH on Wound-Healing: A New Perspective for Wound-Therapy? *Arch. Dermatol. Res.* **2007**, *298*, 413–420. [CrossRef] [PubMed]
31. Jian, L.; Cao, Y.; Zou, Y. Dermal-Epidermal Separation by Heat. *Methods Mol. Biol. Clifton NJ* **2020**, *2109*, 23–25. [CrossRef]
32. Maibach, Y.Z.; Howard, I. Dermal-Epidermal Separation Methods: Research Implications. In *Percutaneous Absorption*; CRC Press: Boca Raton, FL, USA, 2021; ISBN 978-0-429-20297-1.
33. Szoleczky, R.; Budai-Szűcs, M.; Csányi, E.; Berkó, S.; Tonka-Nagy, P.; Csóka, I.; Kovács, A. Analytical Quality by Design (AQbD) Approach to the Development of In Vitro Release Test for Topical Hydrogel. *Pharmaceutics* **2022**, *14*, 707. [CrossRef] [PubMed]
34. Bayan, M.F.; Chandrasekaran, B.; Alyami, M.H. Development and Characterization of Econazole Topical Gel. *Gels* **2023**, *9*, 929. [CrossRef] [PubMed]
35. Binder, L.; SheikhRezaei, S.; Baierl, A.; Gruber, L.; Wolzt, M.; Valenta, C. Confocal Raman Spectroscopy: In Vivo Measurement of Physiological Skin Parameters—A Pilot Study. *J. Dermatol. Sci.* **2017**, *88*, 280–288. [CrossRef] [PubMed]
36. Chen, G.; Ji, C.; Miao, M.; Yang, K.; Luo, Y.; Hoptroff, M.; Collins, L.Z.; Janssen, H.-G. Ex-Vivo Measurement of Scalp Follicular Infundibulum Delivery of Zinc Pyrithione and Climbazole from an Anti-Dandruff Shampoo. *J. Pharm. Biomed. Anal.* **2017**, *143*, 26–31. [CrossRef]
37. Zsikó, S.; Csányi, E.; Kovács, A.; Budai-Szűcs, M.; Gácsi, A.; Berkó, S. Novel In Vitro Investigational Methods for Modeling Skin Permeation: Skin PAMPA, Raman Mapping. *Pharmaceutics* **2020**, *12*, 803. [CrossRef] [PubMed]
38. *ANSI/AAMI/ISO 10993-5:2009/(R)2014*; Biological Evaluation of Medical Devices—Part 5: Tests for in Vitro Cytotoxicity. AAMI: Arlington, VA, USA, 2009; ISBN 978-1-57020-355-8.
39. Ashtikar, M.A.; Verma, D.D.; Fahr, A. Confocal Microscopy for Visualization of Skin Penetration. In *Percutaneous Penetration Enhancers Drug Penetration Into/Through the Skin: Methodology and General Considerations*; Dragicevic, N., Maibach, H.I., Eds.; Springer: Berlin, Heidelberg, 2017; pp. 255–281. ISBN 978-3-662-53270-6.
40. Proksch, E. pH in Nature, Humans and Skin. *J. Dermatol.* **2018**, *45*, 1044–1052. [CrossRef] [PubMed]